# Development of the Yield Stress due to Aging

## Verification of the abc-model based on $K_0$-CRS tests

by

H.B. Polinder

in partial fulfilment of the requirements for the degree of

**Master of Science**
in Civil Engineering

at the Delft University of Technology,
to be defended publicly on Thursday July 11, 2019 at 15:00 PM.

**Thesis committee:**

| | |
|---|---|
| Prof. dr. ir. C. Jommi | TU Delft (Geo-Engineering) |
| Dr. Ir. C. Zwanenburg | TU Delft & Deltares |
| Ir. M.G. van der Krogt | TU Delft & Deltares |
| Ir. W.J. Klerk | TU Delft & Deltares |
| Ir. K.J. Reinders | TU Delft (Hydraulic Engineering) |



TU Delft

Deltares
Enabling Delta Life

# Abstract

Around 55% of The Netherlands is protected by flood defences like dikes. Flood defences must meet requirements which are based on an allowed flood probability. Safety assessments are performed to check whether flood defences meet these requirements. Uncertainties are explicitly included in safety assessments. Uncertainty in soil behaviour is one of the major contributors to failure probability of dikes. Therefore reduction of this uncertainty in soil behaviour leads to potential savings in reinforcement costs.

One of the uncertainties in soil behaviour is the effect of aging on the behaviour of soft clays in compression. Compression behaviour of clay is strongly dependent on the transition from overconsolidated to normal consolidated soil behaviour. This transition phase in plain-strain conditions is indicated by the yield stress. The development of the yield stress due to aging is described by isotach models in terms of creep strains and stiffness parameters. Examples of isotach models are the abc-model and PLAXIS' Soft Soil Creep model (SSC-model). According to those isotach models, a yield stress induced by aging is similar to a yield stress induced by unloading.

This study verifies the development of the yield stress predicted by abc-models based on $K_0$-CRS tests. The test material is remoulded, highly organic, silty clay with a liquid limit of 165% and a plastic limit of 56% (OVP-clay). The determination of the abc-parameters is not straightforward. The value for the creep parameter is easily overestimated due to a slow decrease in excess pore water pressure during a constant stress phase, resulting in stress-dependent strains instead of creep strains. The b-parameter is affected by the gradual transition from overconsolidated to normal consolidated behaviour and by the development of structure during aging. The development of structure is not included in the isotach models and could result in a higher yield stress than predicted by the isotach models. The possible increase of the yield stress due to the development of soil structure is not visible in the test results, but the performed tests indicate softening behaviour after aging phases.

The three dimensional SSC-model simulates no increase in lateral stress during aging. Some studies present data showing that the lateral stresses increase under a constant effective stress in time. Unfortunately, the development of lateral stresses cannot be quantified based on the performed tests due to stick and slip behaviour in the $K_0$-ring during laboratory testing.

Based on the test can be concluded that a minimum yield stress in time can be predicted based on isotach models. An important note is that a yield stress is always obtained with respect to a certain isotach which is dependent on the loading rate and the creep parameter. The shift of the yield stress from the imposed isotach to the reference isotach is often significant in laboratory tests, but not taken into account. Effects of development of structure during aging should be further investigated: it influences the behaviour of the soil in compression and affects the yield stress determination.

# Preface

During my bachelor in Civil Engineering I did two projects in the field of dikes and embankments. I enjoyed those projects and it motivated me to start a master in Geo-Engineering. I do not regret that choice: I liked the combination of Civil Engineering and Engineering Geology. Last year I got the opportunity to start a master thesis at Deltares about aging of soils and the consequences for designing lifecycles of dikes. The scope refined when I started realizing the complexity of processes that underlie definitions like creep and aging. I am proud to present the results of the research on the following pages of this master thesis.

I learned a lot in the last nine months thanks to the graduation committee and Deltares. I want to thank Professor Cristina Jommi for her guidance in the research projects in the last years and Cor Zwanenburg for his time on Wednesdays discussing the results of the tests. I want to thank Mark van der Krogt and Wouter Jan Klerk for their guidance. Among others, their effort in teaching how to write a report is well appreciated! I am grateful for the opportunity to do my master thesis in cooperation with Deltares and with the help of Deltares employees. A special thanks to Mark de Hart, Roeland Tetteroo and Marien Harkes for their work in the laboratory.

I want to thank my parents, brothers, friends, roommates and fellow students. I am blessed with your support!

Herbert Polinder
*Delft, July 2019*

# Table of Contents

# List of Figures

# List of Tables

# 1. Introduction

This introduction contains the problem statement, the research outline and the reading guide of this thesis. The last section of this chapter introduces the test material.

## 1.1 Problem statement

Around 55% of the surface area of The Netherlands is protected by flood defences like dikes. Requirements to flood defences are based on an allowed probability of a flood in the area. Safety assessments are performed to check whether flood defences meet the requirements. Uncertainties are explicitly included in those safety assessments and uncertainty in soil behaviour is one of the major contributors to the failure probability. Reduction of this uncertainty therefore leads to potential savings in reinforcement costs.

The effect of aging on soil behaviour is one of the uncertainties. Aging of soil is defined as changes in the soil without other influences than the passage of time. This thesis focusses on aging of soft clay and its effect on the transition from relatively stiff to less stiff soil behaviour. The stiffer behaviour is related to the so-called overconsolidated state of the soil, while the less stiff behaviour is related to the normal consolidated state. The transition phase in plain-strain conditions is indicated by the yield stress. When working with three-dimensional models the indication for the transition phase is called the yield surface. The yield stress induced by aging (Figure 1a) and the yield stress induced by unloading (Figure 1b) is considered to be similar. Soil models like NEN-Bjerrum, abc-model and PLAXIS Soft Soil Creep model do not consider differences in behaviour between aged and mechanical overconsolidated soils. However, the processes could result in different structures and confining stresses, resulting in differences in soil behaviour of mechanical overconsolidated and aged soils.

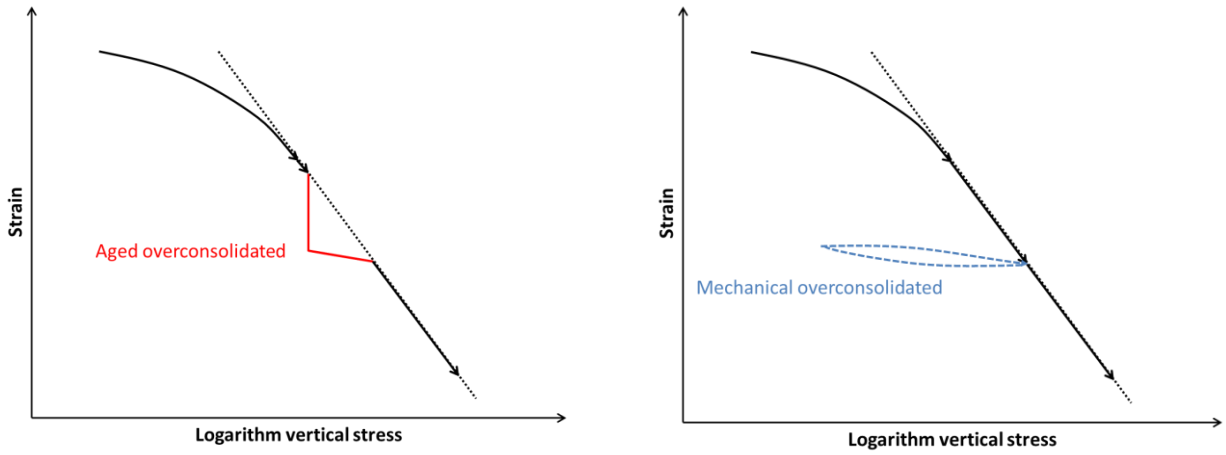


*(a)* *(b)*

**Figure 1: Stress-strain relation for aged overconsolidated soils (a) and mechanical overconsolidated soils (b)**

## 1.2 Research outline

**Problem**
Isotach models describe the consequences of aging in terms of overconsolidation, but it is unsure if clay behaves similar in mechanical (induced by unloading) and aged overconsolidated conditions.

**Goal**
The goal is to obtain differences between aged and mechanical overconsolidated soils, focussing on the transition from relatively stiff to less stiff clay behaviour.

**Approach**
The following approach is used to achieve the goal:

1) Obtain theoretical differences in soil behaviour of aged and mechanical overconsolidated clays.
2) Comparing the behaviour in compression after aging of the performed $K_0$-CRS tests with the behaviour simulated by the abc-model.
    a. The applicability of the abc-model is checked based on stress – void ratio relations obtained with the CRS tests
    b. The abc-parameters are obtained from the tests. A prediction of the development of the yield stress can be made based on the obtained parameters. The ranges of obtained parameters show the applicability of the model as well.
    c. The yield stress and creep strains predicted by the abc-model are compared with the obtained yield stress and creep strains.
    d. The lateral stresses during aging are measured with a $K_0$-ring to verify if lateral stresses increase during aging.

**Research questions**
The following questions are lined out to achieve the goal:

Does the yield stress develop due to aging as predicted by the abc-model and PLAXIS Soft Soil Creep model?

1) What can be theoretical differences in structure between aged and overconsolidated clays?
2) What are indications and possible consequences of development of structure during aging?
3) Which difficulties arise during determination of the abc-parameters?
4) Is the abc-model applicable on the tested clay?
5) Is the transition in soil behaviour indicated by the yield stress described properly by the mathematical formulation of the abc-model and Soft Soil Creep model?

## 1.3 Reading guide

Two diagrams show the structure of the report. The first gives an overview on the topics of the chapters. The second shows how the topics of the sections are connected to each other.

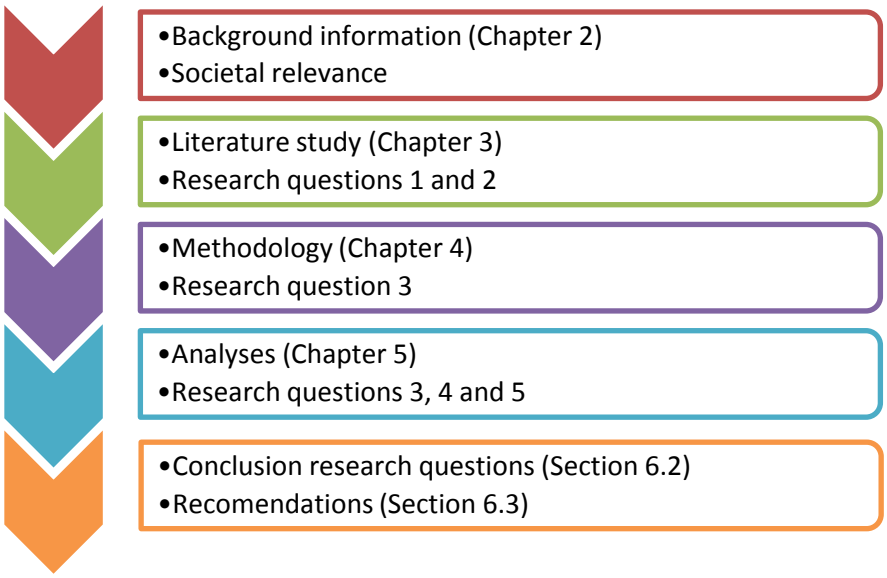


Chapter 2 gives an overview on the societal relevance of this master thesis (Section 2.1), connects aging of soils to dike safety assessments (Section 2.2), describes the similarity between isotach models (Section 2.3) and introduces the PLAXIS Soft Soil Creep model (Section 2.4).

The literature study describes possible differences in fabric of soils with several types of yield stresses (Section 3.1), discusses if lateral stresses could develop during aging (Section 3.2) and describes the differences between natural and remoulded clays (Section 3.3).

Chapter 4 and Chapter 5 focus on the performed (K0-) CRS tests. Chapter 4 describes how tests are used for this research and Chapter 5 discusses the results. The applicability of the abc-model is indicated by the sections about the void ratio and the obtained abc-parameters ranges (Sections 4.2, 4.3, 5.1 and 5.2). The transition from overconsolidated to normal consolidated behaviour is described in the sections about yield stresses and lateral stresses (Sections 4.4, 5.3 and 5.4).

The last chapter concludes on the question: Does the yield stress develop due to aging as predicted by the abc-model and PLAXIS Soft Soil Creep model?

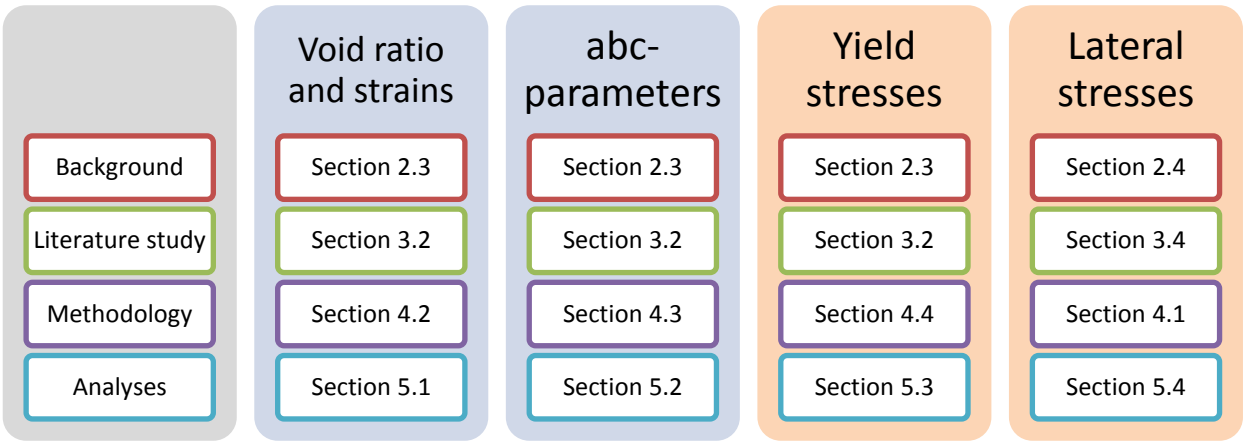

## 1.4 Test material Oostvaardersplassen clay (OVP-clay)


**Figure 2: The Nieuwkoop Formation (Den Haan & Kruse, 2007). The tested material comes from the area around the indication OVP.**

Remoulded Oostvaardersplassen Clay is used for the laboratory tests. The Oostvaardersplassen is a site in the Netherlands which contains soils of the Nieuwkoop Formation. Figure 2 indicates the location with the indication 'OVP'. Most of the Dutch soft soils belong to the Nieuwkoop formation which accumulated after the last glacial period. Due to sea level rise, a large part of the Netherlands became a tidal lagoon protected by a coastal barrier. Rivers flowed into this tidal basin from the east and south. Clay and silt was transported into the basin and sedimentation of those fines occurred in the low energetic environment behind the coastal barrier. During periods of sea level fall (regression) peat accumulated. During sea level rise (transgression) fines were deposited and peat eroded away (Van Loon & Wiggers, 1975).

The OVP-clay is deposited starting around 2000 years ago in fresh to brackish water in the Zuiderzee lagoon. This lagoon was formed after a widening of the connection towards the Waddenzee and North Sea. A lot of thin layers of fine sand and silts can be found in the stratigraphy of the deposition. This lamination is created by wave and storm influences (Van Loon & Wiggers, 1976). The organic material is deposited with an increasing trend of organic material in depth (Cheng, Ngan-Tillard, & Den Haan, 2007). The organic material in the clay layer is sedimentary, which is typically fairly decomposed (Davis, 1997): there is no clear fibre structure in the soil.

Around 400 year ago the opening between the North Sea and the OVP-site became larger. Another layer was formed in a brackish too salty environment, resulting in marine deposits. In 1932 the Zuiderzeedijk was built and 36 year later the Zuiderzee was poldered. Due to human activities the top soil is influenced by fresh water.

In the early nineties some OVP soils were collected and a part of this soil was classified as slightly organic, silty clay. Deltares performed laboratory tests, like triaxial and compression tests, on undisturbed and remoulded samples.

Around the year 2000, triaxial, direct shear and $K_0$-CRS tests were done on remoulded samples in a research project called 'Experimental Research to the Behaviour of Organic Clay' (Tigchelaar, 2001). In this report is stated that the behaviour of samples OVP-clay with a unit weight of approximately 14.0 kN/m$^3$ are representative for Dutch plastic clays. This seems plausible from engineering geology perspective; most plastic clays in the Netherlands have the same genesis and are preserved in comparable conditions. Table 1 indicates the characteristics of the material, which was tested almost 20 years ago. That particular batch had a lower organic content than the tested OVP-clay. Note that the mass content of the organic content is based on the total dry weight, where the mass contents of the particles are based on the total dry weight minus the organic content.

**Table 1: Characteristics of the slightly organic, silty clay**

| | | | |
|---|---|---|---|
| Particle density | $G_s$ | [-] | 2.53 |
| Organic content | OC | [%] | 9.5 |
| Liquid Limit | $W_L$ | [%] | 120 |
| Plastic Limit | $W_P$ | [%] | 37 |
| Mass content clay | | [%] | 26 |
| Mass content silt | | [%] | 71 |
| Mass content sand | | [%] | 3 |

Some of the collected OVP-clay consists of material with a lower unit weight. This material is remoulded in the beginning of April 2017 (Zwanenburg, Lange, & Konstantinou, 2018). After mixing in a vacuum mixer to remove trapped air in the soil, water was added to increase the water content from approximately 143% to 180%. This slurry is consolidated in plane-strain conditions for 172 days under 40 kPa, resulting in remoulded clay with a water content of 114%. Table 2 shows the Atterberg limits of the tested material as described in "POV Macro stability" (Zwanenburg et al., 2018). The Atterberg limits are indications for consistency changes. The change from semi-solid to plastic is called the plastic limit and from plastic to liquid is called the liquid limit. The behaviour of the material changes with its consistency, which is why soft soils can be classified based on the Atterberg limits (Verruijt, 2018). In the same report other properties of the soil are presented which are shown in the same table. The compression parameters of the abc-model and NEN-Bjerrum are discussed in Section 2.3.

**Table 2: Characteristics and model parameters of highly organic OVP-clay**

| | | | | |
|---|---|---|---|---|
| Atterberg limits | Liquid Limit | $W_L$ | [%] | 165 |
| | Plastic Limit | $W_P$ | [%] | 56 |
| abc-model | Direct strain | a | [-] | 0.013 |
| | Virgin compression | b | [-] | 0.18 |
| | Creep | c | [-] | 0.012 |
| NEN-Bjerrum | Unloading – reloading | RR | [-] | 0.024 |
| | Virgin compression | CR | [-] | 0.335 |
| | Creep | $C_\alpha$ | [-] | 0.021 |

# 2. Background

This chapter gives an overview on the societal relevance of the master thesis (Section 2.1), relates aging to dike safety assessments (Section 2.2), describes models that are used to describe aging (Section 2.3) and it ends with background information on the Soft Soil Creep model (Section 2.4).

## 2.1 Societal relevance

An estimated 1900 kilometre of the 3500 kilometre primary flood defences in the Netherlands do not meet the requirements in the first assessment round with the prevailing requirements[1]. Compared with last decade, the costs of dike reinforcements are almost doubled per kilometre and reinforcements of dikes should go almost three times faster than in the past. The total costs of dike reinforcements until 2050 are estimated to be around 11-14 billion euro, taking into account predicted consequences of climate change, subsidence of the hinterland and changes in allowed risks for certain areas (Deelprogramma Veiligheid Deltaprogramma, 2015). Discussions on how to do efficient inspections, maintenances and dike reinforcements are increasing in importance on regional and national scale. As explained in the problem statement, this thesis looks into uncertainty in the development of the yield stress due to aging of clay. More certainty about soil behaviour could lead to savings in reinforcement costs.

## 2.2 Aging of soils and dike safety assessments

Geotechnical engineers doubt if the yield stress obtained with $K_0$-CRS tests results in realistic values. The yield stress is often higher than expected and measured in the field. This causes uncertainty about the development of yield stress due to aging. Creep is one of the prevailing mechanical processes during aging (Schmertmann, 1991). Creep is defined as “time-dependent shear strains and or volumetric strains that develop at a rate controlled by the viscous resistance of the soil structure” (Mitchell & Kenichi, 2005). Explicitly mentioned is that also shear strains are affected by viscous resistance of soil structure. As a logical consequence, shear strength parameters are influenced by aging as well (Bjerrum & Lo, 1963). Therefore aging affects the geometry of dikes, but also their stability. If the yield stress is assumed to be not affected by aging, the modelled shear stress in time will be lower than the shear strength in the field. An overestimation of the yield stress results in larger settlements than expected from the models. This thesis attempts to find a minimum development of yield stress in time due to aging. In addition, it indicates several reasons why the yield stress could be overestimated based on $K_0$-CRS tests.

[1] Presentation “Future Proof Dikes”, F. den Heijer, M. Van, R. Hoogendoorn. 11th December 2018, Deltares Delft

## 2.3 Aging of clay in soil behaviour models

Aging is modelled in time-dependent stress-strain models as creep. Some models are not time-dependent stress-strain models, but time-dependent stress-void ratio models. The void ratio takes initial conditions of soils into account and is a three-dimensional parameter. The void ratio is defined as the volume of pores ($V_{pores}$) over the volume of particles ($V_{solids}$) (Verruijt, 2018):

$$e = \frac{V_{pores}}{V_{solids}}$$

The void ratio is related to the porosity (n) as follows:

$$e = \frac{n}{n-1}$$

If the soil is saturated, the following formulation can be used to obtain the initial void ratio:

$$e = G_s * w$$

$G_s$ is the specific density of the particles:

$$G_s = \frac{\rho_{solids}}{\rho_{water}}$$

And w is the water content:

$$w = \frac{M_{total} - M_{dry}}{M_{dry}}$$

This section summarizes the development of the isotach models.

Terzaghi is considered to be the first who came up with a consolidation theory for fully saturated and homogeneous soils with incompressible solid particles. The theory is a coupled process, the transfer of stress from the pore fluid on the soil skeleton with a rate depending on Darcy's law (Terzaghi, 1925). The following formula predicts the change in void ratio:

$$\Delta\varepsilon = \frac{\Delta e}{1 + e_0} = \frac{C_c}{1 + e_0} * \ log\left(\frac{\sigma_0{}' + \Delta\sigma'}{\sigma_0{}'}\right)$$

Where:

| | | |
|---|---|---|
| Δe | = | change in void ratio, where void ratio = volume voids / volume soil particles [-] |
| ε | = | linear strain = change in height / initial height [-] |
| $e_0$ | = | initial void ratio [-] |
| $C_c$ | = | compression index [-] |
| $\sigma_0'$ | = | initial effective stress [kPa] |
| Δσ' | = | increase in effective stress |

$C_c$ is a material specific empirical constant and can be calculated by dividing the change in void ratio over the change of the logarithm of the effective stress. Terzaghi's stress-strain relation considers no difference in stiffness between overconsolidated and normally consolidated soils. The stress-strain relation is not time-dependent, so aging cannot be simulated by this mathematical formulation.

Buisman introduced around 1940 a formula separating 'direct' and 'secular' compression, respectively consolidation and an endless aging effect. He noted that aging was an effect which occurred linear with the logarithm of time. Koppejan introduced the Koppejan method, a combination of Terzaghi's load compression and Buisman's secular effect (Koppejan, 1948). A problem with this formulation is that the initial condition of the soil is not taken into account. This problem is known as the superposition principle problem. Soil creep does not start after applying load, but soil is typically already in a state where the void ratio has been decreased due to creep.

To solve this, models were developed with time-dependent effective stress – strain (or effective stress – void ratio) relations. Those models are called the isotach models. 'Iso' is equal in Greek and 'tacho' is 'with relation to speed'. The definition of an isotach is an effective stress – strain relation with an equal creep rate along this relation. Šuklje (1957) used the definition isotach in relation to compression of soils for the first time (Heemstra, 2013).

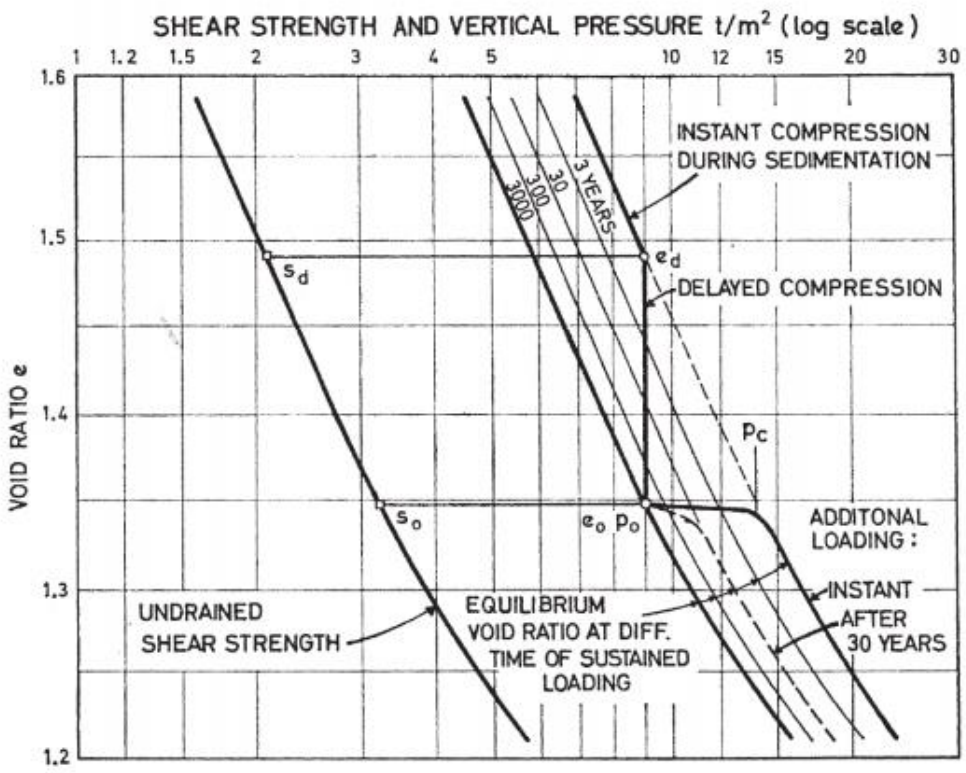


**Figure 3: Illustration of an isotach diagram (Bjerrum, 1967). A relation between the vertical pressure (x-axis), void ratio (y-axis) and time (isotachs).**

Bjerrum (1967) presented a complete model. Figure 3 illustrates the principles of this model. The creep rate is equal along an isotach. The stress-strain relation gets a third dimension with the isotachs. A mathematical formulation of Bjerrum's model can be found in a paper of Garlanger (Garlanger, 1972).

$$\Delta e = C_s * \log \frac{\sigma_p}{\sigma_0'} + C_c * \log \frac{\sigma_f'}{\sigma_p} * C_{\alpha e} * \log\left(\frac{t_1 + t}{t_1}\right)$$

Where:

| | | |
|---|---|---|
| $\Delta e$ | = | change in void ratio [-] |
| $C_s$ | = | unloading / reloading compression index [-] |
| $C_c$ | = | virgin compression index, slope of the isotach [-] |
| $C_{\alpha e}$ | = | delayed compression rate, $\Delta e$ – log(t) relation [-] |
| $\sigma_p$ | = | yield stress [-] |
| $\sigma_0'$ | = | initial effective stress [kPa] |
| $\sigma_f'$ | = | total increase of effective stress [kPa] |
| $t_1$ | = | time to the isotach [days] |
| t | = | variable time [days] |

The stress-strain relation on an isotach line is called virgin compression. The stiffness of an aged or overconsolidated soil is given by the swelling or unloading-reloading index $C_s$. Delayed compression is the decrease in void ratio in time under constant stress.

An alternative for the Bjerrum-model was published by Den Haan about 25 years later. The compression parameters of Den Haan's abc-model are formulated different. Den Haan uses Buisman's terms direct and secular compression, rather than Bjerrum's instant and delayed compression. The difference between the definitions of Den Haan's and Buisman's terms is that according to Den Haan's abc-model, secular compression starts together with direct compression. Figure 4 shows Den Haan's a, b and c parameters in an isotach diagram. On the horizontal axis the natural logarithm of the vertical stress is given, on the vertical axis the natural strain.

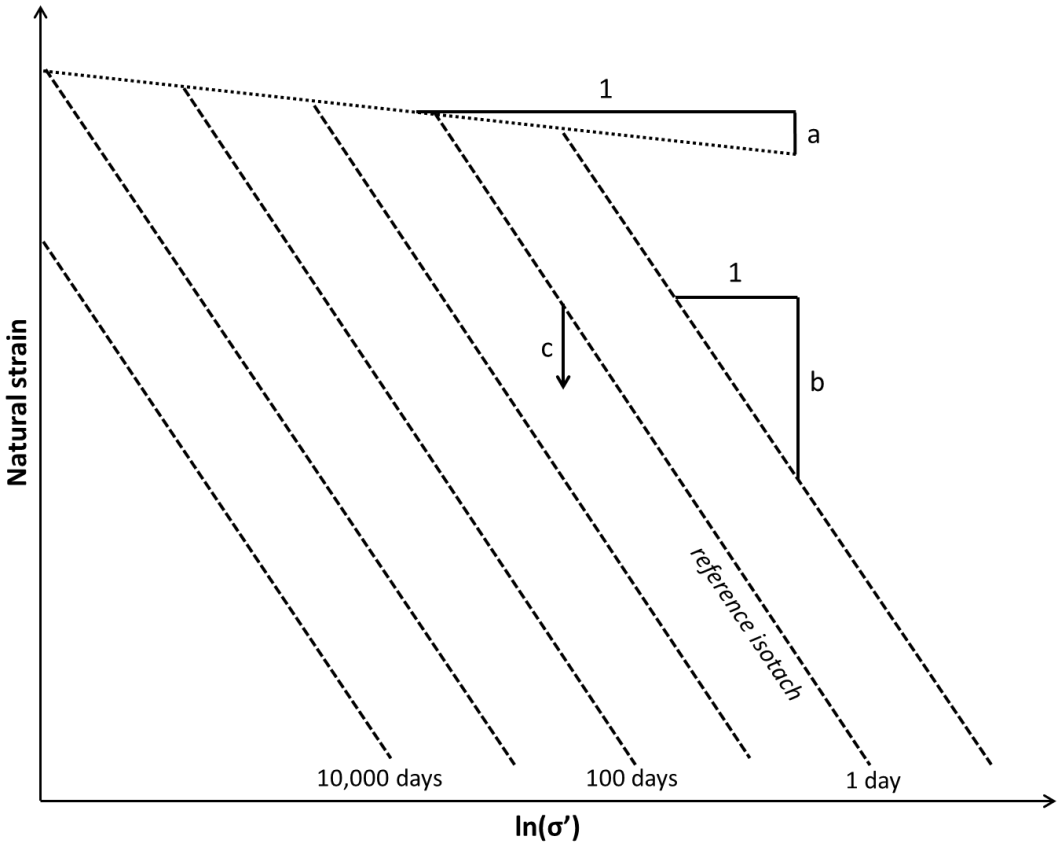


**Figure 4: A schematic illustration of the isotach model of Den Haan. The a-parameter is related to the stiffness in overconsolidated state, the b-parameter to the normal consolidated state and the c-parameter is related to time dependent strains.**

Significant strains can occur in soft soil. Linear strains are not applicable anymore when the strains are around 50%. Figure 5 shows the difference between natural and linear strains. The equations below show how natural strains are related to linear strains.

$$\varepsilon^C = \frac{\Delta h}{h_0}$$

$$\varepsilon^H = \varepsilon_d{}^H + \varepsilon_s{}^H = -\ln(1 - \frac{\Delta h}{h_0}) = -\ln(1 - \varepsilon^C)$$

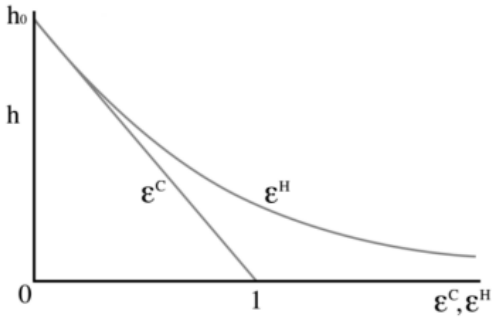


**Figure 5: Natural and linear strain (Deltares, 2016). $\varepsilon^c$ is the linear strain, $\varepsilon^H$ is the natural strain, $h_0$ is the initial height and Δh is the change in height**

The earlier mentioned superposition principle problem is solved by translating the initial state to an intrinsic time. The intrinsic time is defined as the time that the soil would have needed to reach its current stress-strain state under a certain constant effective stress with respect to the reference isotach (Visschedijk, 2010). Den Haan gave the mathematical descriptions of the intrinsic time (Den Haan, 1994):

$$\theta = \frac{c}{\delta\varepsilon_s{}^H / \delta t}$$

$$\theta = t - t_r$$

Where:

| | | |
|---|---|---|
| θ | = | intrinsic time [days] |
| c | = | Den Haan's time-dependent secular compression coefficient [-] |
| $\delta\varepsilon_s{}^H/\delta t$ | = | natural creep rate [$s^{-1}$] |
| t | = | variable time [days] |
| $t_r$ | = | time shift for which the first equation is true [days] |

Note that if the intrinsic time is equal to one day, the time-dependent secular compression coefficient is equal to the creep rate. The one day isotach is the reference isotach and c is by definition the creep rate on the one day isotach. If the intrinsic time is known, one can imagine with help of Figure 3 and Figure 4 that the point at which the soil returns on the isotach can be calculated based on the compression parameters and the in situ stress. This point represents the yield stress. The mathematical formulation below shows how the yield stress and the intrinsic time relate to each other (Ammerlaan, 2011).

$$\theta_1 = \theta_0 * \left(\frac{\sigma_p}{\sigma_0'}\right)^{\frac{b-a}{c}}$$

$$\sigma_{p} = \sigma_0' * \left(\frac{\theta_1}{\theta_0}\right)^{\frac{c}{b-a}}$$

Where:

| | | |
|---|---|---|
| $\theta_1$ | = | intrinsic time [days] |
| $\theta_0$ | = | reference intrinsic time [days] |
| $\sigma_p$ | = | yield stress [-] |
| $\sigma_0$' | = | initial effective stress [kPa] |
| a | = | Den Haan's direct strain parameter [-] |
| b | = | Den Haan's stress-dependent secular parameter [-] |
| c | = | Den Haan's time-dependent secular compression coefficient [-] |

The differences between the Bjerrum and the abc-model are listed below:

- There is a factor between the natural logarithm and the logarithm of ten in the stiffness parameters
- There is a difference between the definitions of the stiffness parameters
- More differences will arise due to the fact that the abc-model uses natural strains while Bjerrum uses linear strains. Natural strains tend to describe soil behaviour of soft soils better.

At the end it does not matter which model would be verified with this thesis. In theory the abc-model describes the soil behaviour best with its natural strains. However, differences for the applied displacements will be very small. The same analysis and conclusions could be made based on Bjerrum's model.

## 2.4 Soft Soil Creep model and the yield surface

The PLAXIS Soft Soil Creep model (SSC-model) describes time dependent compression in relation to strength properties based on the OverConsolidation Ratio (OCR). The OCR is the yield stress over the current stress state in the soil. Some important characteristics of the SSC-model are given in this chapter. Most of them will be in line with the other isotach models.

- The model describes a logarithmic stress-strain relation
- The model works with a time-dependent yield stress
- Irreversible strains are modelled as visco-plastic behaviour
- The model simulates strains in overconsolidated conditions as reversible, so the model behaves elastically in unloading and reloading.

It is unclear if the last assumption is true: it could be that there is an irreversible part in unloading – reloading strain. Therefore direct strain is called in this thesis 'almost elastic' as it is clear that a large part of the strains is elastic.

The SSC-model is a three-dimensional model, so the stress state and the transition from elastic to visco-plastic behaviour should be described in terms of three dimensions. Therefore the Cam-Clay parameters are introduced.

$$p' = \frac{\sigma_{principal}{}' + 2 * \sigma_{lateral}{}'}{3}$$

$$q = \sigma_{principal}{}' - \sigma_{lateral}{}'$$

In which p' is the mean normal stress and q is the deviatory stress. For p' and q is assumed that the lateral stresses are the same in both directions. The ratio lateral stress over principal stress is called the coefficient of earth pressure at rest in plain strain conditions. That means that stresses can be written as:

$$p' = \frac{\sigma_{principal}{}'(1 + 2 * K_0)}{3}$$

$$q = \sigma_1{}'(1 - K_0)$$

Also the stiffness parameters have to be translated to three dimensional parameters. Note that the definitions of the one-dimensional input ABC-parameters of PLAXIS (Vermeer & Neher, 1999) are not the same as the one-dimensional abc-parameters of the abc-model. A conversion from the abc-parameters to the NEN-Bjerrum and Soft Soil Creep parameters is complicated. The abc-model does not work with plastic and elastic strains, but with direct and visco-plastic strains. For a review on the conversion of the abc-parameters in NEN-Bjerrum parameters is referred to an article in Dutch about isotach parameters (Den Haan, Essen, & Visschedijk, 2004). The conversion factor given in this article is added in the Appendix G. The recommendation is to use the alternative Soft Soil Creep model input, the NEN-Bjerrum parameters. The conversion from NEN-Bjerrum to the Soft Soil Creep parameters is given in Table 3.

Table 3: Conversion factors for isotach parameters

| | SSC-model and Bjerrum | |
|---|---|---|
| **Direct strain / elastic behaviour** | $\kappa^* = \frac{2 * C_s}{2.3 * (1+e)}$ | $\kappa^* = \frac{2 * RR}{2.3}$ |
| **Virgin compression** | $\lambda^* = \frac{C_c}{2.3 * (1+e)}$ | $\lambda^* = \frac{CR}{2.3}$ |
| **Creep parameter** | $\mu^* = \frac{C_{\alpha e}}{2.3 * (1+e)}$ | $\mu^* = \frac{C_\alpha}{2.3}$ |

The NEN-Bjerrum parameters have a correcting factor of 2.3 for the change from the logarithm of ten to the natural logarithm. The change from void ratio into volumetric strains can be calculated with a factor one plus the void ratio. The calculated strains are linear strains.

The following formulation is used to calculate the one-dimensional creep strain rate (Vermeer & Neher, 1999).

$$\frac{d{\varepsilon_v}^H}{dt} = \frac{\mu^*}{\theta} * \left(\frac{p'}{p_p}\right)^{\frac{\lambda^* - \kappa^*}{\mu^*}}$$

Where:

$d\varepsilon_v^H/dt$ = The natural volumetric strain rate [-]
$\kappa^*$ = modified Cam-Clay swelling index [-]
$\lambda^*$ = modified Cam-Clay compression index [-]
$\mu^*$ = modified Cam-Clay creep index [-]
$\sigma'$ = effective stress after step n [kPa]
$p_0'$ = initial effective mean stress based on $K_0$ [kPa]
$p_p$ = yield stress [-]
$\theta$ = intrinsic time [days]

The mean effective stress in this p'-q graph is calculated based on soil in $K_0$-conditions. The horizontal stress does not change during aging. The yield stress based on the mean effective stress develops as follows (Vermeer & Neher, 1999):

$$p_p = p_{p0}^{\left(\frac{{\varepsilon_v}^H}{\lambda^* - \kappa^*}\right)}$$

Where:

$p_p$ = yield stress [-]
$p_{p0}$ = initial yield stress [-]
$\varepsilon_v^H$ = natural volumetric strain [-]
$\kappa^*$ = modified Cam-Clay swelling index [-]
$\lambda^*$ = modified Cam-Clay compression index [-]

Instead of calculating the increase in yield stress based on creep strains and intrinsic time, the increase in yield stress is directly calculated by the total amount of creep strains.

Figure 6 shows the yield surface in a p'-q graph, indicating the stress path in $K_0$-conditions with the $K_0$-line. During aging the yield surface (limit state surface in Figure 5) increases (Bjerrum & Lo, 1963; Den Haan, 1994). How the yield surface develops during aging is not clear. It is questionable if the soil stays in $K_0$-conditions during creep, while a yield stress is defined as being on the $K_0$-line. The yield surface could for example rotate towards a more isotropic shape if the lateral stresses increases. The transition during loading after aging could be somewhere below the $K_0$-line.

Some studies indicate that the undrained shear strength increases due to aging (Bjerrum & Lo, 1963; Tang & Tsuchida, 1999). That means that the yield surface not only increases along the $K_0$-line, but also in q direction.

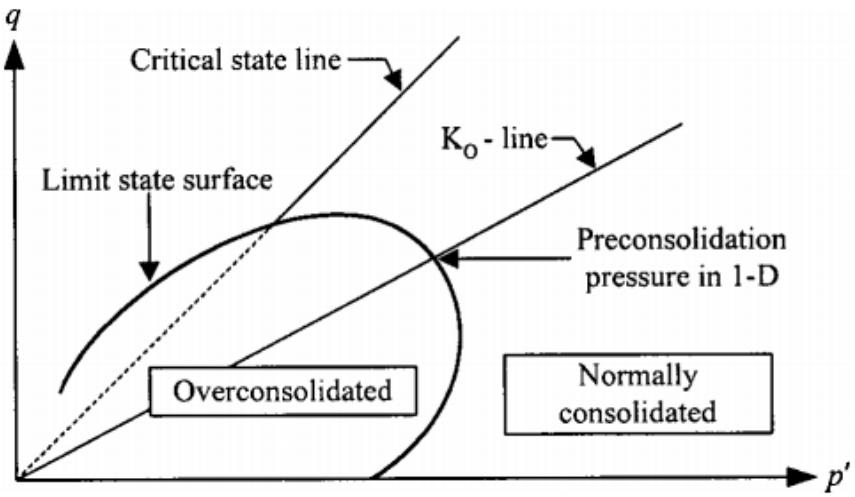


**Figure 6: The yield surface (limit state surface), indicated overconsolidated and normally consolidated conditions with on the $K_0$-line the yield stress (preconsolidation pressure in one dimension) (Augustesen, Liingaard, & Lade, 2004)**

# 3. Literature study

The first two research questions are answered in this chapter.

1) What are theoretical differences in structure between aged and overconsolidated clays?
2) What are indications and possible consequences of development of structure during aging?

Question one is answered in Section 3.2 and 3.4. Question two is the topic of Section 3.3. Section 3.1 is an introduction which links the OVP-clay of Section 1.4 to the literature in this chapter.

The applicability of the isotach models on the silty clay became disputable in this thesis during the literature study. The motivation for the third research question 'Is the abc-parameter applicable on the tested clay?' is explained in Section 3.1.3.

## 3.1 Fabric and characteristics of soft silty clays

The tested clay has a significant organic content and approximately 70 mass percent is silt (Table 4). The fabric and some characteristics of clay, organic material and silt are shortly discussed and linked to expected behaviour of OVP-clay.

Established rules determine how a soil should be classified (NEN-EN-ISO 14688 - 2). Normally this is done per soil layer, but the test material is remoulded: Possible laminated layers in the soil are mixed, resulting in homogeneous, organic, silty clay.

Table 4: Classification of soil particles

| | Soil | Diameter particles [mm] | Void ratio* [-] | Hydraulic conductivity [m/s] |
|---|---|---|---|---|
| **Inorganic fines** | Clay | < 0.002 | 0.40 - 2.00 | $10^{-10} – 10^{-8}$ |
| **Granular material** | Silt | 0.002 – 0.063 | 0.25 - 2.00 | $10^{-8} – 10^{-6}$ |
| **Granular material** | Sand | 0.063 - 2.00 | 0.25 - 1.00 | $10^{-6} – 10^{-3}$ |
| **Organic material** | Peat | | 3.00 - 20.0 ** | $10^{-10} – 10^{-4}$ ** |

* Volume voids / volume particles
**Aljouni (2000)

Figure 7 shows the classification of Dutch soils. The red dots indicate the classification of the OVP-clay: highly organic, silty clay.

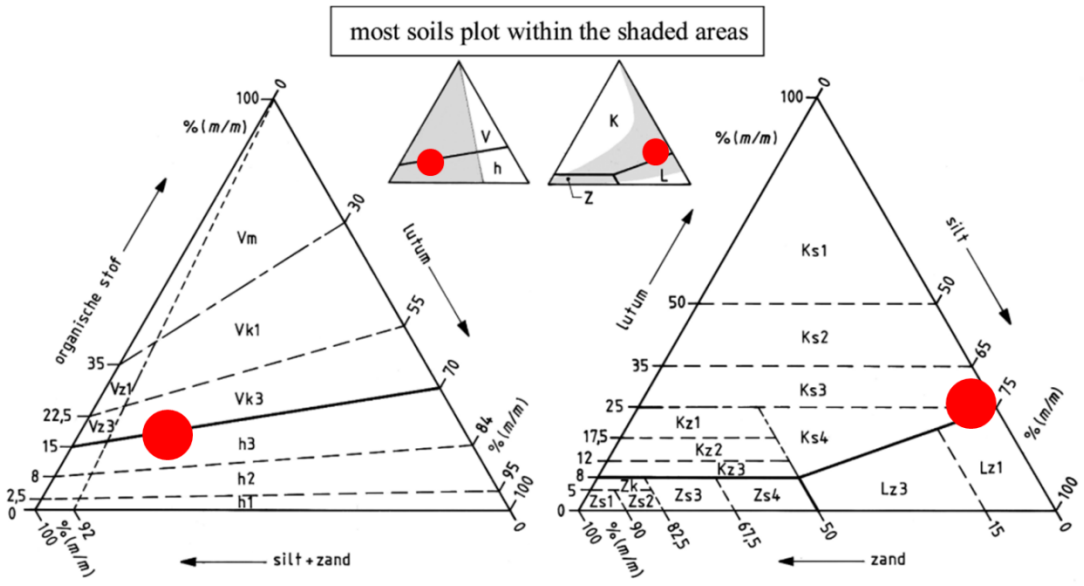


translation of terms and abbreviations:
"organische stof" = organic matter; "lutum" = fines < 2 µm; "silt" = silt; "zand" = sand.
V = "veen" = peat; K, k = "klei" = clay; s = silt; Z, z = "zand" = sand; L = "leem" = loam (silt);
h = "humus" = organics; m = poor in mineral matter.

Figure 7: Classification of Dutch soils (Den Haan & Kruse, 2007)

### 3.1.1 Soft clay

The fabric of a clay is depending on a lot of factors such as particle size, particle shape, particle gradation, clay minerology, organic content, the pore fluid, acidity and deposition modes (Collins & McGown, 1974). This section focusses on factors that could change the structure after its deposition, given an organic content and the conditions of preservation.

A clay particle is a negatively charged and plate or sheet shaped. Figure 8 shows the negatively charged surface and the positively charged edges.

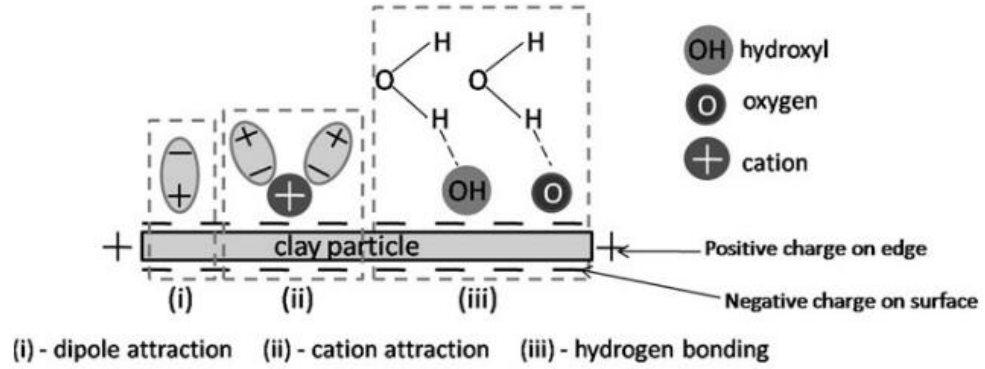


Figure 8: Dipole attraction, cation attraction and hydrogen bonding (Le, Fatahi, & Khabbaz, 2012)

The net negatively charged clay particle attracts (Sridharan & Venkatappa Rao, 1971);

i. the positive sides of dipoles, like water
ii. cat-ions, ions that are dissolved in water like calcium ($Ca^{++}$), magnesium ($Mg^{++}$) and natrium ($Na^{+}$)
iii. hydrogen atoms ($H^{+}$), this hydrogen atoms are bounded to oxygen atoms in pore water and to oxygen particles on the surface of clay particles at the same time

In addition to the three types of bonding above, the negatively charged surfaces attracts positive charged edges. The attraction and repulsion forces and the stress state of the soil, influence the fabric of clay. The fabric of the clay is defined as the arrangement of clay particles relatively to each other and the voids between the particles (Collins & McGown, 1974). If the positively charged edges are attracted to the negative charged surfaces of the clay particles, the particles have a random arrangement. This phenomenon is called flocculation. Dispersion of clays is if the clay particles are parallel structured. The surfaces of the clay particles repulse each other. Compaction generally changes the fabric towards a more dispersed state (Le et al., 2012). Uniform dispersed clays are rare (Bolt, 1956).

Figure 9 gives schematic illustrations of flocculated and dispersed clay structures with edge and (sur)face bonds. Flocculated and dispersed clay particles can form aggregates, further referred to as clay clusters. Those clay clusters can form so called clay peds (Matsuo & Kamon, 1977), which can be seen by eye. That what can be seen by eye is often called macro-structure in literature (Collins & McGown, 1974). In this document macro and micro-porosity is a relative definition, because the macro-structure and corresponding macro-pores are not necessarily visible. The macro-pores are inter-clay-clusters pores, while the micro-pores are intra-clay-clusters pores.

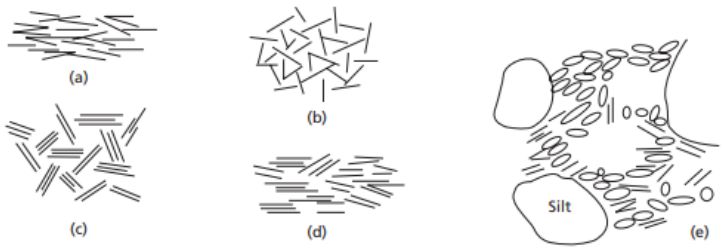


**Figure 9: Clay structures: (a) dispersed clay structure, (b) edge to face flocculated clay structure, (c) edge to edge flocculated, (d) edge to edge dispersed and (e) example of a natural clay structure (Craig & Knappett, 2012)**

The pores of clay are filled with pore fluids. Pore fluids in clay can be distinguished in categories, like:

I. Bounded water as shown in Figure 8.
II. The non-bounded part of pore water in clay clusters**.** Also called micro-structure pore water and linked to the micro-pores (Navarao & Alonso, 2001).
III. Free water between clay clusters. Also called macro-structure pore water, bulk water and linked to the macro-pores (Navarao & Alonso, 2001).

A high amount of free water results typically in large strains in compression (Den Haan & Kruse, 2007). Compaction decreases the water content and typically changes the fabric towards a more dispersed state (Le et al., 2012). Dispersed clays are typically better bonded and less prone to creep than flocculated clays, because the particles are packed closer.

### 3.1.2 Organic soils

The OVP-clay has an organic content around 15%. Its classification is therefore highly organic. The influence of the organic content on physical properties and engineering parameters is significant (Farrell, O'Neil, & Morris, 1993; Den Haan & Kruse, 2007; Nie, Lv, & Li, 2012). However, the soil is remoulded and therefore a constant amount of organic material can be expected in the samples. As mentioned in Section 1.4, the organic material in the OVP-clay is fairly decomposed, which tells us that there is no clear fabric of fibres in the soil.

### 3.1.3 Silt

Silt particles are particles that are between 0.002 and 0.063 mm in their largest dimension. Together with clay they are called fines. That makes sense from sedimentation point of view: the particles settle in low energetic conditions like clayey particles. However, if looked to the fabric, silt seems to be more like sand with a smaller grainsize. The behaviour of silt is certainly not like clay or sand. A unique relation between effective stress and void ratio in normal consolidated conditions is found in studies on clay and sand, but this relation is not found in some silty soils (Nocilla, Coop, & Colleselli, 2006). In literature is referred to 'transitional soils' and soils that do not behave according to the Rendulic's principle. Those soils have no unique normal consolidated behaviour with an effective stress – strain relation and therefore no unique yield stress (Gens & Cataluña, 1985). Knowing that the OVP-'clay' has a mass silt percentage of 70%, the question rises if the isotach models are applicable on the OVP-clay.

## 3.2 Mechanical OCR and apparent OCR's

The mechanical and chemical processes during the development of a yield stress will affect the fabric of the soil. The literature study is used to obtain theoretical differences between OCR's[2]. This could help interpreting the $K_0$-CRS tests. Figure 10 illustrates different OCR's.

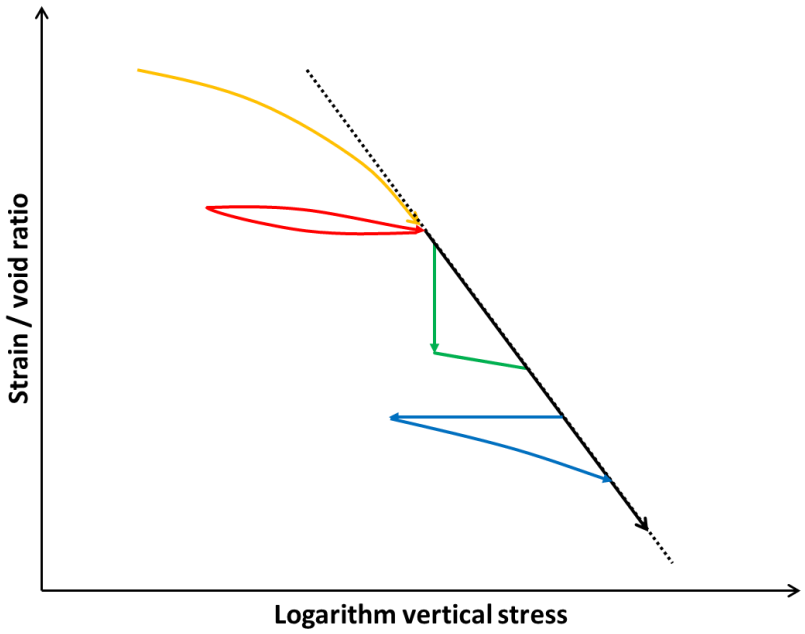


Figure 10: Illustration of several types of OCR's, namely unloading (red and orange), creep (green) and relaxation (blue)

The tested soil is preconsolidated and therefore in overconsolidated state at the beginning of the test. As will be described in Chapter 4, a mechanical, creep or relaxation OCR will be created with the $K_0$-CRS tests. The preconsolidation and the unloading OCR's are mechanical OCR's (Schmertmann, 1991). The soil will age during unloading and reloading as well, but the mechanical OCR will be much larger than the consequences of aging. Creep, like repeated loading and cementation, results in an apparent OCR. The soil is not overconsolidated in the sense that the soil has been prone to a larger load, but the yield stress increased due to another process (Won & Chang, 2007).

Section 3.2.1 discusses mechanical OCR's. Creep OCR is extensively described in Section 3.2.2. Some attention is given to relaxation (Section 3.2.3), repeated loading (Section 3.2.4) and cementation (Section 3.2.5). Section 3.2.6 is a summary of the hypothesis.

[2] The yield stress over the effective stress in the soil

### 3.2.1 Mechanical OCR

The mechanical OCR is an OCR influenced by a load which is larger than the current load. Examples can be found in natural soils that, for example, existed before the last glacial period. The weight of the ice compresses the soil to an overconsolidated state relative to the situation after the ice melted. Another reason for an overconsolidation of soil is if the soils above the soil eroded away, so the layers below the eroded layers have been prone to a higher active vertical stress in the soil than the in situ stress. Erosion can be caused by water flows, wind and ice movements. If the overburden gets smaller, the volume of the soil increases.

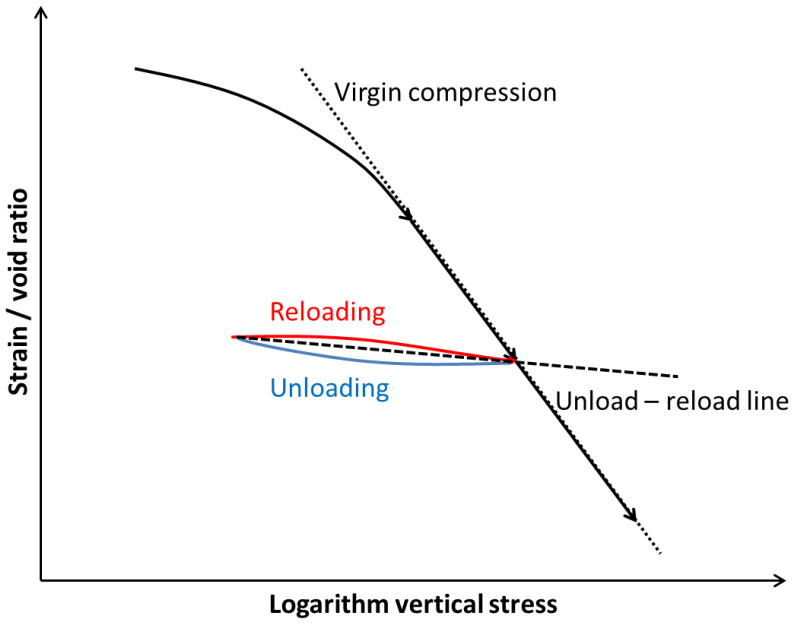


Figure 11: Unloading and reloading

Figure 11 shows an increase in the void ratio during unloading which is about the same as the decrease in reloading. As illustrated in the figure, a hysteresis effect (Mewis & Wagner, 2009) is involved in this unloading-reloading process.

### 3.2.2 Creep

Creep is a mechanical process resulting in an apparent OCR. The OCR is called apparent because there is in fact no 'overconsolidation', no transfer of stresses from pore water to the soil skeleton. Creep is described in several ways with in common that the soil deforms into a new configuration in the soil structure.

There are several terms used to describe creep relative to consolidation. An overview of some of the terms is given in Figure 12. A complete overview of the definitions for this thesis is listed below.

- Primary and secondary compression. Primary compression is related to the time of consolidation: the strains during the dissipation of excess pore water pressure. Secondary compression is the compression after the excess pore water has dissipated and therefore during constant effective stress.
- Instant and delayed compression. Delayed compression is related to all creep strains during, including during the dissipation of excess pore water Instant compression is the total compression minus the influence of delayed compression.
- Direct and secular compression. Direct compression is linked to primary compression. Secular compression is slightly different from secondary compression. Secular compression is defined to be applicable in isotach models, describing creep itself instead of the deformations after consolidation (Heemstra, 2013).
- The Soft Soil Creep model works with reversible and irreversible strains. Those terms are based on a direct and secular compression model. However, it is questionable if direct and secular can be seen as respectively reversible and irreversible strains.

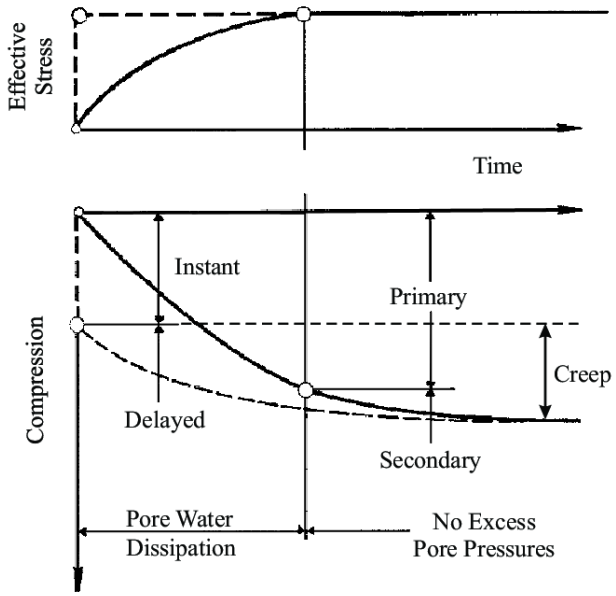


Figure 12: The definitions of primary, secondary, instant and delayed compression (Bjerrum, 1967; Clarke, 2009)

Le, Fatahi & Khabbaz (2012) published a paper called “Viscous behaviour of Soft Clay and Inducing Factors” with five possible causes of creep. The first three are directly linked to the physico-chemical bonds in clays. The last two are a result of the interaction between the macro and micro-structure of clay and the viscosity of the pore fluid.

1. Breakdown of inter-particle bonds
2. Jumping of bonds (Kuhn & Mitchell, 1993; Mitchell & Kenichi, 2005)
3. Sliding particles (Kuhn & Mitchell, 1993)
4. Primary and secondary structure - double porosity
5. Structural viscosity

The aforementioned paper of Le, Fatahi & Khabbaz (2012) gives an elaborated overview, concluding that there is no unified theory which describes creep deformations in soft clays. Some relevant theories are summarized in this section.

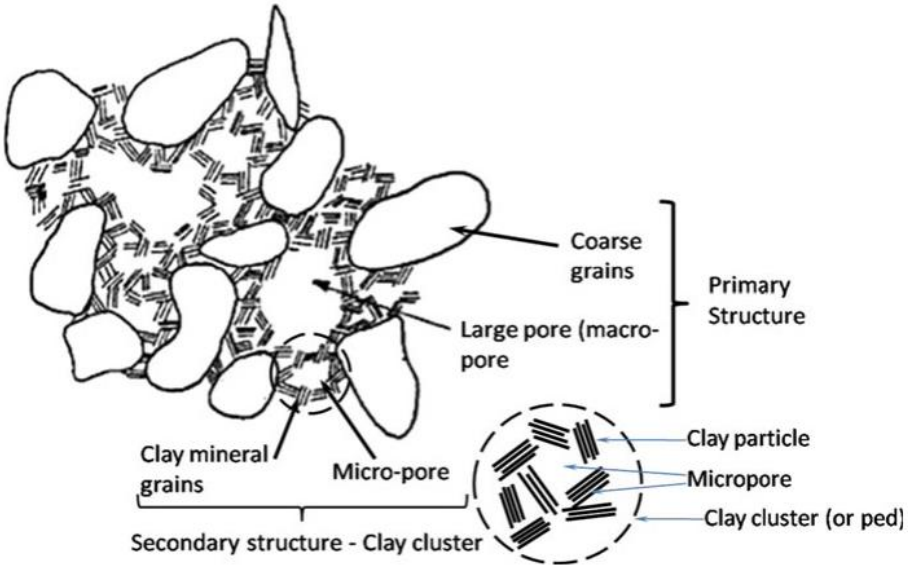


Figure 13: Primary and secondary structure (Le et al., 2012; Zeevaart, 1986)

Figure 13 is a schematic illustration of the primary and secondary structure in clay. The primary structure is formed by clay clusters and coarse grains (if present in the clay). Those form a structure with relatively large pores between the clay clusters and the larger grains. Water in those pores can be called macro-structural water. The secondary structure is formed by clay particles forming clay clusters with microstructural water in the micro-pores (Navarao & Alonso, 2001; Zeevaart, 1986). A mechanism that may cause creep is the flow of microstructural water from micro-pores to macro-pores (Navarao & Alonso, 2001).

As mentioned in Section 3.1.1**,** clay particles attract cations. Those cations increase the viscosity: The resistance against flow through the pores (Navarao & Alonso, 2001). So water close to the clay particles, microstructural water, will have a higher viscosity than water in the macro-pores. Water expelled from a clay sample during consolidation will have less exchangeable cations than water expelled from clay during creep. Based on this hypothesis, Akagi (1994) measured the amount of cations in the expelled pore water during compaction experiments. The conclusion was that the

primary structure is related to consolidation: with increasing effective stress in the soil, the macro-pores are drained. The secondary structure is related to creep deformation of micro-pores in the clay clusters (Akagi, 1994). A few years earlier, based on Mercury Intrusion Porosimetry (MIP) and electron microscopy, was stated that consolidation drains larger pores first: during compression, smaller and smaller macro-pores collapse (Delage & Lefebvre, 1984; Griffiths & Joshi, 1989). Additionally was concluded that the micro-structure was not influenced by the process of transferring stress from the water column on the soil skeleton (Griffiths & Joshi, 1989). It is questioned if MIP tests could be used to make especially the latter conclusion (Griffiths & Joshi, 1990). However, Griffiths' and Joshi's conclusions are in line with the conclusions of Akagi.

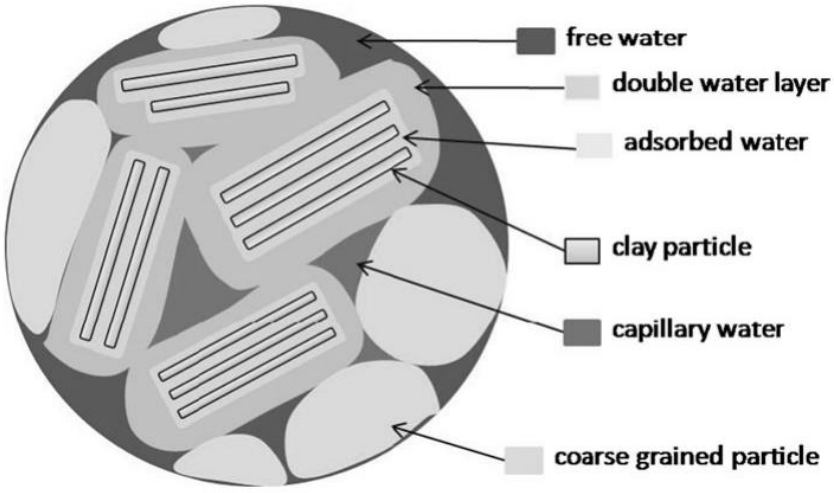


Figure 14: Double water layer around clay particles (Le et al., 2012)

Figure 14 schematizes the theory of a double layer of water. Each clay particle has an absorbed water layer around the periphery of the particle and around the clay cluster another water layer can be observed in which a significant amount of cations are floating. The viscosity of the pore water around the clay particles may be increasing with the distance towards the particles (Barden, 1968). Structural viscosity is a term indicating the increasing resistance against moving caused by the decreasing distance between particles (Bjerrum, 1967).

After consolidation, with decreasing local movements of particles and the flow of water, a stiffening effect occurs. This is caused by the increase of bonds that are made between particles and/or absorbed water molecules when water flow decreases (Barden, 1968). This stiffening is called thixotropic stiffening: reversible and time-dependent increase in stiffness (Mewis & Wagner, 2009) of the micro-structure.

Sridharan and Venkatappa Rao did tests on saturated montmorillonite clay (liquid limit 305% and plastic limit 44%) and saturated kaolinite clay (liquid Limit 49% and plastic limit 29%). They replaced water by eight other pore fluids. Two main mechanisms were distinguished in their tests;

I. Shearing resistance between particles
II. The development of a double layer around the particles

The conclusion was that the first mechanism was dominant in the kaolinite, while the development of a double layer was dominant in the clay with the higher plasticity (Sridharan & Venkatappa Rao, 1973). The tested OVP-clay has a liquid limit of 165% and a plastic limit of 56%, which is between montmorillonite and kaolinite clay.

OVP-clay consists of amorphous organic material and silt. Regardless of the large influence of the organic content, the same phenomenological processes can be used to describe creep in amorphous organic material (Barden, 1968; Berry & Poskitt, 1972). Creep in granular materials results in stiffer and less stiff zones in the soil (Bowman & Soga, 2003). The amount of creep in granular materials with respect to creep in clay is small. The interaction between stiff material and less stiff clay clusters (Bolt, 1956) could be relevant in natural OVP-clay. In the homogeneous remoulded soil is hypothesised that creep is governed by the processes described above, the shear resistance of particles and the development of a double layer around the particles.

### 3.2.3 Relaxation

During relaxation the sample will not deform: the height is kept constant. The soil will creep towards a state in which no stress is transferred to the soil. The soil is in an unloading and aging phase at the same time. Theoretically the microstructural water content will decrease while the macrostructural water content could increase slightly. Expected is a different structure after relaxation and creep. Differences in stiffness parameters will be insignificant.

### 3.2.4 Repeated loading

The repeated loading tests are designed to indicate the influence of repeated loading on the creep rate. Possible causes for this type of repeated loading could be gradual groundwater fluctuations or fluctuations in saturation caused by precipitation. Several studies conclude that repeated and cyclic behaviour is for the largest part undrained, but there are some projects were a drained behaviour is observed (Fujiwara, Ue, & Yasuhara, 1987). To what extent a process can be called drained or undrained is the ratio between the permeability and the rate of transfer of stresses from water to soil structure. There are several factors influencing drained and undrained behaviour in compaction (Fujiwara et al., 1987)**:** the organic content, the load increment ratio, the loading period and the total stress in the soil. This is in line with research that indicated that clay under repeated loading has a higher creep rate than clay under static load (Fujiwara et al., 1987).

### 3.2.5 Cementation

Natural cementation can be caused by several sources, like precipitation of calcite, silica or clays in the pores (Baxter & Mitchell, 2004; Wang & Leung, 2008). Cementation is a chemical mechanism that does not decrease the void ratio, but results in a higher yield stress. If the effective stress is higher than the yield stress, the soil softens until it is back on the isotach (Figure 15). When the isotach is reached, the soil behaves in line with the virgin compression parameter. The relevance of natural cementation in dikes is unclear and has no role in studies of dikes in The Netherlands.

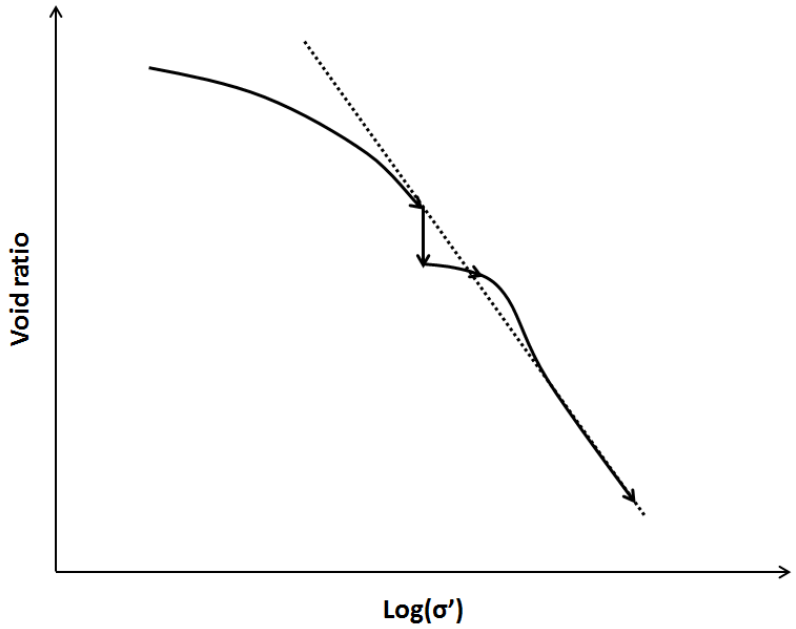


Figure 15: The consequence of cementation of the soil for the stress – void ratio relation: A higher yield stress and softening behaviour until the soil is back on the isotach

### 3.2.6 Summary types of OCR

Creep in clay is a complicated process in which mechanical and chemical processes play a role. During creep mainly the micro-structure will change while mainly the macro-structure is changed by an overburden pressure. Relaxation could have both: changes in the macro-structure and in the micro-structure. Repeated loading increases the creep strain and cementation is not a process that plays a significant role in dikes in the Netherlands.

## 3.3 Remoulded clays and development of structure

As described in the introduction, all tests are done on remoulded soils. Possible differences in the fabric and compressibility with natural soils are described in this section.

The OVP-clay is deposited in fresh to brackish water. Salt in slightly brackish water influences the structure of the clay: the structure is more dispersed than in fresh water (Collins & McGown, 1974). Brackish water is used to remould the OVP-clay to get the same structure. However, natural clays have a more random particle arrangement than remoulded clay. Changes in orientation of the particles are therefore potentially larger in natural clays than in the more dispersed packed remoulded clays (Le et al., 2012). Besides that, remoulded OVP-clay is mixed, while natural OVP-clay is more laminated in structure (Cheng et al., 2007). The vertical hydraulic conductivity will therefore be smaller in natural clays, because the hydraulic conductivity of a clay layer will be smaller than the mixture of several layers. This will influence the consolidation time and the pore water pressure during $K_0$-CRS tests.

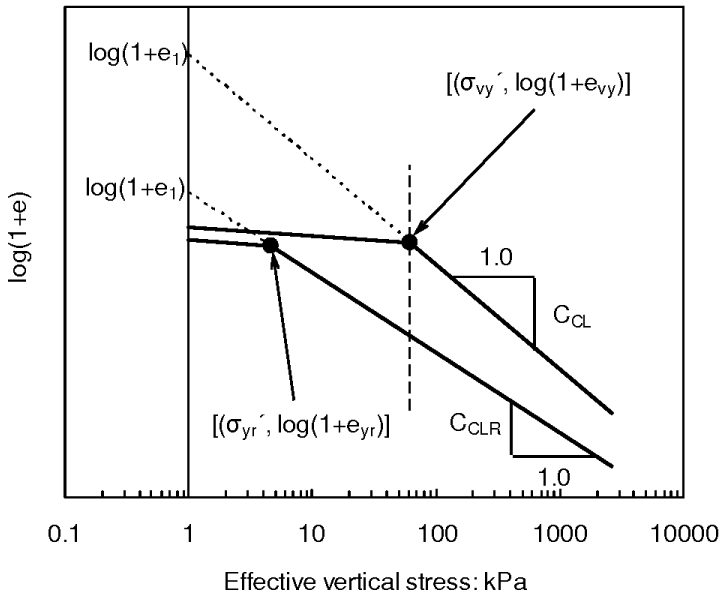


**Figure 16: Remoulded and natural clays (Hong, Zeng, Cui, Cai, & Lin, 2012). The natural soil has a higher yield stress and is less stiff in the post-yield phase**

The difference in compression behaviour of natural and remoulded clays is described and summarized in a paper called “Compression behaviour of natural and reconstituted clays” (Hong et al., 2012). Figure 16 shows typical differences in natural and a remoulded effective stress – void ratio relations. The void ratio is lower at 1 kPa for the remoulded clay, although the water content is equal after preparation of the sample. This has to do with the larger resistance against deformation of natural clays, which is caused by aging processes (Gasparre & Coop, 2008). Figure 16 shows after the yield stress a lower stiffness for the natural clay than for the remoulded clay. As mentioned in Section 3.1.1, remoulded clays are in a more dispersed, higher packed state, which results in a lower creep rate (Le et al., 2012).

Some studies state that in post-yield conditions, the stiffness of the originally better structured and more bonded soil is lower (Burland, 1990; Xu & Zhang, 2018). Burland (1990) relates this further to the macro and micro structure, in which structure is a definition for the combination of fabric and interparticle bonding. Aging in test facilities could change the soil with its 'intrinsic soil properties[3]' towards a simulated natural, better structured state. The compression line of reconstituted clay with its intrinsic properties is called an Intrinsic Compression Line (ICL). Natural soils would have a higher yield stress and a lower stiffness, so at some point the clay will converge to its intrinsic compression line and behave like reconstituted clay (Figure 17). This behaviour looks like the behaviour of a soil that has been prone to cementation (Figure 15).

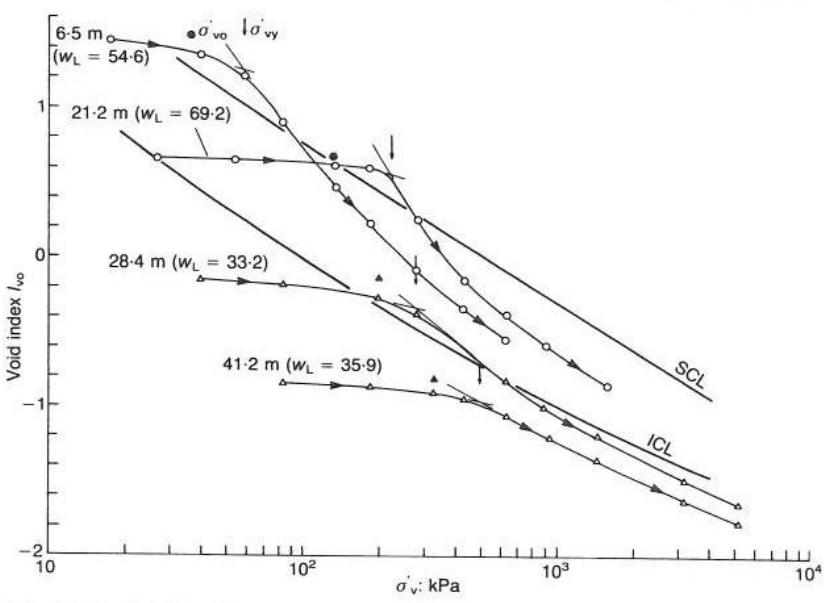


**Figure 17: The intrinsic compression line and natural soils (Burland, 1990)**

[3] Properties of reconstituted clays with a certain water content (Burland 1990)

## 3.4 Confining stresses in plain strain conditions

Differences in developed lateral stresses could result in differences in soil behaviour. The soil stays in $K_0$-conditions[4] during creep in the three-dimensional PLAXIS Soft Soil Creep model. One of the goals of the $K_0$-CRS tests is to check whether the lateral stresses increase during creep. Horizontal stresses are measured to obtain those developments.

The coefficient of earth pressure at rest can be calculated by dividing the horizontal stress over the vertical stress in plain strain conditions.

$$K_0 = \frac{\sigma_h{}'}{\sigma_v{}'}$$

$K_0$ in normally consolidated conditions can be estimated based on the internal friction angle (ϕ') of the soil (Jaky, 1944).

$$K_{0,NC} \approx 1 - \sin\varphi'$$

A low $K_{0,NC}$ value of 0.35 was obtained for the slightly organic OVP-clay (Den Haan, 2003) and 0.35-0.40 for the highly organic OVP-clay (Zwanenburg et al., 2018) with $K_0$-CRS equipment.

$K_0$ in overconsolidated soils can be estimated based on the OCR and the internal friction angle (ϕ') (Mayne & Kulhawy, 1982).

$$K_{0,\mathrm{OC}} \approx (1 - \sin\varphi') * \mathrm{OCR}^{\sin\varphi'} \approx K_{0,\mathrm{NC}} * \mathrm{OCR}^{\sin\varphi'}$$

The mathematical formulation below shows how the OCR increases in time according to the abc-model (Section 2.3).

$$\mathrm{OCR} = \frac{\sigma_p}{\sigma'} = \left(\frac{\theta_1}{\theta_0}\right)^{\frac{c}{b-a}}$$

It is debatable if this creep OCR can be used to calculate the increase in $K_0$. Hanzawa and Kishida (1981) suggested that the $K_0$ value was independent of the OCR induced by creep and chemical bonding: they found that the $K_0$ value of soils prone to creep was similar to values in normally consolidated soils (Hanzawa & Kishida, 1981). Mesri and Castro (1987) concluded based on triaxial tests that the lateral stresses increase during creep. They have linked the increase in $K_0$ to Bjerrum's isotach parameters, resulting in the following mathematical formulation for lateral stress development (Mesri & Castro, 1987)**:**

$$K_{0,\mathrm{OC}} \approx K_{0,\mathrm{NC}} * \left(\frac{t}{t_0}\right)^{\left(\frac{c_\alpha/c_c}{1-c_r/c_c}\right) * \sin\varphi'}$$

They concluded that the measured $K_0$ values in several Holocene clays were in line with their geological age of about 10,000 years.

[4] $K_0$-conditions are defined as the ratio between horizontal and vertical stresses, see Section 2.4

# 4. Methodology

The topic of this chapter is the determination of the input parameters for the abc-model. Creep strain and the development of the yield stress can be predicted based on those parameters. The parameters indicate that the model is applicable if they are consistent over the tests.

## 4.1 $K_0$-CRS tests

$K_0$-CRS tests measure the total stress, pore water pressure and lateral stresses as response to an applied constant rate of displacement. This makes it possible to determine stiffness parameters and permeability in one relatively short test. A cylindrical sample with a height of 20 mm and a diameter of 63 mm is put on top of a porous stone as shown in Figure 18**.** A constant rate of displacement is applied from the bottom on the soil specimen. This pushes the soil against a porous stone and the top cap on the top of the soil. This top cap pushes against a piston which is connected to a load cell (Figure 19). This load cell measures the force that is applied on the sample. At the bottom of the sample the pore water pressure is measured, while the horizontal (also named lateral stresses) are measured around one third from the bottom of the sample.

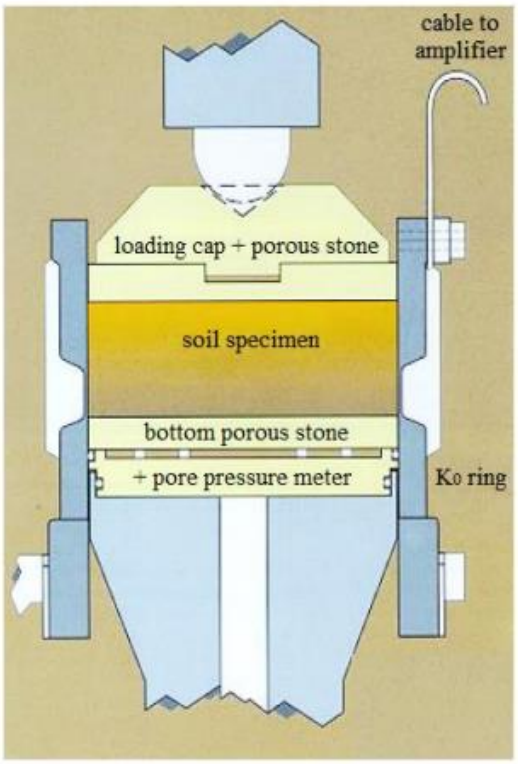


Figure 18: Schematization of the $K_0$-CRS test setup (Houkes, 2016)

In Constant Rate of Strain (CRS) tests not the rate of strain is constant, but the rate of displacement. This becomes important at large strains: a constant rate of strain if the soil is half of its initial height should be half of the initial strain rate, while a constant displacement rate neglects this decrease in initial height. The difference is small for the applied strains in the performed test.

In Section 5.4 will be shown that a yield stress should always be obtained with respect to a known isotach. If the isotach is unknown, not only the yield stress has no reference, also the creep parameter cannot be obtained as the intrinsic time is unknown (Section 2.3). The soil is

automatically on an isotach in normal consolidated conditions with a constant rate of strain: An isotach is an equal creep strain line. Assuming that the direct strain parameter is constant along an isotach, the creep parameter will be constant as well.

A constant rate of displacement can be imposed in a triaxial test as well. It is possible to allow almost no displacement in lateral direction with triaxial tests (Mesri & Castro, 1987), which makes it possible to simulate $K_0$-CRS tests. It would also be possible to do the test with different imposed coefficients of earth pressure at rest. This would make it possible to verify the shape of the yield surface after aging. However, the tests are expensive and the test setups were not available in a climate room. The latter is important for creep tests: temperature influences creep strains significant.

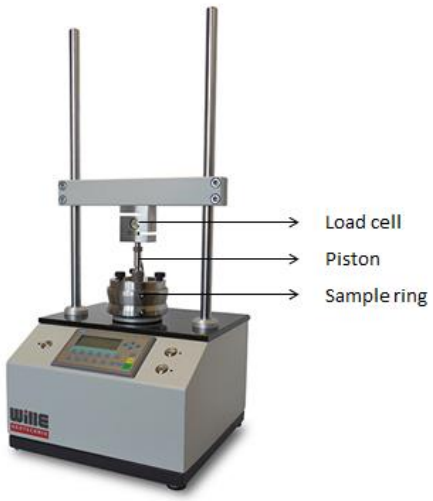


Figure 19: CRS test set up (Wille Geotechnik)

### 4.1.1 Displacement rate

Choosing a rate of displacement is a combination of the recommendations from regulations (Ozer, Lawton, & Bartlett, 2012) and experience with the material and the test setup. The suitable rate of displacement for the OVP-clay is 0.036 mm/hour. It is not too fast to generate water pressures above 10% of the total stress, but high enough to determine the consolidation coefficient based on the test (Zwanenburg et al., 2018). The consolidation coefficient is off topic for this thesis, while normally this is one of the important parameters determined based on $K_0$-CRS test results.

### 4.1.2 Ring friction

Due to friction between the ring and the soil, a part of the stresses is not applied on the samples but on the ring around the samples. Based on CRS test with a load cell under and above the ring was concluded that the ring friction was only 5% of the stress at 30% axial strain and less for smaller strains (Tigchelaar, 2001). The low lateral stress coefficient of the soil in combination with the low friction coefficient of the ring, results in low friction stresses at the boundaries of the sample and therefore an almost uniform stress distribution over the sample. However, when $K_0$ increases, the ring friction increases as well. Note that the load cell registers the stress at the top of the sample while the displacement is applied on the bottom: The ring friction will not be registered and its exact height is not important for the goals of this thesis.

### 4.1.3 Lateral stresses

The yield stress is a one-dimensional parameter in plain-strain conditions. If the soil is not in its $K_0$ conditions during aging, a yield surface is needed to indicate the transition from overconsolidated to normal consolidated behaviour. To indicate the yield surface, not only the principal direction, but also the lateral direction is needed. The Cam-Clay p' – q axis are used, see Section 2.4.

The aforementioned $K_0$-ring is a ring that needs very small displacements to measure the forces in lateral direction. The displacements are in the order of $40*10^{-3}$ mm at 800 kPa (Gareau, Molenkamp, & Sharma, 2006). The volume change in lateral direction is therefore neglected**.** Figure 20 illustrates the mechanism.

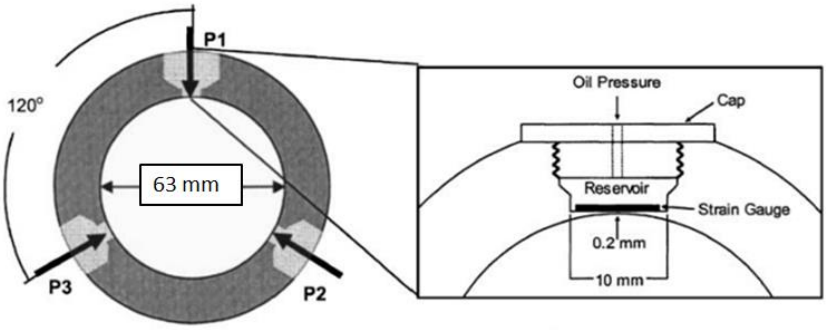


Figure 20: The $K_0$-ring (Gareau et al., 2006)

The $K_0$-ring measures the lateral pressure on three places on the side of the sample. The initial height of the sample is 20 mm and the maximum displacement is smaller than 25%. The strain gauges are placed below half of the sample height, so compression will not disturb the measurements of the $K_0$-ring. It is known that the measurements of this ring are showing stick and slip behaviour, especially at low stresses.

### 4.1.4 Sample preparation

The samples are cut out of a block that is preserved for around a year in a climate room. The clay is wrapped up in plastic so no water can escape from the material. Slices are cut off from the block and four samples can be made from each slice. The samples are cut into a 20mm high ring with a diameter of 63 mm. The height of the sample could be slightly smaller, but would not be larger than this 20 mm. After measuring the weight of the sample and ring, the sample is wrapped in foil. The samples are built into the test setup (Figure 18) as follows.

- The $K_0$-CRS samples are pushed into the $K_0$-ring, which is placed in the CRS machine. To make sure no water is trapped on the bottom of the sample, water is allowed to escape at the place where the water pressure is measured. Meanwhile the ring is filled with water.
- The CRS samples stay in the ring and are placed in the CRS machines. Water is added and the test can be started.

### 4.1.5 General test plan

The test is divided in three parts:

1. Loading to the isotach
2. Development of the yield stress
3. The sample is brought back on the isotach

The isotach is assumed to be reached at 75 kPa with the chosen displacement rate. This assumption is based on $K_0$-CRS tests on the same soil with the same pre-consolidation pressure (Zwanenburg et al., 2018).

A yield stress is developed for each sample in one of the four ways as described below and summarized in Table 5 (Chapter 5). One sample (sample 19) is used as reference: the piston is displaced until 125 kPa before creating a yield stress.

- Unloading. A mechanical yield stress is created by unloading the soil. The pressure is reduced with the same displacement rate as the sample has been loaded. Directly after unloading, reloading starts with the same displacement rate as used before.
- Aging. The development of an OCR under a constant effective stress is called aging. The stress is held constant by adapting the displacement rate.
- Relaxation, a constant height for a certain time. Den Haan and Kamao (2003) suggested calculating the creep parameter based on the relaxation phase of a soil. Hypothesised is that this inverse way of measuring the creep rate could result in another type of structure than the structure of a soil with a mechanical or aged OCR.
- Repeated loading. Some studies indicate that loading cycles result in softer behaviour of the clay (Fujiwara et al., 1987) and therefore faster creep aging. In some preliminary performed simulations with the PLAXIS Soft Soil Creep model, this is not the case: less creep is simulated than normal due to the lower effective stress on average.

The stress-strain position is brought back from the overconsolidated position. Displacement goes further along the isotach. Expected is that the isotach in the last step will be the same as the one in the first step.

## 4.2 Void ratio

Stress – void ratio relations of the $K_0$-CRS tests give an indication of the applicability of the isotach models. Results of $K_0$-CRS tests are often presented in stress-strain diagrams, as the abc-parameters are calculated based on strains. Strains are neglecting initial conditions of the samples like porosity and degree of saturation. Based on the void ratio initial conditions are taken into account. Figure 21 is an illustration of expected soil behaviour in compression of one soil with different initial void ratios based on strains (a) and void ratio (b).

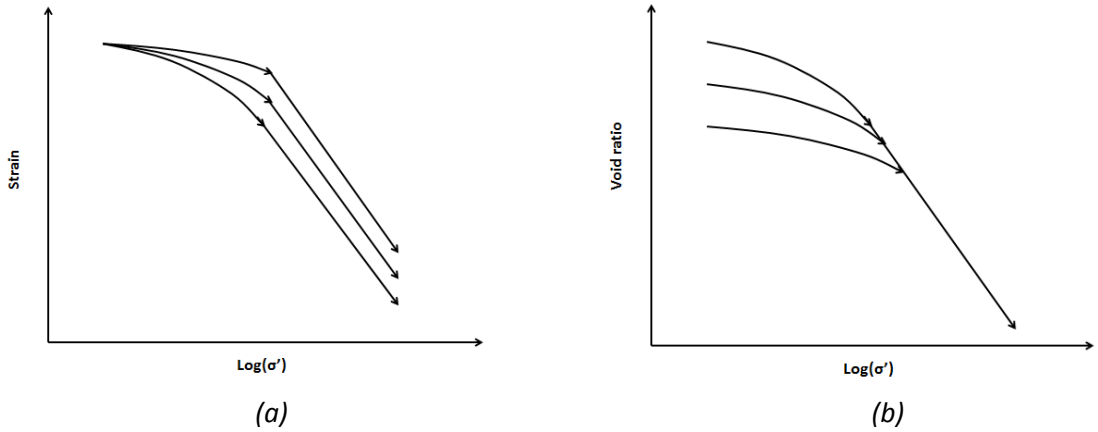


Figure 21: Stress-strain (a) and stress-void ratio (b) relation of the same soil with different initial conditions

There are several ways to determine the initial void ratio. For all the methods the specific gravity of the soil is needed. The specific gravity ($G_s$) is determined for every sample in the laboratory. This soil property is the density of the particles divided by the density of water. A pycnometer is used to calculate the unit weight of the OVP-clay particles (NEN-EN-ISO 17892-3:2016) and the density of water is assumed to be equal to 1 g/cm$^3$.

**1. Dry weight and total theoretical volume of the sample**

The volume of the particles can be determined based on the specific density and the dry weight of the sample. The theoretical volume of the sample minus the particle volume gives the volume of the pores. The volume of the particles over the volume of the pores is the initial void ratio. Assumed is that the sample volume is equal to the theoretical volume of the sample and that the soil is completely saturated.

**2. Water content after test and obtained strain after test**

Based on the specific density and the water content after the test, the void ratio after the test can be determined. The theoretical initial height minus the recorded height after the test divided by the dry weight results in the void ratio that is lost during the test. The void ratio after the test plus the void ratio that is lost, gives the initial void ratio. Assumed is than that the sample volume is equal to the theoretical volume of the sample. Small deviations in initial height could result in differences in initial void ratios.

**3. Water content after test and mechanical measured height after test**

The void ratio after the test is determined in the same way as method 2. The theoretical initial height minus the height after the test (measured by the lab technicians) divided by the dry weight of the soil results in the void ratio that is lost during the test. The void ratio after the test plus the void ratio that is lost, gives the initial void ratio. The height of the sample and the water content after the test could be affected by swelling after the piston of the K0-CRS device is removed. This method takes this change into account. Assumed is than that the sample volume is equal to the theoretical volume of the sample. The potential error in the calculated void ratio is larger than the error of method 2: an extra measurement error appears from the measurement accuracy with which the height of the sample is measured.

## 4.3 Determination of a, b and c parameter

The determination of Den Haan's abc-parameters is not entirely straight forward and easy. Aljouni (2000) stated in his PhD thesis that "the process of obtaining b and c is very complicated and unclear" for highly organic materials. According to this PhD thesis, it is an optimization process of data fitting based on trial error and interpolation (Aljouni, 2000). A clarifying paper called "Obtaining isotach parameters from a CRS $K_0$-Oedometer" was published a few years later (Den Haan & Kamao, 2003). The paper analysis results of $K_0$-CRS tests on OVP-clay.

The b-parameter can be found based on the imposed isotach.

$$b = \frac{\Delta\varepsilon}{\Delta\ln(\sigma)}$$

Note that the stress is a total stress, which is almost the same as the effective stress with low pore water pressures. The b-parameter can be seen as a product of the direct strain parameter (a-parameter) and the creep parameter (c-parameter). Although it is conceptually hard to understand the physical meaning of the direct strain parameter, it is easy to obtain the parameter based on an unloading-reloading phase: the mean of the unloading and reloading strain divided by the natural logarithm of the decrease in stress. Appendix G shows that the parameter obtained in this way is depending on how far the soil is unloaded.

$$a = \frac{\Delta\varepsilon_{unloading-reloading}}{\Delta\ln(\sigma)}$$

A more precise approach is the change in strain rate divided by the change in stress rate, times the stress in the soil just after a change in displacement rate. If the time step is chosen small enough, the creep rate will be negligible with respect to the direct strain parameter.

$$a = \frac{\Delta\, {}^{\delta\varepsilon}/_{\delta t}}{\Delta\, {}^{\delta\sigma}/_{\delta t}} * \sigma$$

The creep parameter can be obtained in the following two ways according to Den Haan and Kamao (2003): a constant effective stress phase and a relaxation phase. The most obvious way to determine c is keeping the CRS device on a constant stress level for some time. That results in the following expression for c, in which θ is the intrinsic time:

$$c = \frac{\Delta\varepsilon}{-\Delta\ln({}^{\delta\varepsilon}/_{\delta\theta})}$$

This method is questioned by Den Haan & Kamao, 2003. They stated that the control system is not good enough to keep a constant stress in the soil, the pore water pressure would vary during the test and the ring friction is unknown during such a constant stress phase. The varying pore water pressure and the imperfect strain-controlled constant effective stress are related. With new control systems it is possible to keep the soil almost at a constant stress level. This is shown in Appendix D. The height of the ring friction is taken into account as explained in Section 4.1.2: The system measures the stress in the sample and keeps the stress level constant, even if the ring friction increases.

A relaxation phase can also be used to obtain the creep parameter. This method assumes that relaxation is the inverse behaviour of creep. The height of the sample is kept constant for 16 hours. Under the decreasing stress level, the soil creeps without changing its volume. When the decrease of the stress is fitted against the intrinsic relaxation time, a fit can be made based on the following mathematical formulation (Den Haan & Kamao, 2003):

$$\sigma_v{}' = \sigma_{vR}{}' \left( 1 - \frac{b-a}{c} * \frac{d\sigma_{vR}{}'/dt}{\sigma_{vR}{}'} * \theta \right)^{-\frac{c}{b-a}}$$

Assuming that the parameters for direct strain and the isotach parameter are known, the creep parameter can be obtained by fitting to a certain dataset.

The c-parameter is equal to the creep strain rate at the reference isotach (Section 2.3). Both the reference isotach and the c-parameter are unknown. The displacement rate can be related to the reference isotach if the c-parameter is known (Section 5.3.2). An iterative process is needed to get the c-parameter and the intrinsic time between the imposed and reference isotach (Section 5.2.3 and Section 5.3.2). This illustrates the difficulty in abc-parameter determination.

## 4.4 Determination of the yield stress

The yield stress is a point on the yield surface in plain-strain conditions. There are several methods to determine the yield stress. A comparison between methods to determine the yield stress is not part of the thesis. For a review is referred to Gorzic, Lunne and Pande (2003). The choice is made for the well-known and easy to use Casagrande method. There is a broad experience of working with this method, although the method is particular sensitive for drawing inaccuracies.

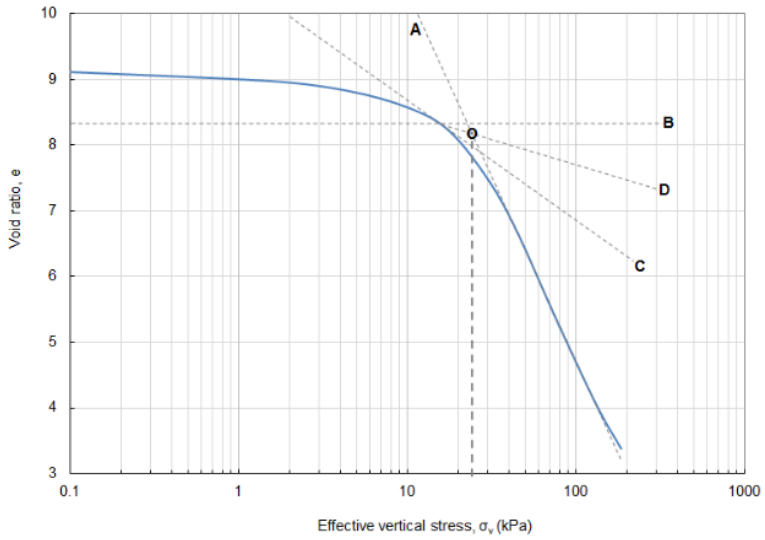


Figure 22: The Casagrande method to determine the yield stress (Houkes, 2016)

Figure 22 shows an effective stress – void ratio graph with the four lines needed to obtain the yield stress.

A. Line A is the isotach for which the yield stress is determined. Another displacement rate leads to another stress – void ratio relation.
B. Line B is a line through the void ratio at which the curvature of the obtained stress – void ratio is at its maximum.
C. A tangent line at the maximum curvature is drawn.
D. A bisector is drawn.

The intersection between A and D is called the yield stress. The Casagrande method gives generally consistent results if there is a well-defined transition from overconsolidated to normal consolidated behaviour (Grozic, Lunne, & Pande, 2003). Note that this is often not the case for remoulded soils (Burland, 1990). Besides that, stiff soils like silty clays have in general a gradual transition from overconsolidated to normal consolidated behaviour (Gasparre & Coop, 2008).

# 5. Results tests

22 Constant Rate of Strain (CRS) tests are performed on OVP-clay in a climate chamber with a constant temperature of 10 degrees Celsius. 16 tests gave useful results on yield stresses and abc-parameters. Eight out of ten CRS tests with $K_0$-ring gave useful lateral stresses measurements. Table 5 shows the programs of the tests. The tests with the samples indicated in green are the tests with lateral stress measurements. The tests indicated with orange have no lateral stress measurements. The tests indicated in red are not used in the analyses. Appendix A explains why some of the tests are not used. The most important reasons are a power failure (e.g. sample 7, 15) and computer updates (e.g. sample 7, 21 and 22).

Table 5: Overview performed tests

| Sample | Machine | Program 75 kPa | Program 125 kPa |
|---|---|---|---|
| 1 | 1 | 1 day relaxation | |
| 2 | 2 | Unloading reloading | Unloading reloading |
| 3 | 3 | Unloading reloading | Unloading reloading |
| 4 | 4 | 1 day relaxation | |
| 5 | 2 | 1 day aging | |
| 6 | 1 | 1 day aging | |
| 7 | 4 | 50 days aging | |
| 8 | 2 | 10 days aging | |
| 9 | 1 | Unloading reloading | Unloading reloading |
| 10 | 1 | 10 times 70-75 kPa | |
| 11 | 3 | 1.7 days aging | |
| 12 | 1 | 10 times 65-75 kPa | |
| 13 | 3 | 10 days aging | |
| 14 | 2 | 10 days aging | |
| 15 | 1 | 30 days aging | |
| 16 | 1 | 30 days aging | |
| 17 | 3 | Repeated loading | |
| 18 | 3 | 10 times 70-75 kPa | |
| 19 | 1 | Reference 75 kPa | 1 day aging |
| 20 | 3 | 10 times 72.5-77.5 kPa | |
| 21 | 3 | 10 times 70-80 kPa | Relaxation |
| 22 | 2 | Reference 75 kPa | 1 day aging |

## 5.1 Void ratio

Section 4.2 describes the methods that can be used to determine the void ratio. The void ratio is used to validate if the soil can be modelled with isotach models. All the methods to determine the initial void ratio use the specific gravity of the soil. The obtained average specific gravity is 2.31 with a coefficient of variation over 22 samples smaller than 1%. Appendix B shows the results.

The described methods are compared with the ideal isotach behaviour as shown in Figure 23**.** This perfect isotach behaviour of samples from one block remoulded clay has typically a small range of initial void ratios and the stress converges to an imposed isotach. Figure 24 on the next page shows (a) the method based on the obtained strain at the end of the test, (b) the results for the dry weight method and (c) the method based on the measured height after the test.

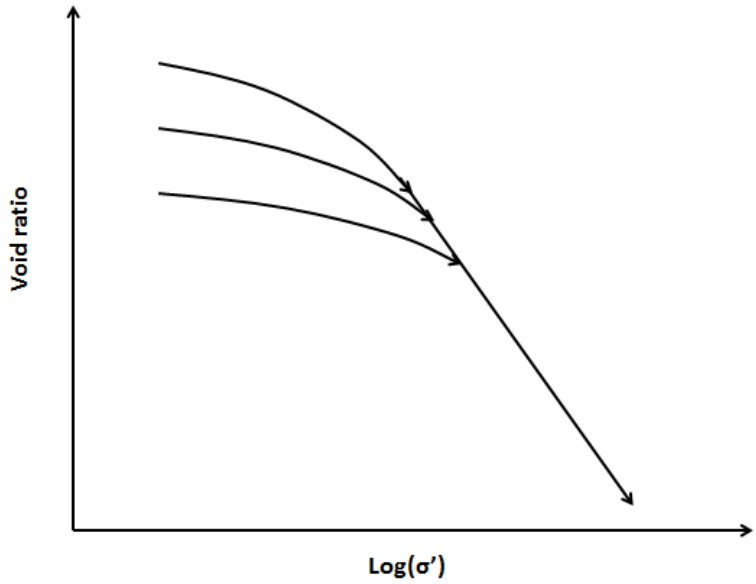


Figure 23: Ideal isotach behaviour in which there is a unique stress-void ratio relation

The best way to determine the initial void ratio is based on water content after test and obtained strain (a). The isotach behaviour of converging towards an isotach is best visible when the void ratio is determined based on this method. The found initial void ratios are between 2.70 and 2.85. The initial void ratios of method (b) are significant lower indicating that the soil is not completely saturated in initial conditions: the ratio between water content before and after the tests is small with respect to the amount of obtained strains. The potential error in calculating the void ratio is larger for method (c), as there is an extra measurement error in measuring the height of the sample after the test. The largest uncertainty for the methods is the initial height, which could be lower than the assumed 20.0 mm. The consequence of an initial height of 19.9 is given for one of the samples in Figure 24**.**

It is not clear if the soil behaves perfectly according the isotach models: there seems to be a range of relations between effective stress and void ratio. However, the error margin is larger than the obtained differences. As discussed in Section 3.1.3, the behaviour of 'transitional' soils is known for its non-unique stress-strain relation in normal consolidated conditions. The next section gives an overview on the parameters found with the $K_0$-CRS tests. The obtained ranges of the abc-parameters indicate the applicability of the model on the test material as well.

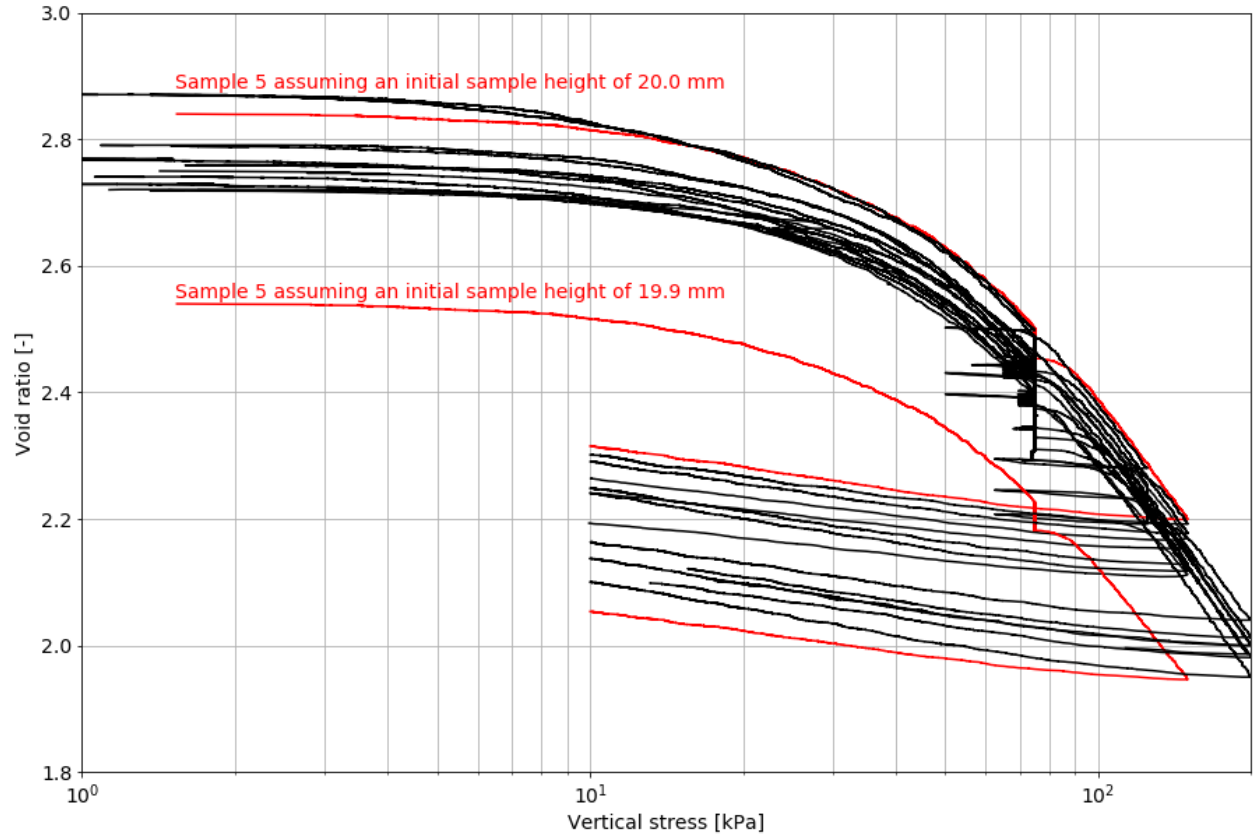


(a) Vertical stress – void ratio relation based on water content after test and obtained strain. The estimated maximum error in initial yield stress is around 0.3 and is indicated for one of the samples

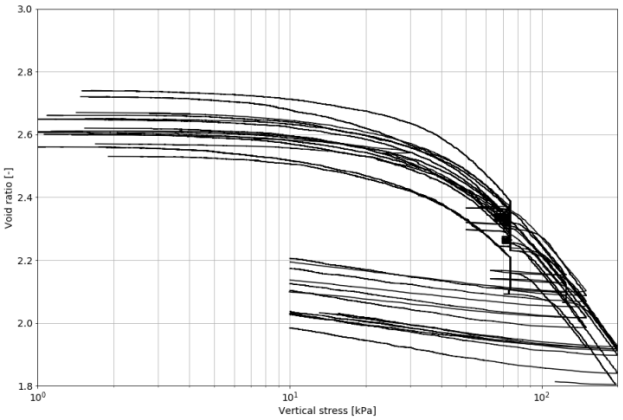


(b) Vertical stress – void ratio relation based on water content before test. This assumes that the clay samples are completely saturated, which is not the case

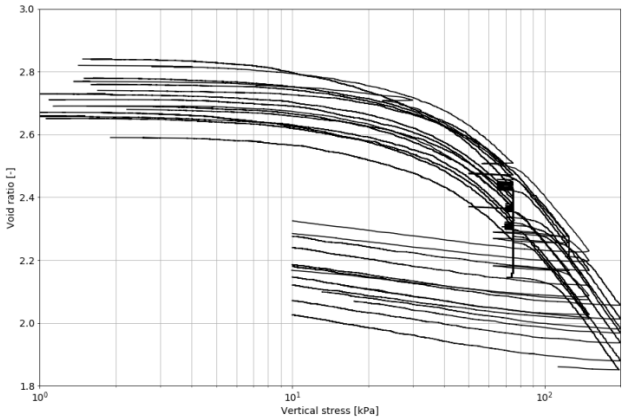


(c) Vertical stress – void ratio relation based on water content and measured height after test. The maximum error in the yield stress is twice as large as based on method (a)

**Figure 24: Comparison of three possible ways to determine the initial void ratio**

## 5.2 abc-parameters

Chapter 4 explains how the abc-parameters are determined. The obtained parameters are compared with the reported parameters on the same clay (Zwanenburg et al., 2018). The obtained virgin compression, direct strain and creep parameter are discussed.

### 5.2.1 Virgin compression

The virgin compression parameter of the abc-model is called b. The parameter can be called the isotach parameter: this parameter times the natural logarithm of the vertical effective stress gives a line at which the creep strains in time are constant. Table 6 gives the local b values around the presented stresses.

**Table 6: b-parameter around the presented vertical stresses. The character A represents Aging, UR Unloading-Reloading, R Relaxation and RL Repeated Loading.**

| | Stress [kPa] | 72.5 | 90 | 100 | 120 | 130 | 140 | 160 | 185 |
|---|---|---|---|---|---|---|---|---|---|
| **Reference** | **19** | 0.09 | 0.12 | 0.13 | 0.14 | A | A | 0.14 | 0.15 |
| **UR** | **2** | 0.10 | 0.10 | 0.13 | 0.13 | UR | 0.13 | | |
| **UR** | **3** | 0.10 | 0.11 | 0.12 | 0.12 | UR | 0.12 | | |
| **UR** | **9** | 0.09 | 0.12 | 0.13 | 0.14 | UR | 0.14 | | |
| **R** | **4** | 0.09 | R | R | 0.13 | 0.13 | 0.14 | | |
| **A 1 day** | **5** | 0.11 | A | 0.13 | 0.14 | 0.16 | 0.15 | | |
| **A 1 day** | **6** | 0.11 | A | 0.13 | 0.14 | 0.15 | 0.15 | | |
| **A 1.7 days** | **11** | 0.11 | A | A | 0.15 | 0.15 | 0.16 | | |
| **A 10 days** | **8** | 0.11 | A | A | 0.12 | 0.15 | 0.16 | 0.15 | 0.17 |
| **A 10 days** | **13** | 0.12 | A | A | 0.15 | 0.15 | 0.16 | | |
| **A 20 days** | **14** | 0.11 | A | A | 0.12 | 0.16 | 0.15 | 0.17 | 0.17 |
| **A 30 days** | **16** | 0.09 | A | A | A | 0.15 | 0.15 | 0.17 | 0.17 |
| **RL** | **10** | 0.10 | RL | 0.13 | 0.15 | 0.15 | 0.14 | 0.16 | 0.16 |
| **RL** | **12** | 0.10 | RL | 0.14 | 0.14 | 0.14 | 0.15 | 0.16 | 0.16 |
| **RL** | **18** | 0.12 | RL | 0.13 | 0.14 | 0.16 | 0.16 | 0.16 | 0.17 |
| **RL** | **20** | 0.10 | RL | 0.11 | 0.14 | 0.11 | 0.14 | 0.15 | 0.15 |

From Table 6 can be concluded that the transition from overconsolidated to normal consolidated is gradual for the tested material. The virgin compression parameter (b) will be around 0.11 during aging at 75 kPa. The low values for the Unloading-Reloading graphs and for sample 19 at 140 kPa could have to do with the gradual transition from stiff, almost elastic to visco-plastic behaviour. Another cause could be the difference in structure with less macro-pore volume than aged samples. The Repeated Loading samples are slightly stiffer (lower b value) in its post yield stage than the Aged samples.

### 5.2.2 Direct strain parameter

Table 7 shows the direct strain parameter as obtained in three unloading-reloading tests. The direct strain parameter at 75 kPa is unexpected high with respect to the other obtained parameters. The first part of test 9 showed unexpected high horizontal stresses as well. There is chosen to work with a direct strain parameter of 0.013 as it is the average of the measured values of the two more reliable tests and the same value is found in literature. The higher a-parameters at 125 kPa with respect to the 75 kPa a-parameters are caused by a higher created OCR. The a-value is also influenced by the natural strain level at which the unloading-reloading phase is performed.

Table 7: Values a-parameter

| Samples | | 75 kPa | | 125 kPa | | 160 kPa | |
|---|---|---|---|---|---|---|---|
| # | Machine | a | OCR | a | OCR | A | OCR |
| 2 | 2 (K0-CRS) | 0.011 | 1.5 | 0.019 | 2.0 | | |
| 3 | 3 (CRS) | 0.015 | 1.5 | 0.016 | 2.0 | | |
| 9 | 1 (K0-CRS) | 0.064 | 1.5 | 0.018 | 2.0 | | |
| *CRS1 | | | | | | 0.013 | 2.0 |
| *CRS13 | | | | | | 0.013 | 2.0 |

*Test with conventional $K_0$-CRS equipment on the same material gave the following values (Zwanenburg et al., 2018)

### 5.2.3 Creep parameter

Calculating the creep parameter as suggeted in Section 4.3 did not result in consistent values. The calculated values based on an aging phase are strongly depending on the chosen time span at which the derivative of strain to time is calculated. The fit through the decrease in stress during relaxation is neither succesfull. Appendix C shows the results.

The range of creep strains at a given time is much smaller than the range of calculated creep parameters. Figure 25 **g**ives the strains in time for the eight aging stages at 75 kPa. By plotting the logaritmic trendlines of four samples that have aged for more than one day, a clear time-dependent strain relation is found. An iterative calculation resulted in a creep parameter of 0.00635. This c-parameter corresponds to an imposed isotach of 0.15 days (Section 5.3.2). Therefore the strains after one day aging are plotted at a reference time of 1.15. The trendline is formulated as follows:

$$creep\ strain\ = creep\ parameter * \ln(time\ [days]) + strain\ at\ reference\ isotache$$

The plotted data is selected from a continue data range and can be found in Appendix E**.**

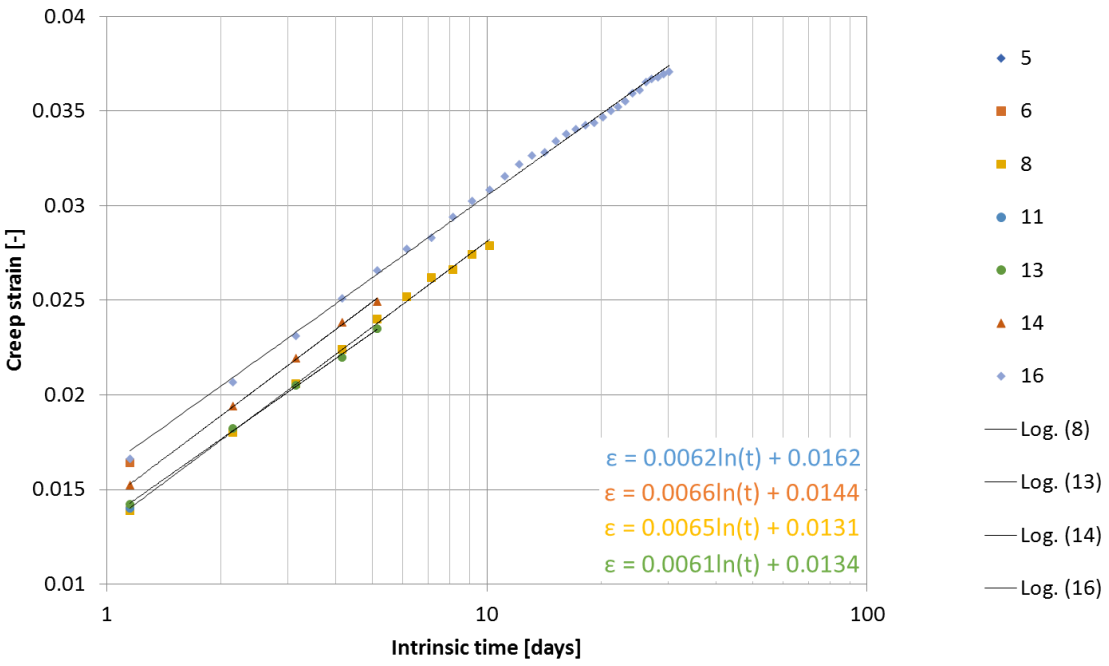


Figure 25: Creep strains plotted as function of the intrinsic time

With a creep parameter of 0.00635, the expected creep strain at the reference isotach would be:

$$\varepsilon = 0.00635 * \ln(0.15) = -0.012$$

During the first 0.85 day (one day reference isotach - 0.15 day isotach), the creep strain is on average 0.0023 to large. This is 120% of the creep strain that would be calculated with the obtained c-parameter. Therefore is concluded that it is better to work with an aging or relaxation phase of more than one day, to make sure that there is no excess pore water pressure in the soil.

The strains during repeated loading are not analysed further. They did not give consistent results with respect to time and strains. All repeated loading phases took shorter than one day. The first day of the aging tests did not give a consistent creep rate as well, so comparing the strains has no added value.

## 5.3 Yield stress

This section consists of two parts. The first part deals with a possible cause of overestimation of the yield stress. After that, predicted OCR's are compared with obtained OCR's.

### 5.3.1 Indications of development of structure

The vertical stress – natural strain of a one day aged sample (5) is compared with samples that have aged ten days (8) and 1.7 days (11). Figure 26 shows that the longer aging sample (8, green line) softens with respect to the shorter aged sample (5, orange line). When looked to a vertical stress – void ratio diagram, this phenomenon is less obvious as shown by Figure 27. But still, Figure 27 indicates that the one day aging sample gives a stiffer response in the post-yield phase than the longer aged samples.

The softer behaviour of the longer aged samples after aging could be interpreted as that structure is broken down and that the soil returns to its unique stress - void ratio relation (Burland, 1990) as explained in Section 3.3. If we hypothesise that the repeated loading samples can develop less structure than the aged samples, we can hypothesise that structure develops during aging: Table 7 showed a higher b-value for aged samples than for repeated loading samples and therefore the stiffness of the aged samples is lower in the phase after the transition zone. The significance of the hypothesised development of structure is small for the performed tests: we have seen that the differences in b-value are small.

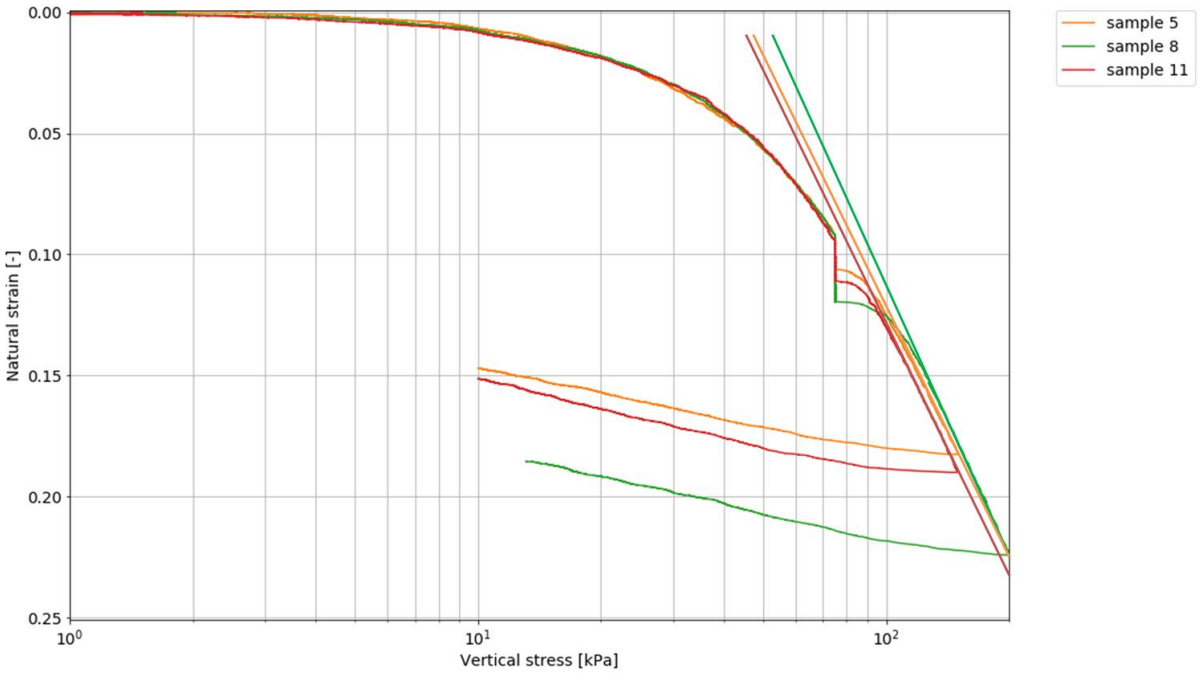


**Figure 26: Indication of development of structure in vertical stress – strain plots. Samples 5, 8, 11 are respectively aged one, ten and 1.7 days**

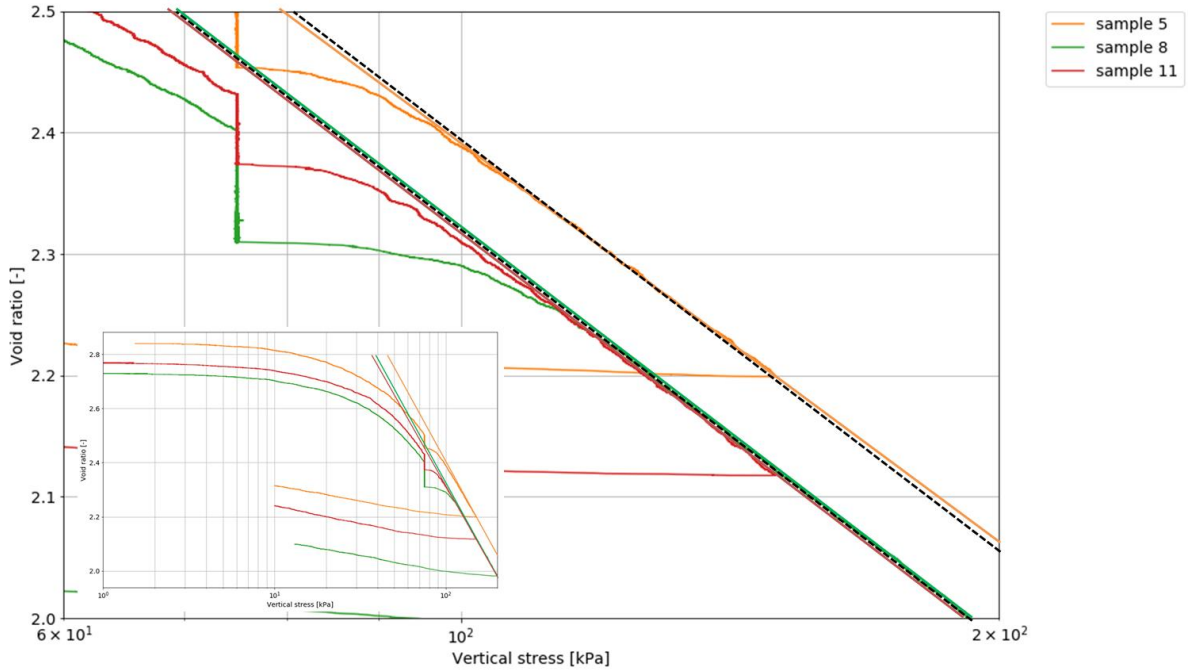


**Figure 27: Possible softening behaviour in stress – void ratio plots. The black dotted lines are parallel lines and the initial conditions are indicated in the subfigure. Sample 5 (orange) has a higher stiffness then samples 8 and 11 that aged longer.**

Figure 28 is the result of an analysis to determine abc-parameters and the yield stress in remoulded OVP-clay (Zwanenburg et al., 2018). It shows a change in stiffness: especially after the relaxation phase the stiffness of the soil decreases. To obtain the yield stress the red line is plotted which is fitted to the stiffness at the end of the tests after a relaxation phase. For this thesis, the blue line is plotted to obtain the yield stress. In that way eventual stress-dependency and aging effects on the stiffness are eliminated from the analyses. The estimation based on the blue line gives still a significant overestimation for this particular case, but is closer to the preconsolidation pressure of 40 kPa.

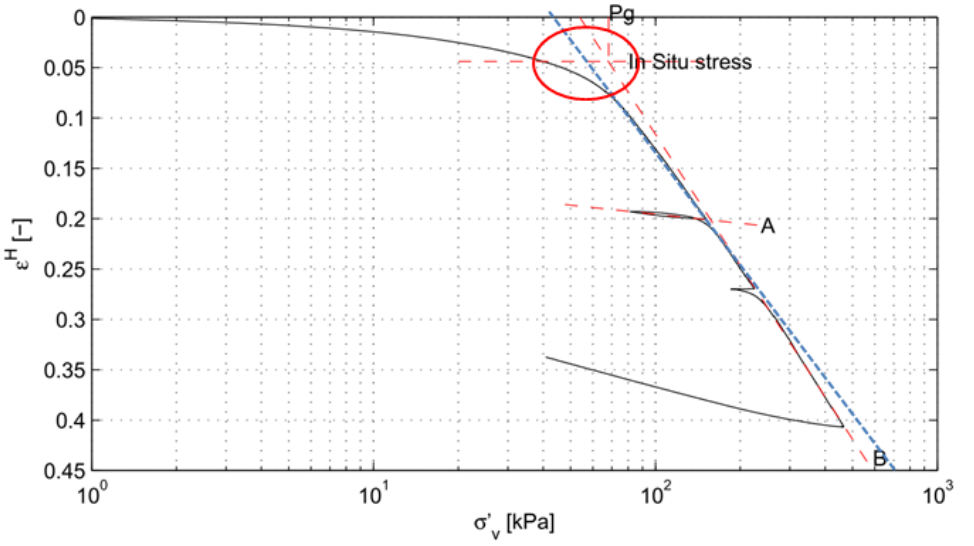


**Figure 28: Determination of the yield stress (Zwanenburg et al., 2018). The red line is the isotach normally used to determine the yield stress. The blue line is an alternative, resulting in a yield stress that is closer to the preconsolidation pressure for the tested soil.**

### 5.3.2 Comparison yield stresses data and model

Section 2.3 describes the expected development of the yield stress during aging. The mathematical formulation for the expected OCR with respect to the reference isotach is given below. The stiffness parameters are obtained in the previous section of this chapter.

$$OCR = \frac{\sigma_p}{\sigma_0'} = (\theta)^{\frac{c}{b-a}} = (\theta)^{\frac{0.00635}{0.11-0.013}} = t^{0.065}$$

This theoretical development of the OCR is compared with the OCR's created with the performed aging tests. The method of yield stress determination is described in Section 4.4.

The obtained OCR's of the aged samples and the repeated loaded samples[5] are shown in Figure 29. The yield stresses after aging of samples 5, 6, 8, 11, 13, 14, 16 and reference sample 19 are used. Figure 29 shows the fit through the aged samples in green. The predicted OCR based on the obtained abc-parameters is plotted in red.

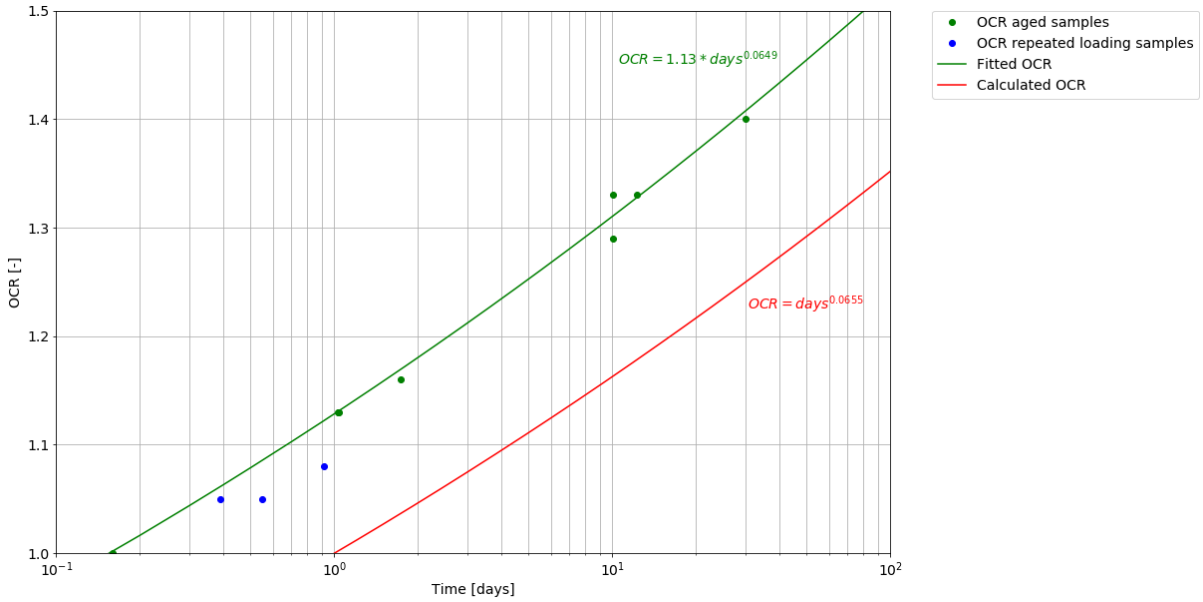


**Figure 29: Obtained OCR on 0.15 days isotach (green line) and predicted OCR on the reference isotach (red line).**

The obtained OCR is based on the isotach related to the displacement rate, while the calculated OCR is based on the one day (reference) isotach. This is illustrated in Figure 30: the green line illustrates the imposed isotach related to the displacement rate in the test. The red line is the reference isotach and the grey line is the 10 days isotach.

[5] As mentioned in Section 5.2.3, there is no consistency between time, strains and stress path in the repeated loading samples. This data is not used in the analysis.

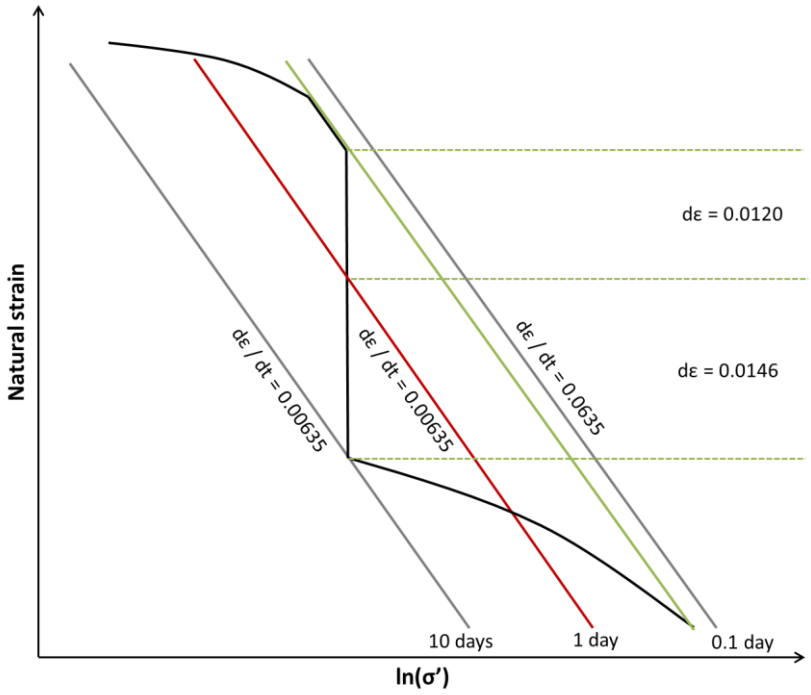


Figure 30: Aging and the reference isotach. The black line illustrates a 10 days aging test like sample 8 and how it is related to the imposed isotach in green, the reference isotach in red and the 10 days isotach in grey.

The imposed isotach is on the 0.15 day isotach. Note that this is depending on both the c-parameter and the displacement rate (dε/dt).

$$\theta = \frac{c}{d\varepsilon/dt} = \frac{0.00635}{0.036/20 * 24} = 0.15\ days$$

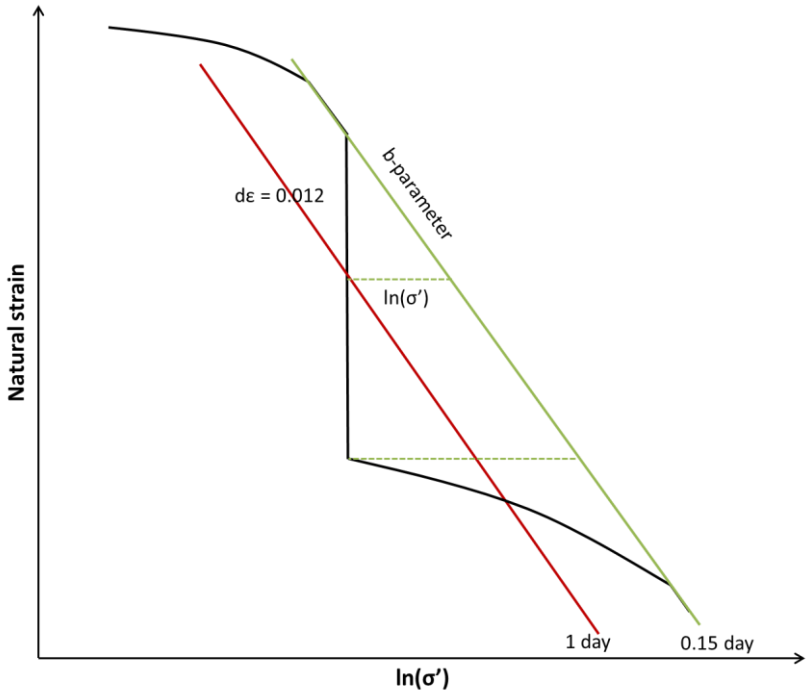


Figure 31: The stress relation between the reference (red) and the imposed (green) isotach

The shift between the one day isotach and the 0.15 isotach can be calculated with the obtained b parameter and the theoretical strain between the imposed and reference isotach (Figure 31).

$$\varepsilon = c * \ln(\theta) = |0.00635 * \ln(0.15)| = 0.012$$

The local b value is approximately 0.11:

$$\ln(\sigma') = \frac{\varepsilon}{b} = \frac{0.012}{0.11} = 0.109$$

The yield stress and the OCR are not related to the natural logarithm of the stress, but the stress itself, so:

$$e^{0.109} = 1.12$$

The same calculation is made based on the parameters from literature.

$$\theta = \frac{c}{d\varepsilon/dt} = \frac{0.012}{0.036/20 * 24} = 0.28\ days$$

$$\varepsilon = c * \ln(\theta) = |0.012 * \ln(0.28)| = 0.015$$

$$\ln(\sigma') = \frac{\varepsilon}{b} = \frac{0.015}{0.18} = 0.0833$$

$$e^{0.0833} = 1.09$$

Both calculated OCR and fitted OCR are plotted over 50 years in Figure 32. The calculated OCR based on data in literature (Zwanenburg et al. 2018) is plotted with the blue line. The reference OCR is multiplied by the factor calculated above**.** Note that normally the reference isotach is used to define the OCR, so the imposed OCR is divided by the calculated factor between the imposed and reference isotach.

From Section 3.3 can be concluded that the development of structure should result in higher yield stresses than expected from the model. According to that section, aging is not only a matter of creep, but of development of structure as well. It is hypothesized that the consequences of this phenomenon for the yield stress will become measurable when tests with longer aging times are performed. The measurement inaccuracies of the performed tests are much larger than the hypothesised increase in yield stress caused by the consequences of development of structure.

Note that the conclusions made in this section are based on tests performed in a climate room with strain-controlled constant stress phases. Changes in temperature and stress conditions could result in different creep strains.

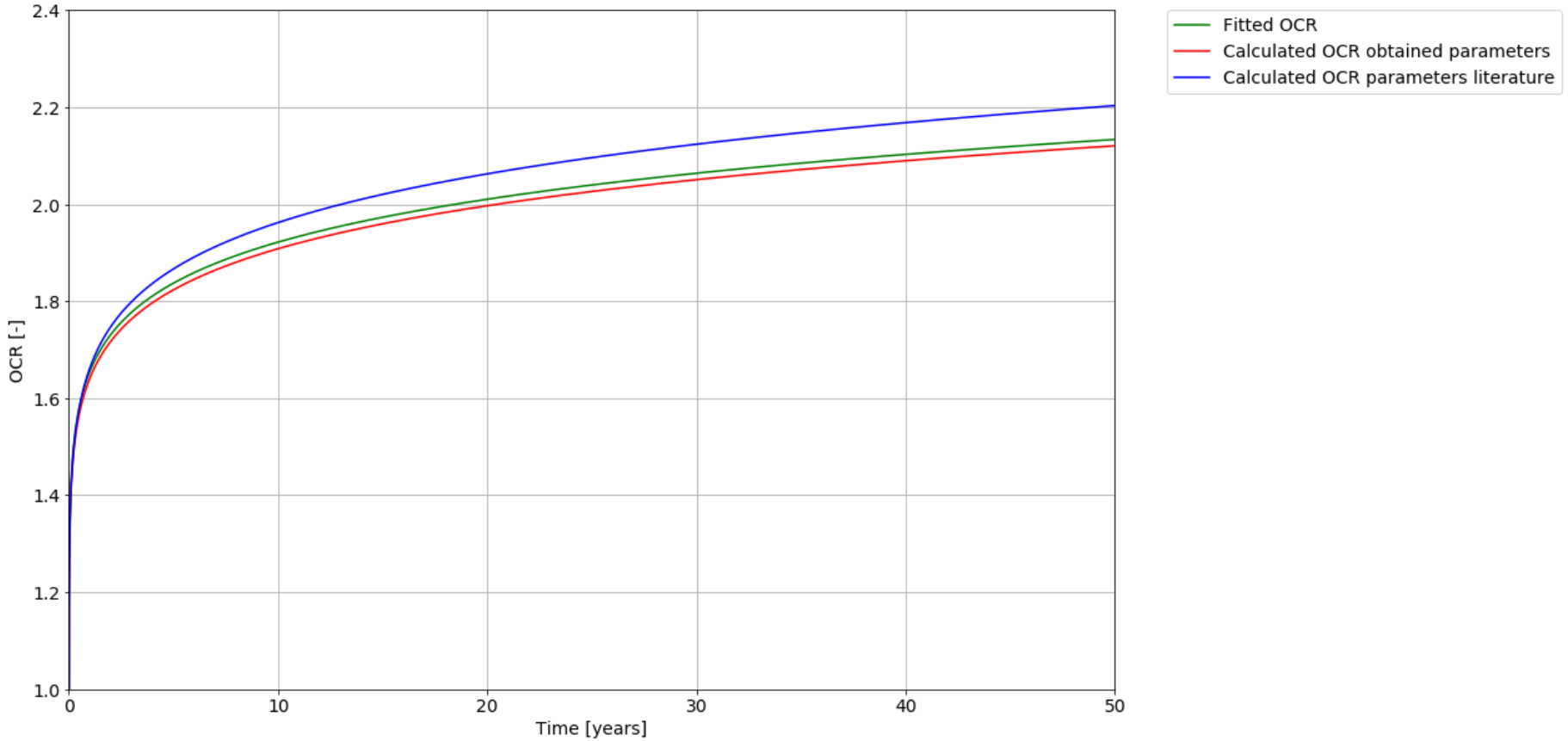


Figure 32: Predicted OCR in 50 years

$$Trendline\ obtained\ OCR = fitted\ OCR = 1.13 * t^{0.0649}$$

$$Calculated\ OCR\ obtained\ parameters\ = 1.12 * \left(\frac{t}{1}\right)^{\frac{0.00635}{0.11-0.013}} = 1.12 * t^{0.065}$$

$$Calculated\ OCR\ parameters\ literature\ = 1.09 * \left(\frac{t}{1}\right)^{\frac{0.012}{0.18-0.013}} = 1.09 * t^{0.072}$$

## 5.4 Sensitivity analysis OCR

From Section 5.2 could be concluded that the determination of the abc-parameters is quite arbitrary, but the OCR in time can be predicted based on the determined parameters as shown in the previous section. The maximum and minimum of the obtained parameters are shown in Table 8. This section shows the sensitivity of the model for possible outcomes of OCR in time. The range of Table 8 is based on obtained values in the performed tests together with the values for the same material in the report of Zwanenburg et al. (2018) and a paper of Den Haan and Kamao (2003)[6]. At the end of this section is looked into the consequences of a shift from the reference isotach to the isotach imposed in the performed tests.

**Table 8: Range of obtained abc-parameters OVP-clay**

| Parameter | Minimum | Maximum |
|---|---|---|
| **a** | 0.010 (Den Haan and Kamao 2003) | 0.019 (own data) |
| **b** | 0.110 (own data) | 0.180 (Zwanenburg et al. 2018) |
| **c** | 0.006 (own data) | 0.012 (Zwanenburg et al. 2018) |
| **m = (b-a)/c** | 7.6 | 28.3 |

First is focused on the a-parameter. Figure 33 shows the influence of the a-parameter on the OCR in time. The colours indicate a range for the predicted OCR with a maximum value of 0.019 and a minimum of 0.010 for the a-parameter. The other two parameters are combinations of parameters from Table 8.

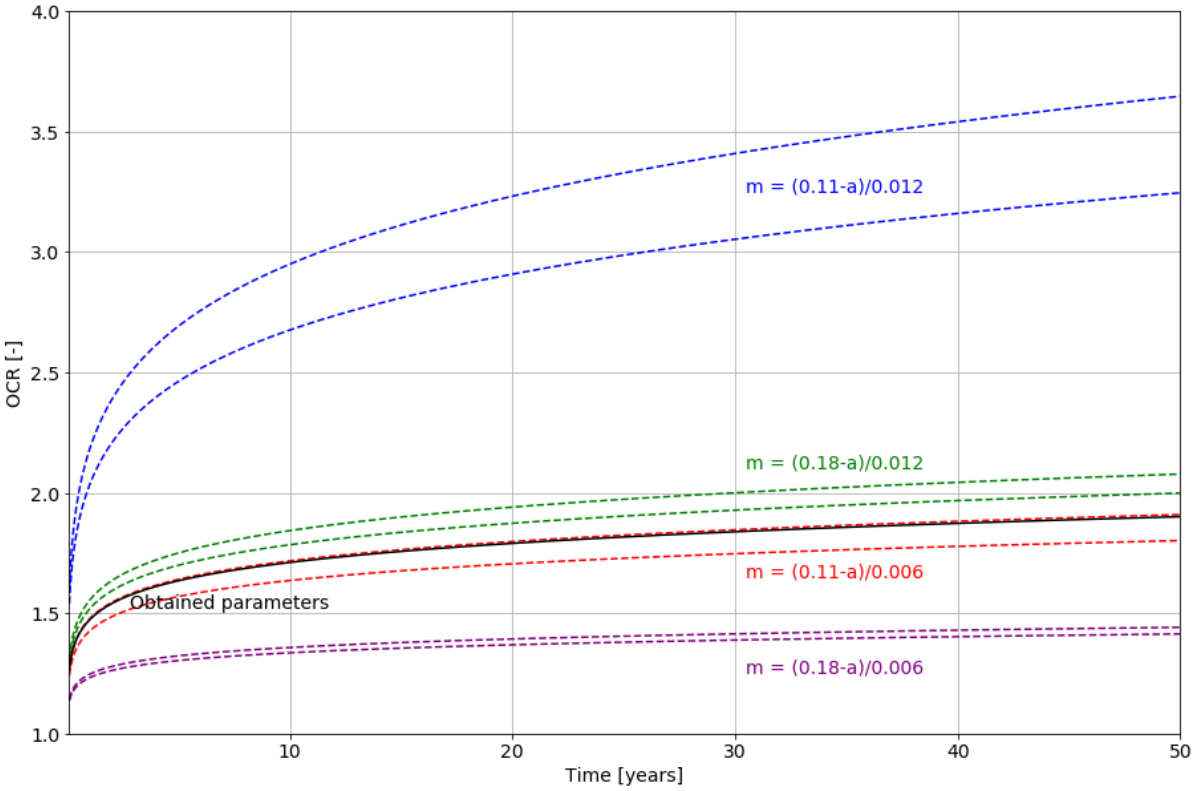


**Figure 33: Sensitivity analysis a-parameter**

[6] The paper deals with the determination of the parameters based on $K_0$-CRS tests on OVP-clay.

From Figure 33 can be established that the a-parameter does not have a large influence on the OCR. The influence of the a-parameter is larger when the b/c ratio is smaller. However, it is unlikely that a ratio of 8.3 would be found: the c-parameter is in that case determined based on a relaxation phase at 240 kPa, while the b value is obtained based on the stress-strain relation around 75 kPa. Therefore this scenario is left out of consideration for the rest of the analysis. The OCR in time based on the obtained parameters is given with the black line in Figure 33 and is similar to the red lines in the other figures.

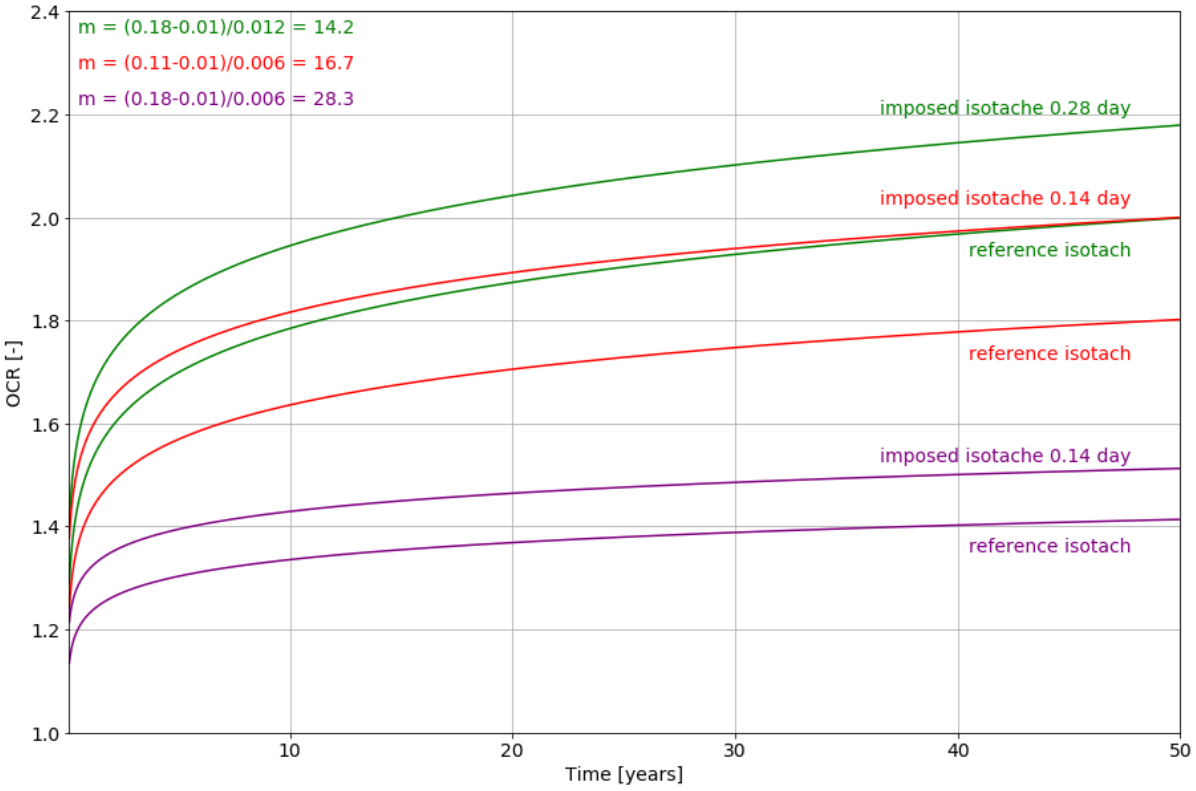


Figure 34: Sensitivity analysis b/c ratio

The a-parameter is held constant at 0.01, while the b/c ratio is varied. Figure 34 indicate that the OCR is strongly affected by the ratio b/c. Important to remember is that the b-parameter of 0.11 is not the intrinsic b-value, because the soil is in the transition phase between overconsolidated and normal consolidated (Section 5.2.1). The lower value of 0.11 corresponds with the stiffness on the isotach in the stress range in which the c-parameter is obtained. If the intrinsic b-value would be used, the OCR will be predicted by the purple line.

As discussed in the previous section, a factor for the shift towards the reference isotach should be used if the obtained OCR's are compared with the model. If we calculate the factors for the used range of parameters of Table 8 we end up with Table 9**.** The previous section explains the shift in more detail. An example of a shift calculation is given below:

$$\theta = \frac{c}{d\varepsilon/dt} = \frac{0.012}{0.036/20 * 24} = 0.28\ days$$

$$\varepsilon = c * \ln(\theta) = |0.012 * \ln(0.28)| = 0.015$$

$$\ln(\sigma') = \frac{\varepsilon}{b} = \frac{0.015}{0.11} = 0.136$$

$$e^{0.136} = 1.15$$

**Table 9: The shift factor from imposed to reference isotach**

| # | a | B | C | b/c | factor |
|---|---|---|---|---|---|
| **1** | 0.01 | 0.11 | 0.012 | 9.2 | 1.15 |
| **2** | 0.01 | 0.18 | 0.012 | 15 | 1.09 |
| **3** | 0.01 | 0.11 | 0.006 | 18.3 | 1.11 |
| **4** | 0.01 | 0.18 | 0.006 | 30 | 1.07 |

The shift of the yield stress to the reference isotach is often not presented and not taken into account. The related isotach is unknown if the test is stress controlled.

The last analysis looks into the influence of the loading rate. The abc-parameters of number 3 from Table 9 are used: b = 0.11 and c = 0.006. The shift factor is calculated as explained in the last section and the calculation is shown for the 0.05 day isotach.

$$\theta = \frac{c}{d\varepsilon/dt} = \frac{0.006}{0.108/20 * 24} = 0.05\ days$$

$$\varepsilon = c * \ln(\theta) = |0.006 * \ln(0.05)| = 0.018$$

$$\ln(\sigma') = \frac{\varepsilon}{b} = \frac{0.018}{0.11} = 0.163$$

$$e^{0.163} = 1.18$$

Table 10: The shift factor and imposed isotach as a function of the loading rate

| Loading rate [mm/hr] | Isotach [days] | Shift factor |
|---|---|---|
| **0.005** | 1.0 | 1.0 |
| **0.012** | 0.42 | 1.02 |
| **0.036** | 0.14 | 1.12 |
| **0.108** | 0.05 | 1.18 |
| **0.360** | 0.01 | 1.29 |

Table 10 shows that the obtained OCR can be 118% of the OCR on the reference isotach if the loading rate is 20 times higher than the loading rate related to the reference isotach. Those displacement rates will be applied during CRS tests. The shift from imposed to reference isotach is not negligible for conventional displacement rates as applied in the performed tests.

## 5.5 Lateral stresses

In Section 3.4 is concluded that the lateral stresses could increase during aging. This section shows the results from the tests with $K_0$-rings. If the lateral stresses would increase during aging, the stress path would be schematized by the illustration of Figure 35 (a). Figure 35 (b) shows a stress path with an aging phase without any changes in lateral stresses.

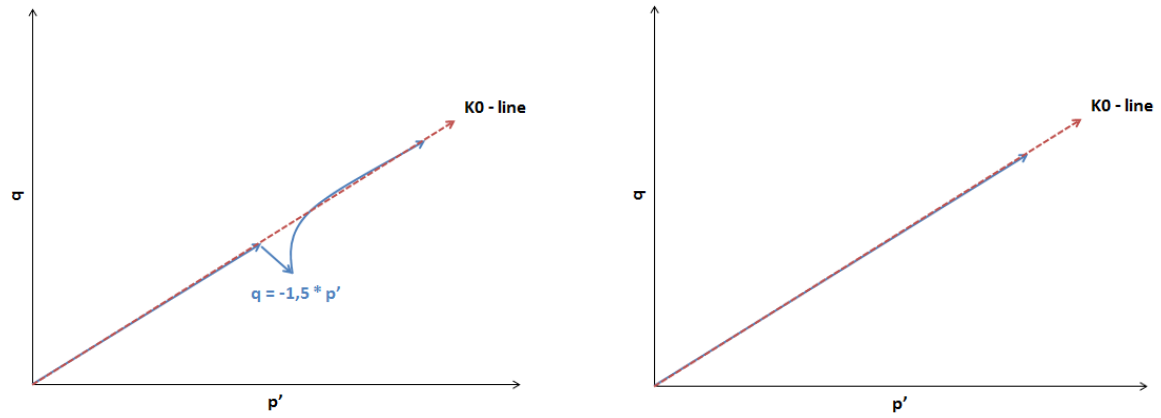


*(a)* *(b)*

**Figure 35: Stress paths with an aging phase with (a) and without (b) increase in lateral stresses during creep**

The question is if and how fast lateral stresses increase during aging. Unfortunately the performed $K_0$-CRS tests cannot be used to verify the changes in lateral stresses due to the stick and slip behaviour. However, there is a trend in which the soil behaviour tends towards an isotropic state during a constant effective stress phase. The horizontal and vertical stress in time graphs of a one day aging and a ten days aging test (respectively sample 5 and 8) are shown in Figure 36 on the next page**.** Figure 37 gives the p'-q graphs of those two samples. The p'-q graphs show a decrease in lateral stresses (increase in deviatory stress q) when aging starts and there after a decrease in lateral stresses. A few other p'-q graphs can be found in Appendix F**.**

The development of the $K_0$ as function of the OCR is given in Section 3.4. Note that if there is no increase of horizontal stresses due to aging, the structure of a mechanical and creep OCR are different. The lateral stresses during aging have to increase to have the same confining stresses as a mechanical OCR.

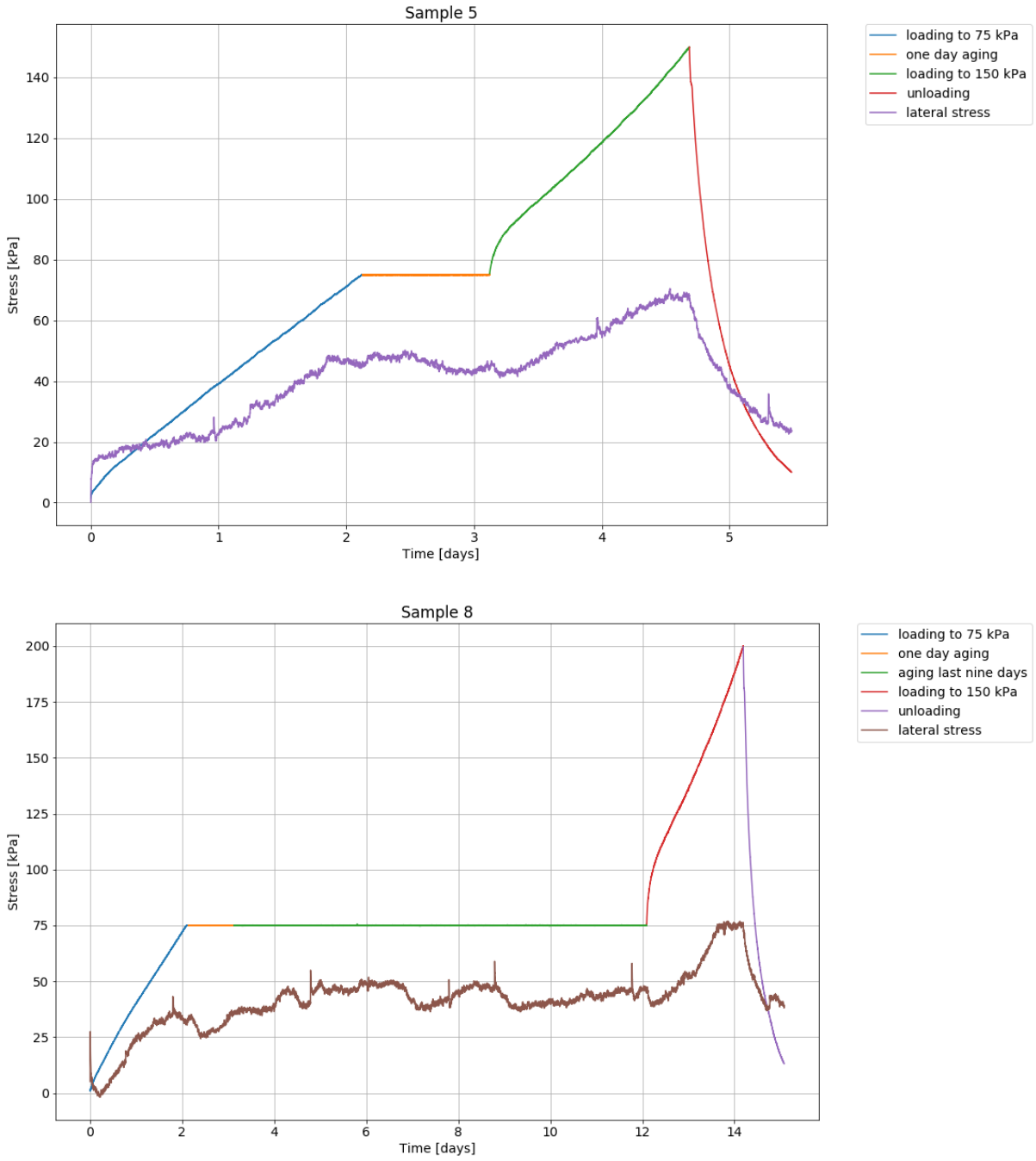


Figure 36: Measured vertical and horizontal stress in time

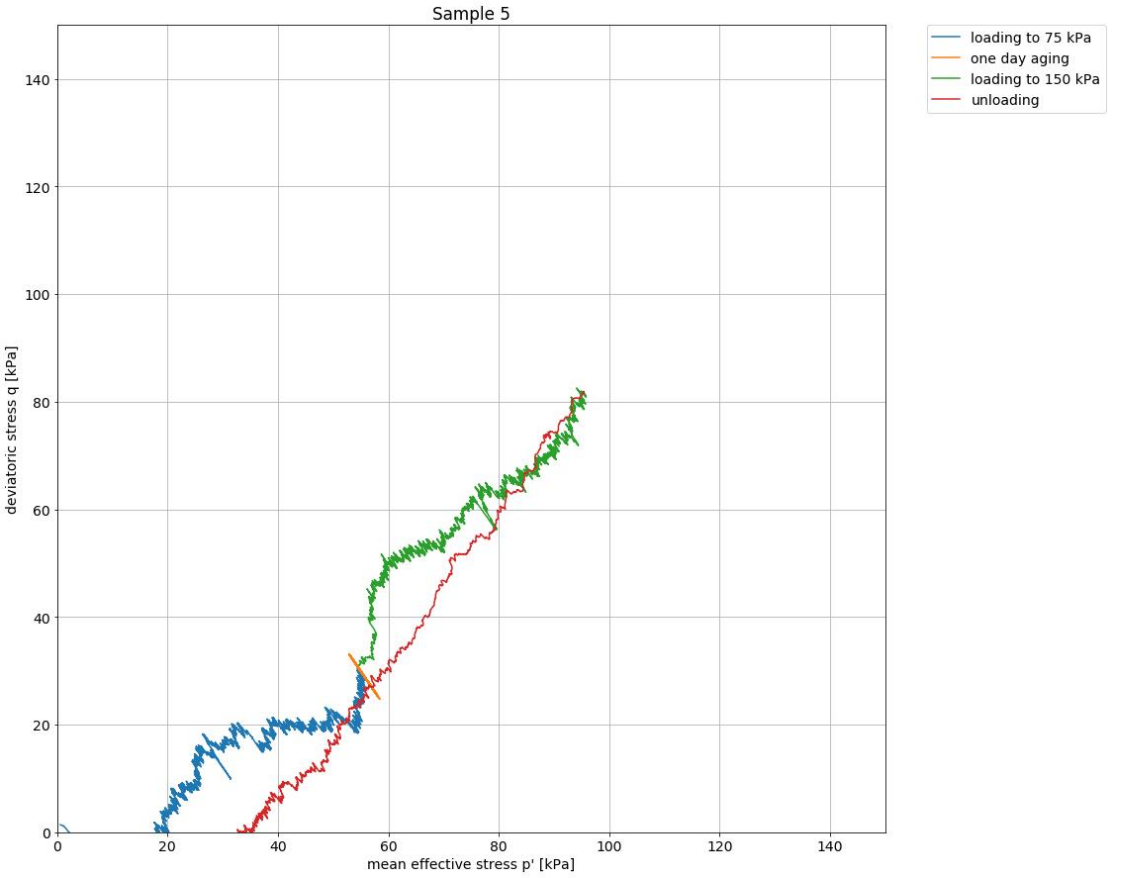


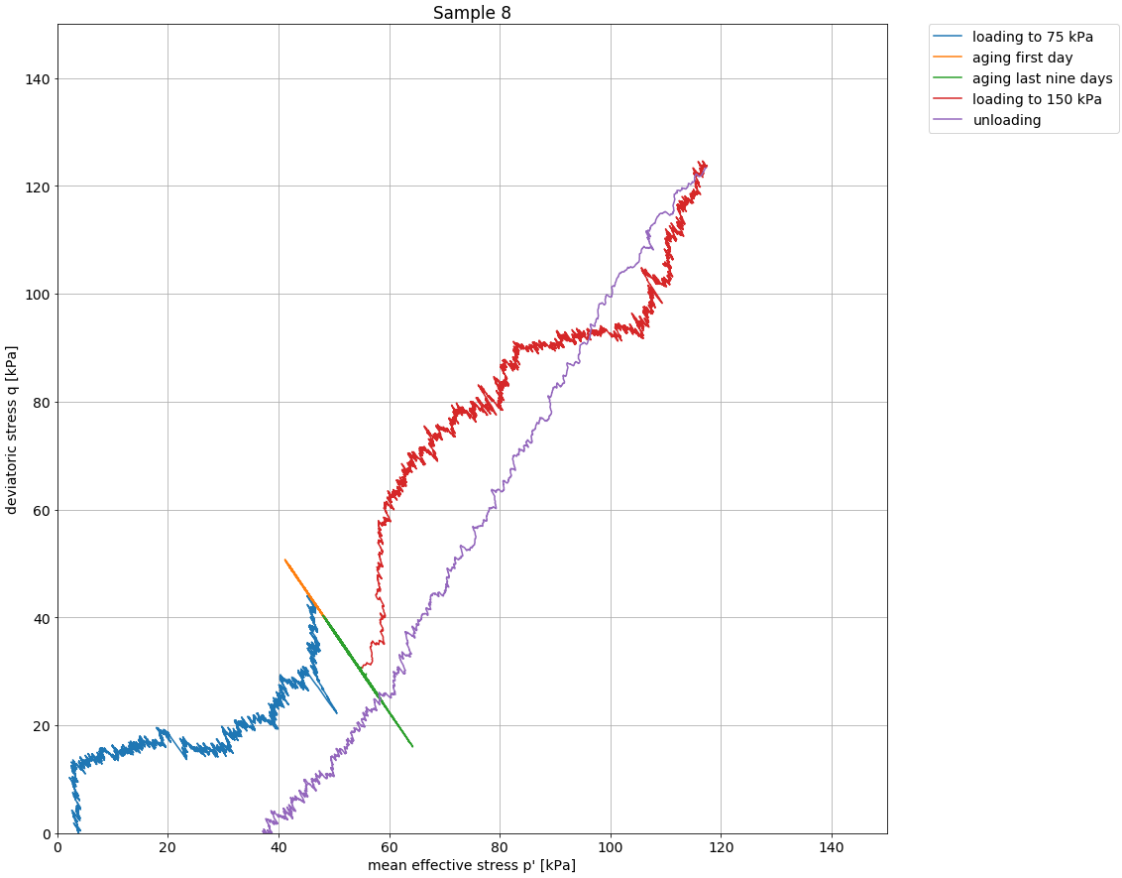


**Figure 37: Obtained stress paths**

## 5.6 Discussion results

The obtained relations of the vertical stress - void ratio of the tests are not unique. In the literature study is indicated that this could be expected for silty clays, because 'transitional soils' would not have this unique relation. However, the estimated error range is larger than the obtained stress – void ratio range.

The parameter that links the stress-void ratio relation to time is the c-parameter. The creep parameter for the performed analyses is obtained based on the intrinsic time – strain graph of several days. The other used methods to determine the c-parameter did result in a large range of values, probably caused by the effects of the dissipation of excess pore water in the first hours of relaxation and aging.

The obtained b-parameter used for the prediction of the yield stress is not the intrinsic b-parameter. According to the b-parameters in literature the value would be around 0.18. This value is obtained for high stresses above the range that can be expected in soft soils below dikes. The aging tests are performed at 75 kPa, which is equivalent to more than 7 meters of soil on top of the clay. Questioned can be if the OVP-clay ever reaches this intrinsic b-value. Probably it is better to work with the obtained stiffness in a certain stress range when soils have a gradual transition from overconsolidated to normal consolidated behaviour.

Unfortunately the lateral stress measurements are hard to interpret due to stick and slip behaviour of the soil in the measurement devices. However, there is a trend in the obtained data in which the soil behaviour tends towards an isotropic state during a constant effective stress phase. Note that the lateral stresses increases with a mechanical OCR and a difference with the development of lateral stresses during aging would be a difference between aged and overconsolidated clay.

The yield stress is an indication for the transition between overconsolidated and normal consolidated soils. Normal consolidated soils are following a certain stress-strain relation (an isotach). The yield stress is obtained with respect to this imposed isotach, which is often not the reference isotach. Yield stresses should be compared and validated based on a reference. This reference is unknown if the displacement rate is unknown, which is the case in stress-controlled laboratory tests and also during construction in the field. The actual difference will be small for low displacement rates, but is significant for the displacement rates in the laboratory tests.

# 6. Conclusions and recommendations

## 6.1 Conclusion

The goal of the thesis is to obtain differences between aged and mechanical overconsolidated soils, focussing on the transition from relatively stiff to less stiff clay behaviour. The answer on the main research question is given after dealing with the following research questions:

**1) What are theoretical differences in aged and overconsolidated clays?**

Differences can be caused by the differences in soil configuration of aged and overconsolidated clays. The virgin compression decreases mainly the macro-pore volume, while the micro-pore volume is changed due to creep. These types of differences are captured in the structure of the soil. The lateral stresses for a given OCR of aged and mechanical overconsolidated samples could be different as well.

**2) What are indications and possible consequences of development of structure during aging?**

Development of structure has two components: development in fabric and an increase in lateral stress. The effects of the development of structure can be seen in the difference between natural and remoulded clay samples. The yield stresses of natural soils are higher than predicted based on isotach models. Softening behaviour can be observed in the post-yield phase of those soils.

Some studies describe an increase in lateral stresses during creep. It is not possible to quantify the increase of lateral stresses in the performed tests due to the stick and slip behaviour of the clay in the $K_0$-CRS test.

**3) Which difficulties arise during determination of the abc-parameters?**

The virgin compression parameter seems to be stress and structure-development dependent, which makes it hard to choose a value for this b-parameter. The a-parameter changes with the imposed OCR, so the difficulty is the question how far the soil should be unloaded to obtain the direct strain parameter. Another difficulty is the overestimation of the creep parameter due to direct strains that are considered to be creep strains in the first hours of relaxation or constant stress phases. When worked with a relaxation phase, fitting the data to obtain the c-parameter seems to be arbitrary. For both methods, aging and relaxation, an iterative process is needed to define the creep parameter based on the reference isotach.

**4) Is the abc-model applicable on the tested clay?**

The obtained stress-void relations of the OVP-clay seem to have no unique relation. However, the obtained range is smaller than the range of void ratios for a given stress that could be obtained when small measurement errors are taken into account. Therefore is concluded that it is likely that there is a unique relation between stress and void ratio. Also the small range of creep parameters indicates that the abc-model is applicable on the remoulded OVP-clay.

Note that the obtained virgin compression parameter shows a gradual transition from overconsolidated to normal consolidated soil behaviour. This gradual transition and the earlier mentioned consequences of structure development are not taken into account by the isotach models.

**5) Is the transformation from overconsolidated soil behaviour to normal consolidated soil behaviour in the aging tests described properly by the mathematical formulation of the abc-model and Soft Soil Creep model?**

The observed transitions from overconsolidated to normally consolidated state are properly predicted by the isotach models. The development of the yield stress is dependent on the ratio of the virgin compression parameter (b-parameter) over the creep parameter (c-parameter). The parameter related to the behaviour in overconsolidated conditions (the a-parameter) has a small influence on the prediction of the yield stress.

The goal of the thesis is to observe differences between aged and overconsolidated soil behaviour in compression. Because the transition between overconsolidated and normal consolidated behaviour plays an important role, the main question is as follows:

**Does the yield stress develop due to aging as predicted by the isotach model of Den Haan?**

A minimum yield stress in time can be predicted based on the isotach models. Isotach models assume that there is no difference between aged and mechanical overconsolidated yield stresses, but the performed $K_0$-CRS tests indicate that there could be differences if structure develops in the soil. The yield stress of a structured soil is higher and after the structure is broken down, the soil shows softening behaviour. The increase in yield stresses due to the development of structure is too small to obtain in the performed tests, but there are indications of softening behaviour after an aging phase. No quantification can be made of the development of lateral stresses in the performed tests, but the lateral stresses seem to increase with OCR.

The overestimation of the yield stress based on $K_0$-CRS tests results in uncertainty about the capability modelling aging with isotach models. This master thesis indicates two possible causes of overestimation of the yield stress:

1) The effects of structure development during aging
2) The shift from the imposed isotach to the reference isotach that is often not taken into account

The first cause is related to the method of yield stress determination. The yield stress is often determined with the Casagrande method. This method uses the b-parameter which could be too large if the soil softens, resulting in a significant overestimation.

The second cause has to do with the fact that the yield stress is obtained with respect to an imposed isotach. Yield stress determination and comparison should be done based on the reference isotach, which is typically not the same as the imposed isotach. The overestimation is increasing with the rate of displacement. A high displacement rate is often chosen in laboratory tests, causing a significant overestimation of the yield stress.

## 6.2 Recommendations

The b-parameter seems to be stress-dependent in the performed tests due to the gradual transition from overconsolidated to normal consolidated behaviour. Besides that, the b-parameter seems to be influenced by aging phases like relaxation. Therefore is suggested to obtain the b-parameter around a stress level which is in the range of field conditions. The determination of the b-parameter should be done before a constant effective stress or relaxation phase in laboratory tests. That obtained b-parameter should also be used to determine the yield stress if worked with the Casagrande method. Determination of the yield stress based on the stress-strain relation at large strains can easily result in an overestimation of the yield stress if there is some softening behaviour in the soil.

Determination of the c-parameter based on a relaxation phase did not result in a c-parameter that is consistent with the creep parameters found based on a constant stress phase. Fitting the decrease of stress in time seems to be arbitrary. This is probably caused by the effects of consolidation in the first hours of relaxation. It is recommended to work with aging phases longer than a day to be sure no stress-dependent strains are interpreted as creep strains.

The development of structure is not significant in the performed tests, which makes it hard to make conclusions about the consequences of this process. Therefore differences between aging in isotach models and aging of soils should be further investigated based on a longer aging time. This could be done by putting a load on top of a remoulded clay block and test the behaviour of the clay after a day, week, month, quarter and year. Triaxial tests can be used to test several stress paths and see how the yield surface changes due to aging. $K_0$-CRS tests could be used to determine the development of structure.

Another important recommendation is studying the increase in lateral stresses during aging. The results of the $K_0$-rings are not very useful due to stick and slip behaviour. Measuring lateral stresses in an embankment over a few months after construction gives insight in the development of lateral stresses in time. It is also possible to simulate aging in triaxial behaviour and prevent lateral deformation by increasing the cell pressure (Mesri and Castro 1987).

# References


Akagi, H. (1994). A Physico-Chemical approach to the Consolidation Mechanism of Soft Clays. *Soils and Foundations*, *34*(4), 43–50.

Aljouni, M. A. (2000). *Geotechnical Properties of Peat and related Engingeering Problems*. University of Illinois.

Ammerlaan, P. R. M. (2011). *Proefterpen project Bloemendalenpoldre te Weesp*.

Augustesen, A., Liingaard, M., & Lade, P. V. (2004). Evaluation of Time-Dependent Behavior of Soils. *International Journal of Geomechanics*, *4*(3), 137–156. https://doi.org/10.1061/(ASCE)1532-3641(2004)4:3(137)

Barden, L. (1968). Primary and secondary consolidation of clay and peat. *Geotechnique*, *18*, 1–24.

Baxter, C. D. P., & Mitchell, J. K. (2004). An experimental study on the aging of sands. *Journal of Geotechnical and Geoenvironmental Engineering*, *130*(October), 1051–1062. https://doi.org/10.1061/(ASCE)1090-0241(2004)130

Berry, P., & Poskitt, T. (1972). The consolidation of peat. *Geotechnique*, *22*(1), 27–52. https://doi.org/10.1680/geot.1972.22.1.27

Bjerrum, L. (1967). Engineering Geology of Norwegian Normally-Consolidated Marine Clays as Related to Settlements of Buildings. *Géotechnique*, *17*(2), 83–118. https://doi.org/10.1680/geot.1967.17.2.83

Bjerrum, L., & Lo, K. Y. (1963). Effect of Aging on the Shear-Strength Properties of a Normally Consolidated Clay. *Géotechnique*, *17*(2), 83–118. https://doi.org/10.1680/geot.1963.13.2.147

Bolt, G. H. (1956). Physico-Chemical Analysis of the Compressibility of Pure Clays. *Géotechnique*, *6*(2), 86–93. https://doi.org/10.1680/geot.1956.6.2.86

Bowman, E. T., & Soga, K. (2003). Creep, Ageing and Microstructural change in Dense Granular Materials. *Soils and Foundations*, *43*(4), 107–117.

Burland, J. B. (1990). On the compressibility and shear strength of natural clays. *Géotechnique*, *40*(3), 329–378. https://doi.org/10.1680/geot.1990.40.3.329

Cheng, X. H., Ngan-Tillard, D. J. M., & Den Haan, E. J. (2007). The causes of the high friction angle of Dutch organic soils. *Engineering Geology*, *93*, 31–44. https://doi.org/10.1016/j.enggeo.2007.03.009

Clarke, S. D. (2009). *Enhancement of the BRICK constitutive model to incorporate viscous soil behaviour*. University of Sheffield.

Collins, K., & McGown, A. (1974). The form and function of microfabric features in a variety of natural soils. *Géotechnique*, *24*(2), 223–254. https://doi.org/10.1680/geot.1974.24.2.223

Craig, R. F., & Knappett, J. A. (2012). *Craig's Soil Mechanics*.

Davis, J. H. (1997). The peat deposits of Florida their occurrence, development and uses. *Florida Geological Survey*.

Deelprogramma Veiligheid Deltaprogramma. (2015). *Synthesedocument Veiligheid Achtergronddocument B1*.

Delage, P., & Lefebvre, G. (1984). Study of the structure of a sensitive Champlain clay and of its evolution during consolidation. *Canadian Geotechnical Journal*, *21*, 21–35. https://doi.org/10.1139/t84-003

Deltares. (2016). D-SETTLEMENT User Manual.

Den Haan, E. J. (1994). *Vertical compression of soils*. TU Delft. https://doi.org/uuid:b8dc88e0-f400-4d86-9a2e-4e00b68d0472

Den Haan, E. J. (2003). Sample disturbance of soft organic Oostvaardersplassen clay. In *Proc. Int. Symp. on Deformation Characteristics of Geomaterials* (Vol. 1, pp. 49–55). Lisse.

Den Haan, E. J., Essen, H. M., & Visschedijk, M. A. . (2004). Isotachenmodellen: Help, hoe kom ik aan de parameters? *Geotechniek*, 62–69.

Den Haan, E. J., & Kamao, S. (2003). Obtaining Isotache parameters from a CRS K0-Oedometer. *Soils and Foundations*, *43*(4), 203–214.

Den Haan, E. J., & Kruse, G. (2007). Characterisation and engineering properties of Dutch peats. *Taylor & Francis Group, London, UK*.

Farrell, E. R., O'Neil, C. O., & Morris, A. (1993). Changes in the mechanical properties of soils with variations in organic content. *Proc., International Workshop on Advances in Understanding and Modeling the Mechanical Behavior o f Peat, Delft, Netherlands*, 19–25.

Fujiwara, H., Ue, S., & Yasuhara, K. (1987). Secondary Compression of Clay under Repeated Loading. *Soils and Foundations*, *27*(2), 21–30.

Gareau, L. F., Molenkamp, F., & Sharma, J. (2006). An improved oedometer apparatus to measure lateral stress during testing. *Geotechnical Testing Journal*, *29*(3), 200–206. https://doi.org/10.1520/GTJ12341

Garlanger, J. E. (1972). The consolidation of soils exhibiting creep under constant effective stress. *Géotechnique*, *22*(1), 71–78.

Gasparre, A., & Coop, M. R. (2008). Quantification of the effects of structure on the compression of a stiff clay. *Canadian Geotechnical Journal*, *45*(9), 1324–1334. https://doi.org/10.1139/t08-052

Gens, A., & Cataluña, U. P. De. (1985). A State Boundary Surface for soils not obeying Rendulic ' s principle, 473–476.

Griffiths, F. J., & Joshi, R. C. (1989). Change in pore size distribution due to consolidation of clays. *Géotechnique*, *39*(1), 159–167. https://doi.org/10.1680/geot.1990.40.2.303

Griffiths, F. J., & Joshi, R. C. (1990). Discussions: Change in pore size distribution due to consolidation of clays. *Géotechnique*, *40*(1), 303–309. https://doi.org/10.1680/geot.1990.40.2.303

Grozic, J. L. H., Lunne, T., & Pande, S. (2003). An oedometer test study on the preconsolidation stress of glaciomarine clays. *Canadian Geotechnical Journal*.

Hanzawa, H., & Kishida, T. (1981). Fundamental considerations on undrained strength characteristics of alluvial marine clays. *Soils and Foundations*, *21*(1), 39–50.

Heemstra, J. (2013). Met Buisman naar de isotachen. *Geotechniek*, (April), 30–33.

Hong, Z.-S., Zeng, L.-L., Cui, Y.-J., Cai, Y.-Q., & Lin, C. (2012). Compression behaviour of natural and reconstituted clays. *Géotechnique*, *62*(4), 291–301. https://doi.org/10.1680/geot.10.P.046

Houkes, C. B. (2016). *Review and validation of settlement prediction methods for organic soft soils, on the basis of three case studies from the Netherlands*. TU Delft.

Jaky, J. (1944). The coefficient of earth pressure at rest. *J. of the Society of Hungarian Architects and Engineers*, 355–358. Retrieved from https://ci.nii.ac.jp/naid/10007807963/en/

Koppejan, A. W. (1948). A formula combining the Terzaghi load compression relationship and the buisman secular time effect. *Proc. 2nd ICSMFE, Rotterdam, 1948*, *3*, 32–37.

Kuhn, B. M. R., & Mitchell, J. K. (1993). New Perspectives on Soil Creep. *Journal of Geotechnical Engineering*, *119*(3), 507–524.

Le, T. M., Fatahi, B., & Khabbaz, H. (2012). Viscous Behaviour of Soft Clay and Inducing Factors. *Geotechnical and Geological Engineering*, *30*(5), 1069–1083. https://doi.org/10.1007/s10706-012-9535-0

Matsuo, S., & Kamon, M. (1977). Microscopic Study on Deformation and Strength of Clays. In *Proceedings of the 9th international conference on soil mechanics and foundation engineering* (pp. 201–204). Tokyo, Japan.

Mayne, P. W., & Kulhawy, F. H. (1982). K0 – OCR relationships in soil. *Journal of the Geotechnical Engineering*, *108*(GT6), 851–872. https://doi.org/10.1016/0148-9062(83)91623-6

Mesri, G., & Castro, A. (1987). Ca / Cc Concept and K 0 during Secondary Compression. *Journal of Geotechnical EngineeringJournal of Geotechnical Engineering*, *113*(3), 230–247.

Mewis, J., & Wagner, N. J. (2009). Thixotropy. *Advances in Colloid and Interface Science*, *147–148*, 214–227. https://doi.org/10.1016/j.cis.2008.09.005

Mitchell, J. K., & Kenichi, S. (2005). Time Effects on Strength and Deformation. In *Fundamentals of Soil Behavior* (pp. 465–522).

Navarao, V., & Alonso, E. E. (2001). Secondary compression of clays as a local dehydration process. *Geotechnique*, *51*(10), 859–869.

Nie, L., Lv, Y., & Li, M. (2012). Influence of organic content and degree of decomposition on the engineering properties of a peat soil in NE China. *Quarterly Journal of Engineering Geology and Hydrogeology*, *45*(4), 435–446. https://doi.org/10.1144/qjegh2010-042

Nocilla, A., Coop, M. R., & Colleselli, F. (2006). The mechanics of an Italian silt: an example of 'transitional' behaviour. *Géotechnique*, *56*(4), 261–271. https://doi.org/10.1680/geot.2006.56.4.261

Ozer, A. T., Lawton, E. C., & Bartlett, S. F. (2012). New method to determine proper strain rate for constant rate-of-strain consolidation tests. *Canadian Geotechnical Journal*, *49*(1), 18–26. https://doi.org/10.1139/t11-086

Schmertmann, B. J. H. (1991). The Mechanical Aging of Soils. *Journal of Geotechnical Engineering*, *117*(9), 1288–1330.

Sridharan, A., & Venkatappa Rao, G. (1971). Shear strength behavior of saturated clays and the role of the effective stress concept. *Geotechnique*, *29*(2), 177–193.

Sridharan, A., & Venkatappa Rao, G. (1973). Mechanisms controlling volume change of saturated clays and the role of the effective stress concept. *Géotechnique*, *23*(3), 359–382. https://doi.org/10.1680/geot.1973.23.3.359

Tang, Y. X., & Tsuchida, T. (1999). The development of shear strength for sedimentary soft clay with respect to aging effect. *Soils and Foundations*, *39*(6), 13–24.

Terzaghi, K. (1925). *Erdbaumechanik auf bodenphysikalischer grundlage*.

Tigchelaar, J. (2001). *Eindrapportage Experimenteel onderzoek van het gedrag van organische klei*.

Van Loon, A. J., & Wiggers, A. J. (1975). Holocene lagoonal silts (formerly called “sloef”) from the Zuiderzee. *Sedimentary Geology*, *13*(1), 47–55. https://doi.org/10.1016/0037-0738(75)90049-4

Van Loon, A. J., & Wiggers, A. J. (1976). Primary and secondary synsedimentary structures in the lagoonal almere member (Groningen formation, Holocene, the Netherlands). *Sedimentary Geology*, *16*, 89–97.

Vermeer, P. A., & Neher, H. P. (1999). A soft soil model that accounts for creep. *Beyond 2000 in Computational Geotechnics - 10 Years of PLAXIS International*. https://doi.org/10.1201/9781315138206-24

Verruijt, A. (2018). Theory and Applications of Transport in Porous Media An Introduction to Soil Mechanics (pp. 17–19).

Visschedijk, M. (2010). Isotachen berekeningen op een sigarendoosje. *Geotechniek*, 1–10.

Wang, Y.-H., & Leung, S.-C. (2008). A particulate-scale investigation of cemented sand behavior. *Canadian Geotechnical Journal*, *45*(1), 29–44. https://doi.org/10.1139/T07-070

Won, J. Y., & Chang, P. W. (2007). The causes of apparent overconsolidation in the Namak marine deposit, Korea. *Geotechnique*, *57*(4), 359–365. https://doi.org/10.1680/geot.2007.57.4.365

Xu, B., & Zhang, N. (2018). Determination of compression curve of in-situ soil considering soil disturbance (Vol. 162, pp. 213–216).

Zeevaart, L. (1986). Consolidation in the intergranular viscosity of highly compressible soils. *Consolidation of Soils: Testing and Evaluation*, *892*, 257–281. https://doi.org/10.1520/STP34619S

Zwanenburg, C., Lange, D. A. de, & Konstantinou, M. (2018). *POVM Validatie uitgangspunten en lange termijnontwikkeling*.

# Appendix

**Appendix A:** Summary tests

| Start test | Sample | Machine | Program 75 kPa | Program 125 kPa | Note |
|---|---|---|---|---|---|
| 18-12-18 | 1 | 1 | 1 day relaxtion | | High strains at begin of the test, data unreliable |
| 18-12-18 | 2 | 2 | Unloading-reloading | Unloading-reloading | |
| 18-12-18 | 3 | 3 | Unloading-reloading | Unloading-reloading | Top cap - piston alligment not perfect, peak in vertical stress |
| 18-12-18 | 4 | 4 | 1 day relaxtion | | Relaxation instead of aging |
| 09-01-19 | 5 | 2 | 1 day aging | | |
| 17-01-19 | 6 | 1 | 1 day aging | | Sample is called sample 6 extra in Deltares database. Original sample 6 did not result in a useful dataset due to top cap - piston alligment problems |
| 17-01-19 | 7 | 4 | 50 days aging | | Three files, power failure (16th Februari) + windows update (6th March): A part of the data during aging seems to be missing. |
| 23-01-19 | 8 | 2 | 10 days aging | | |
| 23-01-19 | 9 | 1 | Unloading reloading | Unloading reloading | K0-measurements unusual, unloading-reloading stiffness at 75 kPa 4 times higher than samples 2 and 3 |
| 30-01-19 | 10 | 1 | 10 times 70-75 kPa | | |
| 30-01-19 | 11 | 3 | 1.7 days aging | | |
| 06-02-19 | 12 | 1 | 10 times 65-75 kPa | | |
| 06-02-19 | 13 | 3 | 10 days aging | | Power failure (16th of Februari) during day 10. No K0-ring measurement data |
| 06-02-19 | 14 | 2 | 10 days aging | | Power failure (16th of Februari) during day 8. No K0-ring measurement data |
| 14-02-19 | 15 | 1 | 30 days aging | | Test stopped after power failure (16th Februari) |
| 19-02-19 | 16 | 1 | 30 days aging | | No K0-ring measurement data. Computer failure (6th of March) |
| 21-02-19 | 17 | 3 | 10 times 60-80 kPa | | Other program then planned |
| 28-02-19 | 18 | 3 | 10 times 70-75 kPa | | |
| 27-03-19 | 19 | 1 | Reference 75 kPa | 1 day aging | |
| 11-03-19 | 20 | 3 | Repeated loading | | |
| 18-03-19 | 21 | 3 | 10 times 70-80 kPa | Relaxation | Missing data |
| 29-03-19 | 22 | 2 | Reference 75 kPa | 1 day aging | Missing data |

**Appendix B:** Void ratio

The Lost on Ignition (LOI), specific gravity ($G_s$) and the initial void ratio ($e_0$) are presented in the graph below. The b and c parameter are shown as well. There is no correlation found between the parameters.

| Sample | LOI [%] | $G_s$ [-] | $\rho_{bulk}$ [g/cm$^3$] | $e_0$ [-] | b 72.5 kPa | c |
|---|---|---|---|---|---|---|
| 1 | 17 | 2.30 | | | | |
| 2 | 17 | 2.31 | 1.36 | 2.72 | 0.10 | |
| 3 | 17.2 | 2.31 | 1.36 | 2.72 | 0.10 | |
| 4 | 16.8 | 2.31 | 1.33 | 2.75 | 0.09 | |
| 5 | 16.5 | 2.31 | 1.35 | 2.84 | 0.11 | 0.0092 |
| 6 | 17.4 | 2.31 | 1.38 | 2.87 | 0.11 | 0.0052 |
| 7 | 17.2 | 2.31 | | | | |
| 8 | 17.3 | 2.31 | 1.32 | 2.73 | 0.11 | 0.0057 |
| 9 | 17.5 | 2.31 | 1.34 | 2.87 | 0.09 | |
| 10 | 17.5 | 2.32 | 1.34 | 2.79 | 0.10 | |
| 11 | 17.1 | 2.31 | 1.37 | 2.77 | 0.11 | 0.0065 |
| 12 | 16.7 | 2.31 | 1.35 | 2.76 | 0.10 | |
| 13 | 17.1 | 2.31 | 1.32 | 2.79 | 0.12 | 0.0078 |
| 14 | 17.5 | 2.30 | 1.36 | 2.72 | 0.11 | 0.0077 |
| 15 | 17.7 | 2.31 | | | | |
| 16 | 17.4 | 2.29 | 1.38 | 2.76 | 0.09 | 0.006 |
| 17 | 17.4 | 2.31 | | | | |
| 18 | 17.6 | 2.31 | 1.36 | 2.72 | 0.12 | |
| 19 | 17.2 | 2.30 | 1.36 | 2.69 | 0.09 | |
| 20 | 17.6 | 2.30 | | | | |
| 21 | 17.5 | 2.30 | | | | |
| 22 | 17.2 | 2.31 | | | | |
| **Mean** | **17.2** | **2.31** | **1.35** | **2.77** | **0.103** | **0.007** |
| **CoV** | **2%** | **0%** | **1%** | **2%** | **10%** | **19%** |

**Appendix C** Creep parameter relaxation

The c-parameter can be determined based on the following mathematical formulation:

$$\sigma_v{}' = \sigma_{vR}{}' \left( 1 - \frac{b-a}{c} * \frac{d\sigma_{vR}{}'/dt}{\sigma_{vR}{}'} * \theta \right)^{-\frac{c}{b-a}}$$

The data is fitted on t = 0.25 days and therefore θ = 0.15 + 0.25 = 0.4 days.

$$\sigma_v' = (\sigma_{vR}{}' + 3) \left( 1 - \frac{0.11 - 0.013}{c} * \frac{d\sigma_{vR}{}'/dt}{\sigma_{vR}' + 3} * \theta \right)^{-\frac{c}{0.11-0.013}}$$

The fit with a c-parameter equal to 0.016 is given below. This value is significant higher than the obtained 0.006 in the report.

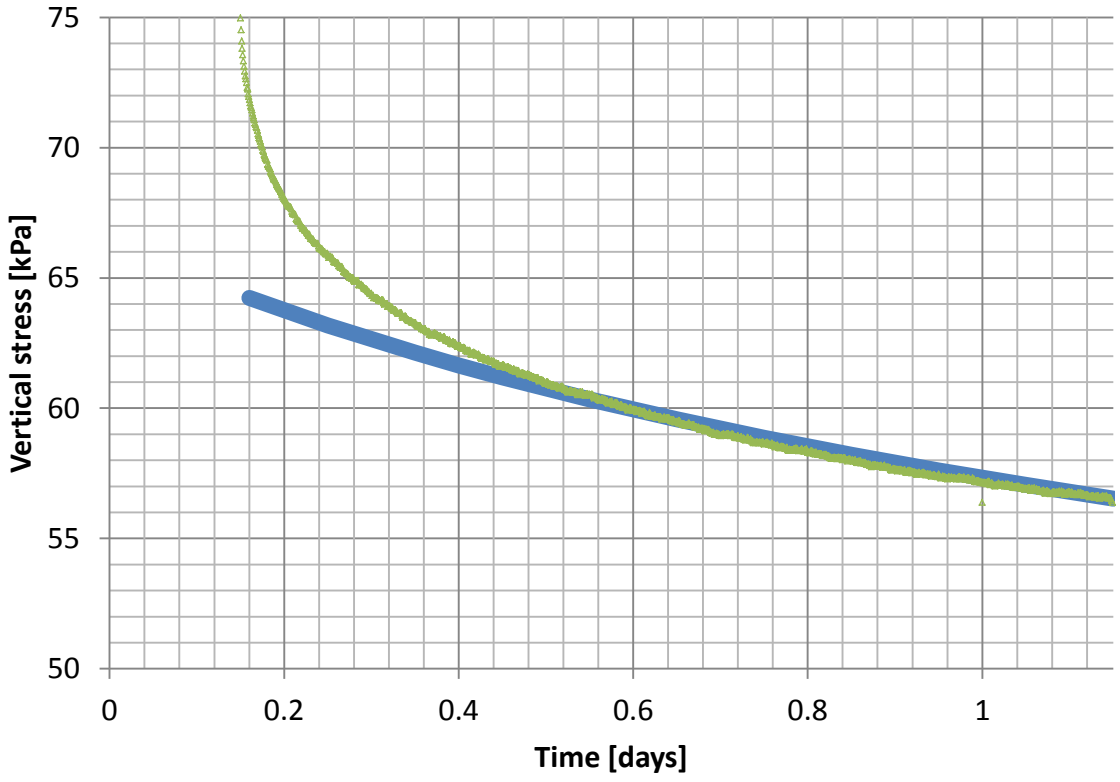

**Appendix D** Calculated creep parameters

The table below shows the obtained c-parameters determined based on the creep strains and creep rate as described in Chapter 4.

$$c = \frac{\Delta\varepsilon}{-\Delta \ln(\delta\varepsilon/\delta t)}$$

| Sample | Aging | b | c | b/c |
|---|---|---|---|---|
| **5** | **1 day** | 0.11 | 0.0092 | 11.5 |
| **6** | **1 day** | 0.11 | 0.0052 | 20.4 |
| **8** | **10 days** | 0.11 | 0.0057 | 19.6 |
| **11** | **1 day** | 0.11 | 0.0065 | 16.5 |
| **13** | **5 days** | 0.12 | 0.0078 | 15.5 |
| **14** | **5 days** | 0.11 | 0.0077 | 14.0 |
| **16** | **30 days** | 0.09 | 0.0060 | 15.3 |

**Appendix E** Creeps strain in time

The time spans that are us to obtain parameters are given in the table of Appendix D.

The natural strain as function of time:

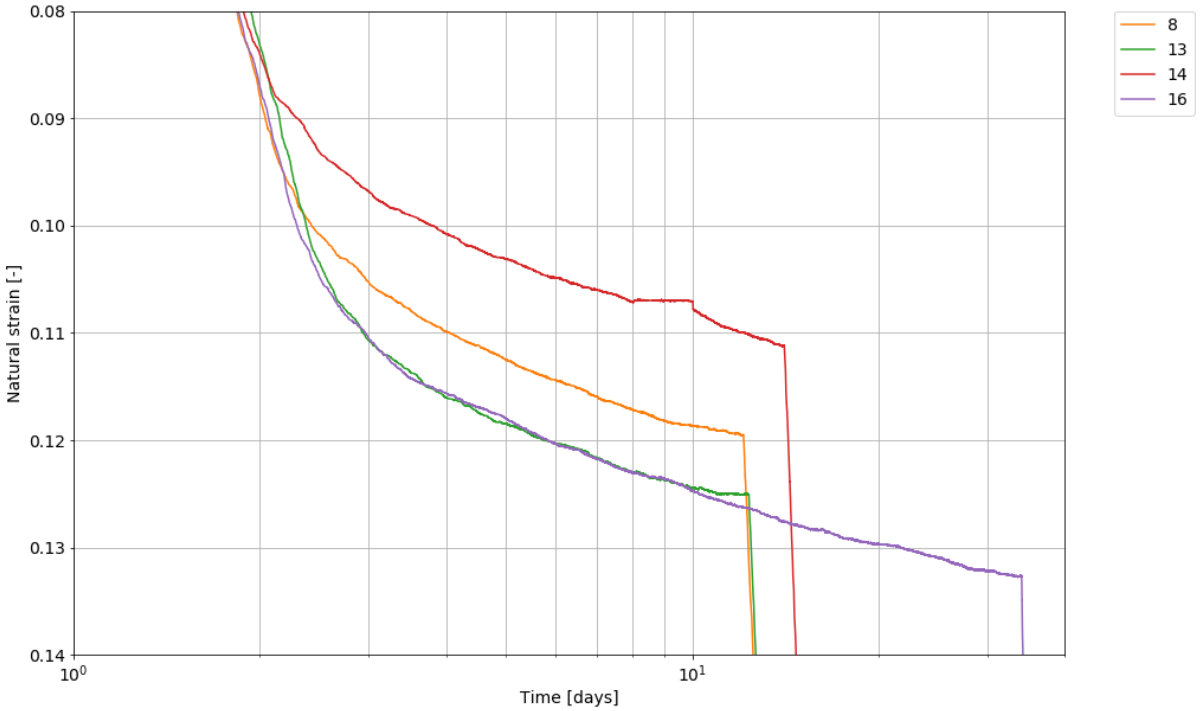


The void ratio as function of time:

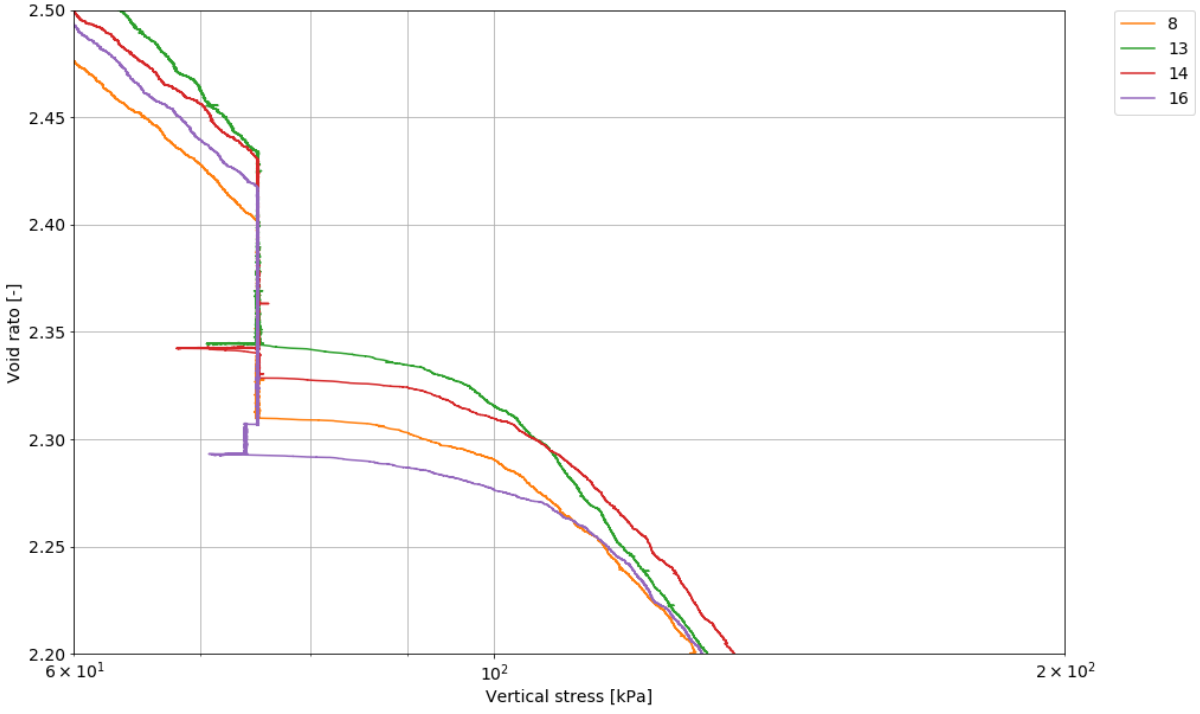

The vertical stress as function of time:

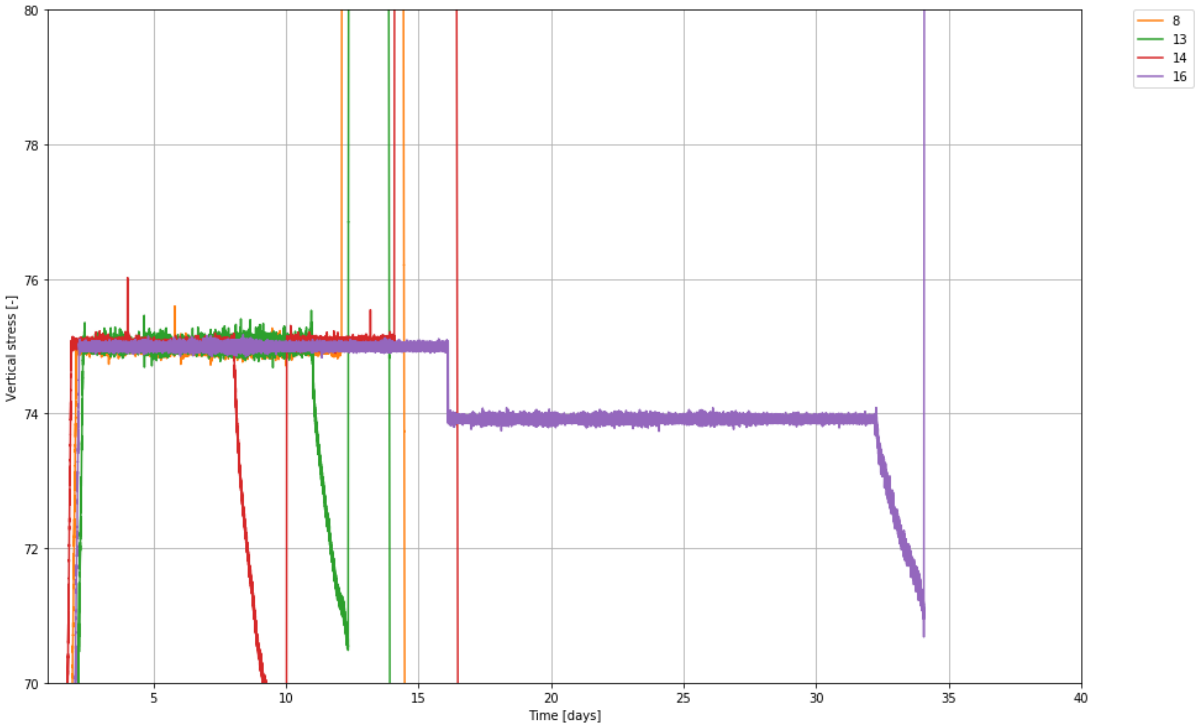


It is clear that it is possible to hold the vertical stress at a certain level. The change between aging and loading back to the isotach results often in a short reloading phase. But the consequences of computer updates and a power failure are also visible.

**Appendix F** Stress paths

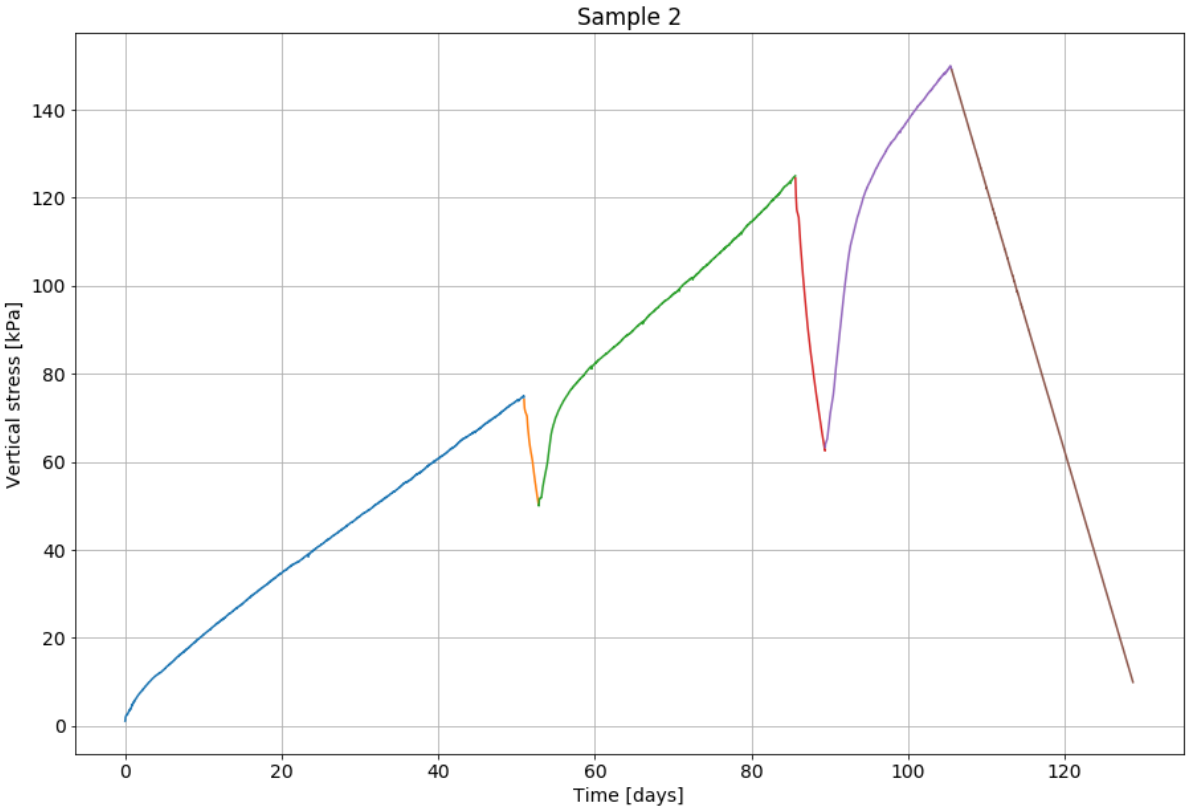


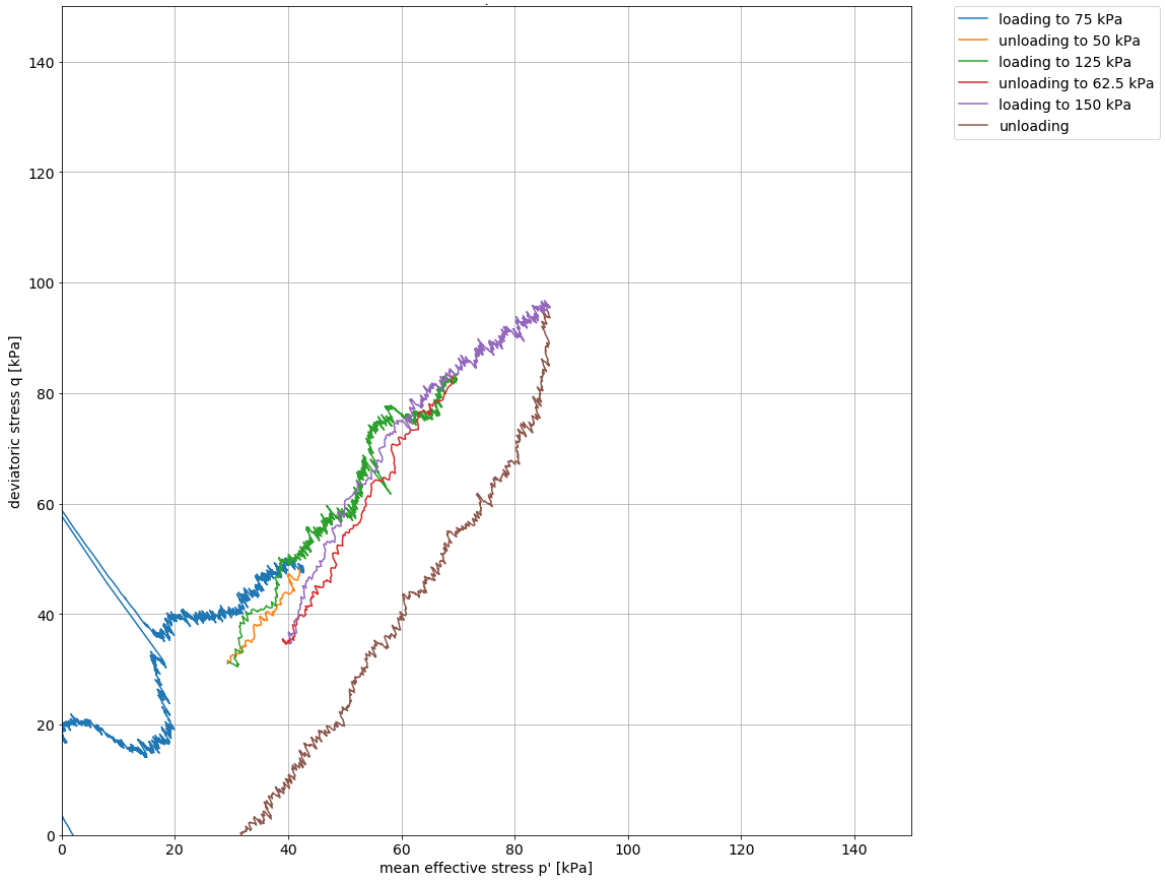

**Sample 5**

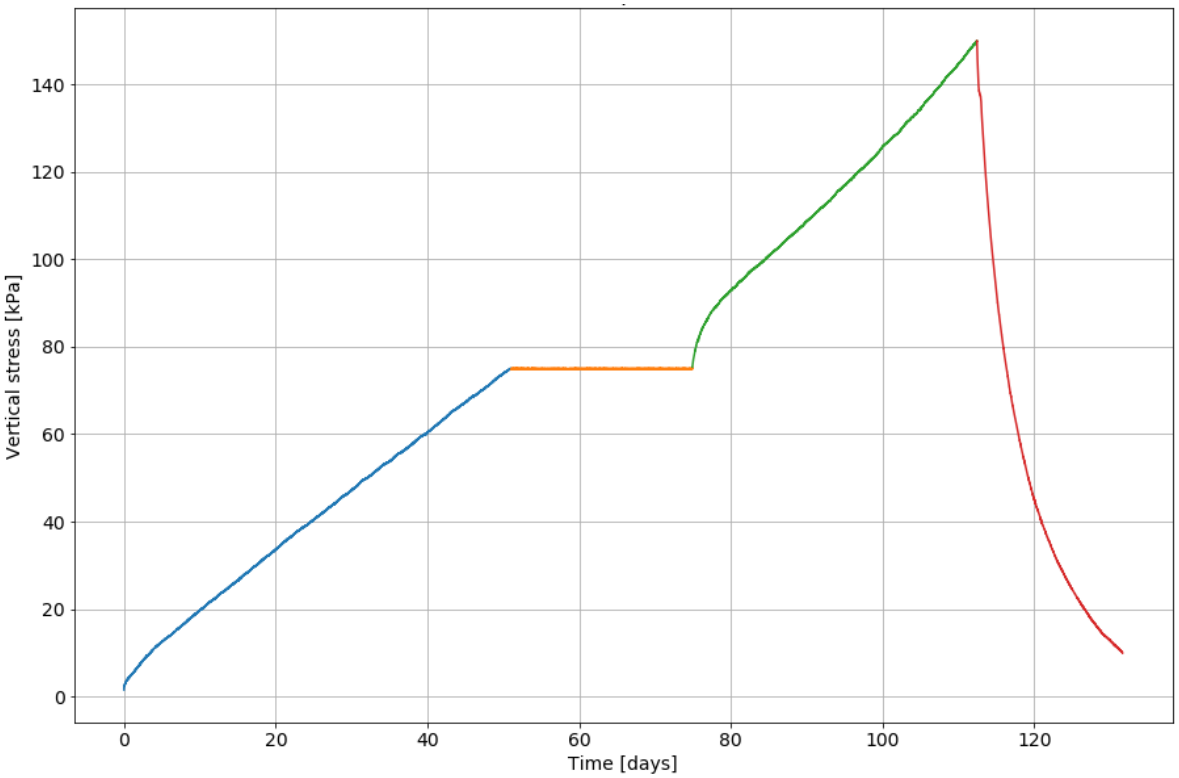
Vertical stress [kPa]
Time [days]
0
20
40
60
80
100
120
140

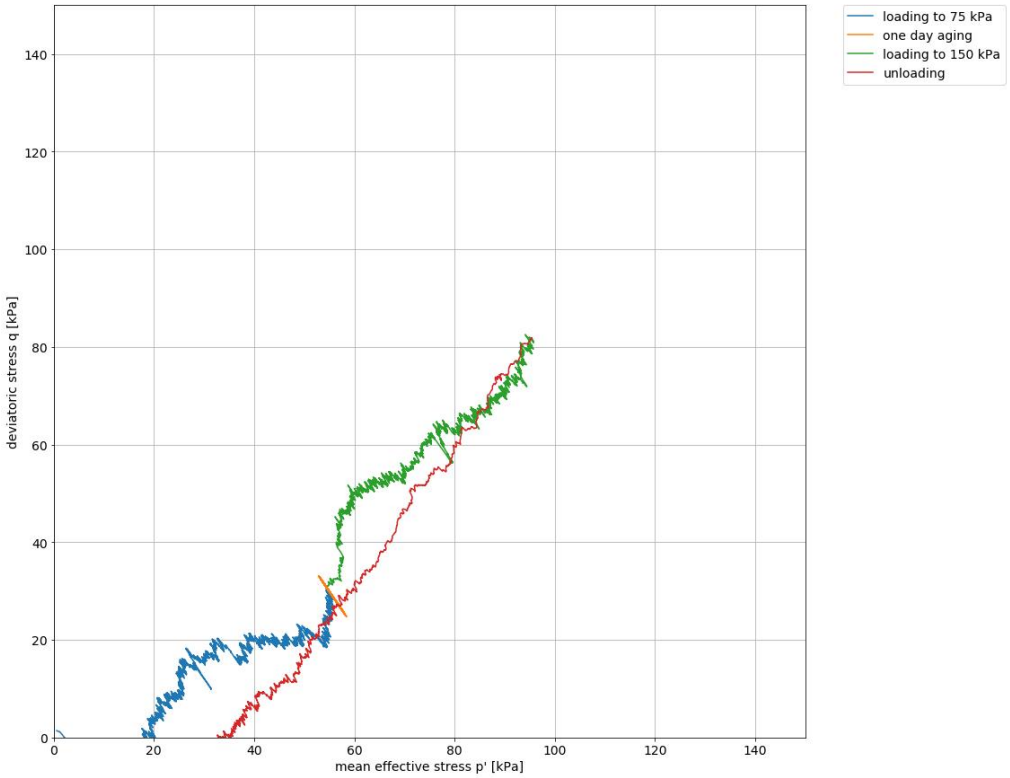
loading to 75 kPa
one day aging
loading to 150 kPa
unloading
deviatoric stress q [kPa]
mean effective stress p' [kPa]
0
20
40
60
80
100
120
140

## Sample 8

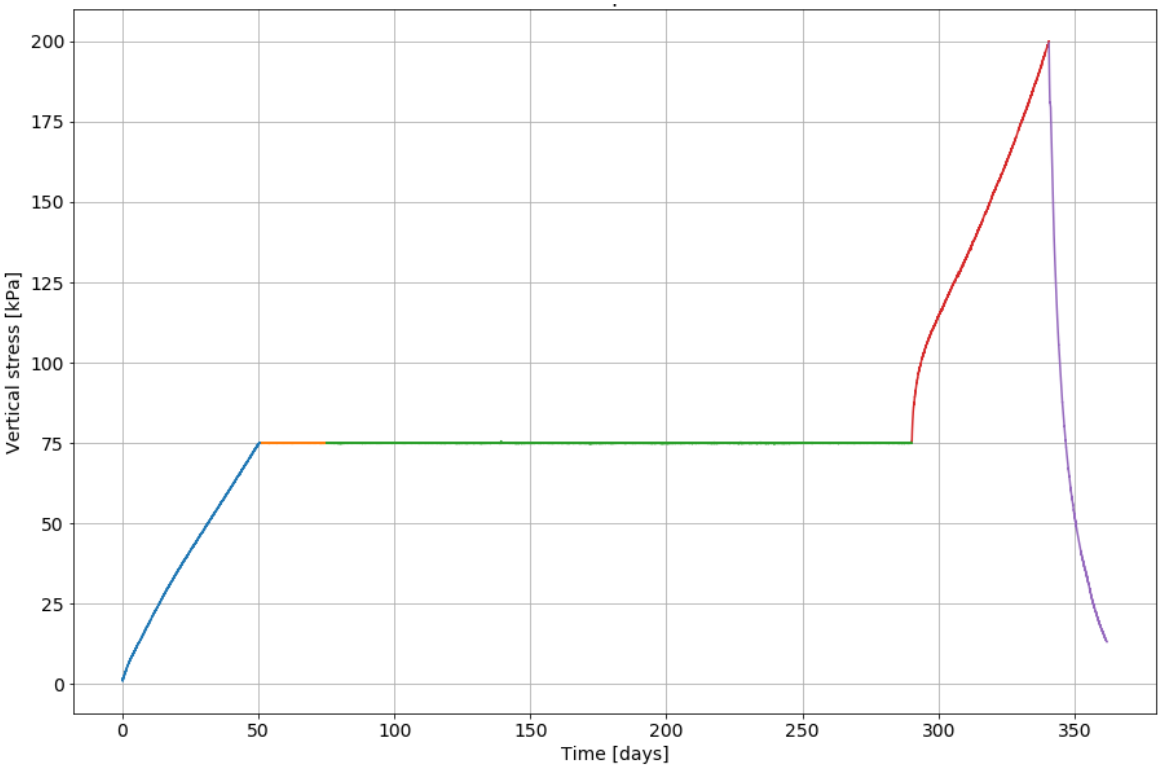
Vertical stress [kPa]
Time [days]
0
25
50
75
100
125
150
175
200
0
50
100
150
200
250
300
350

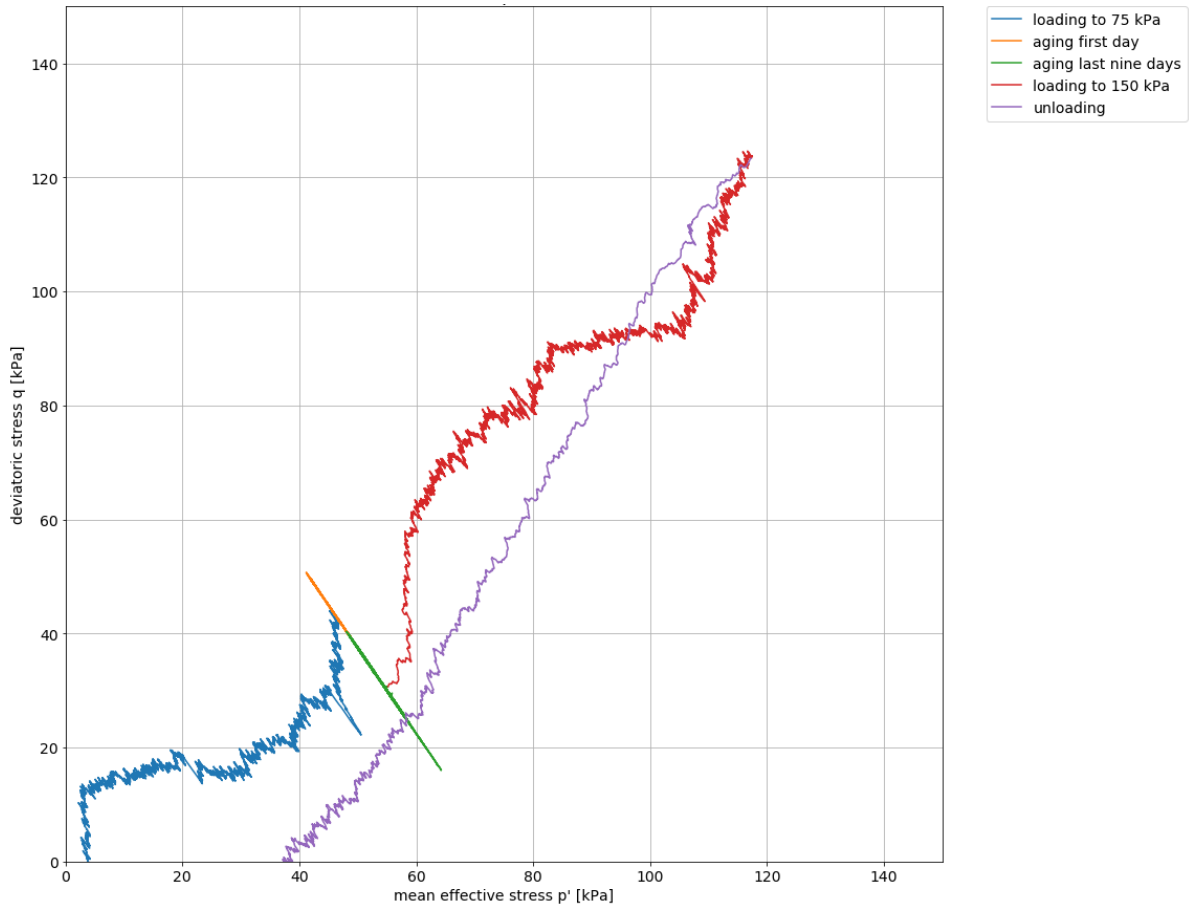
deviatoric stress q [kPa]
mean effective stress p' [kPa]
loading to 75 kPa
aging first day
aging last nine days
loading to 150 kPa
unloading
0
20
40
60
80
100
120
140

## Sample 10

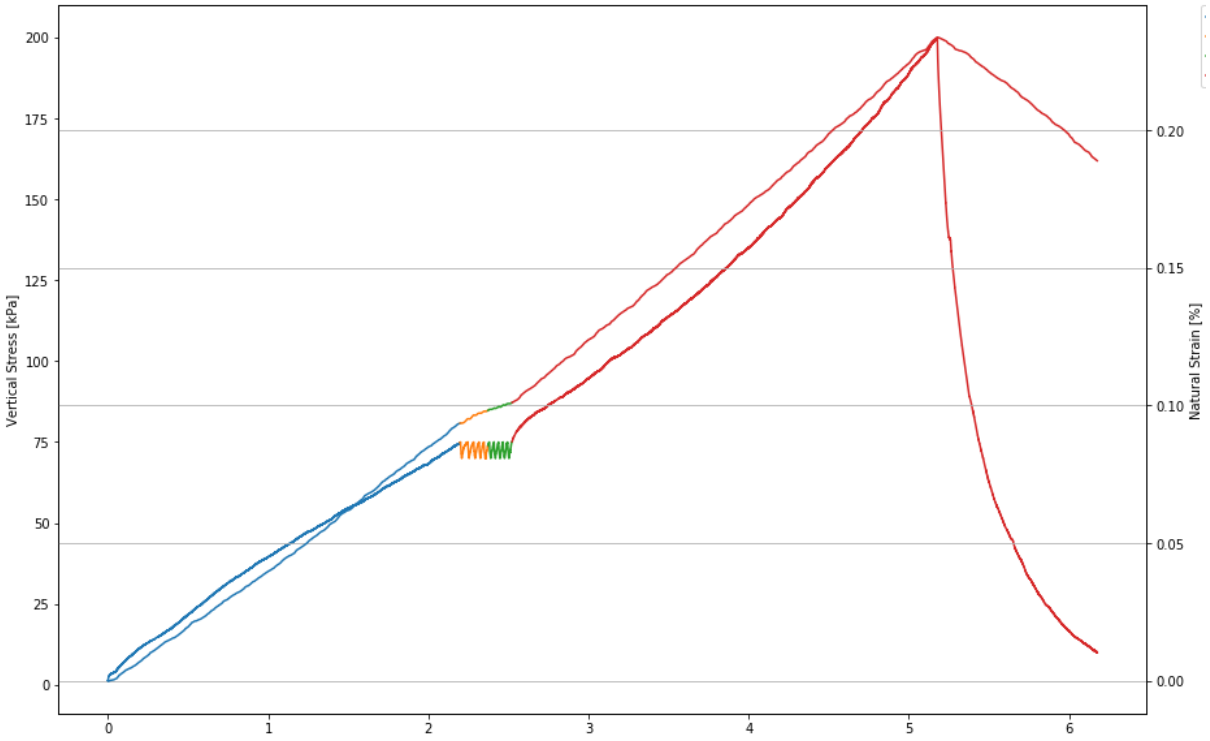
Vertical Stress [kPa]
Natural Strain [%]
200
175
150
125
100
75
50
25
0
0.20
0.15
0.10
0.05
0.00
0
1
2
3
4
5
6

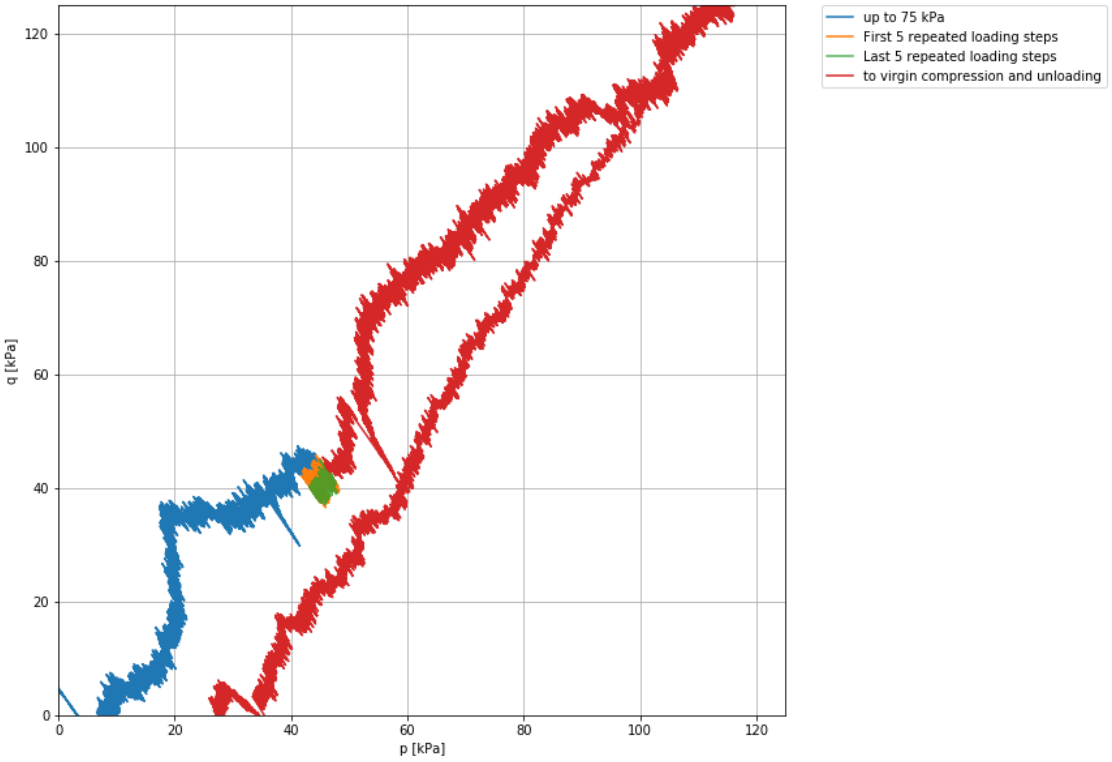
q [kPa]
p [kPa]
120
100
80
60
40
20
0
0
20
40
60
80
100
120
up to 75 kPa
First 5 repeated loading steps
Last 5 repeated loading steps
to virgin compression and unloading

## Sample 12

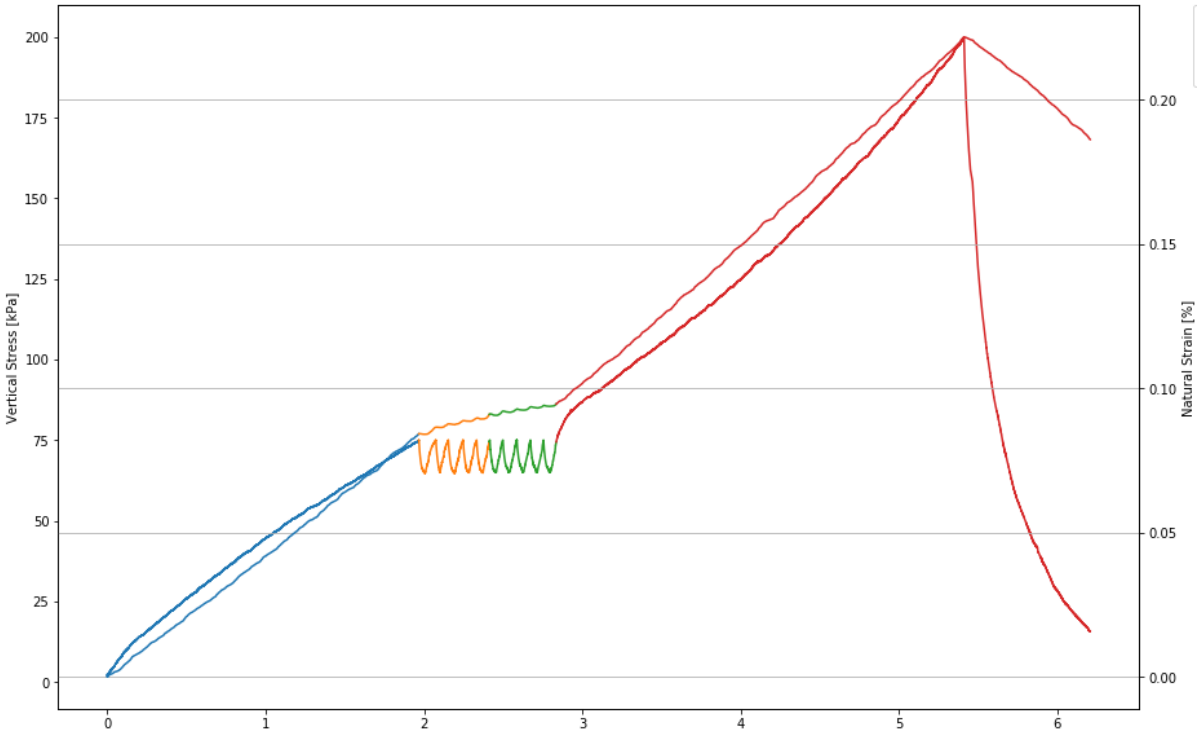
Vertical Stress [kPa]
Natural Strain [%]
0
25
50
75
100
125
150
175
200
0.00
0.05
0.10
0.15
0.20
0
1
2
3
4
5
6

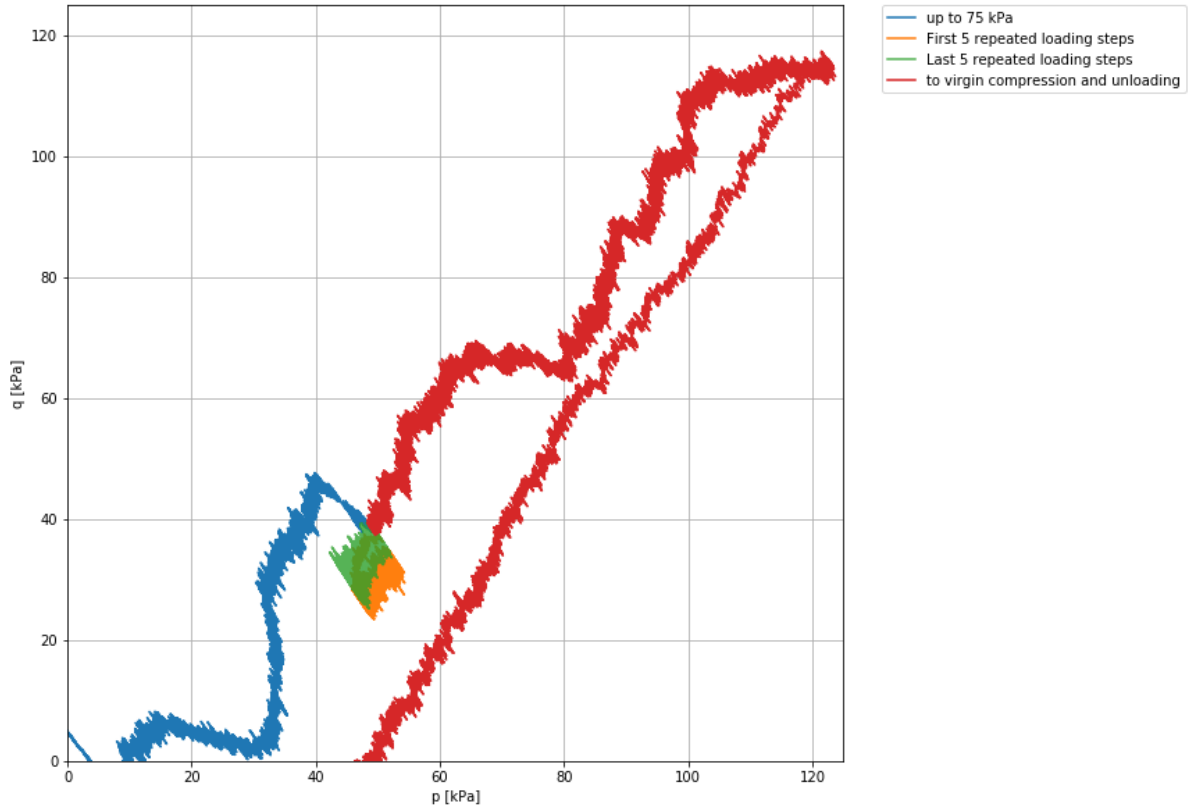
q [kPa]
p [kPa]
0
20
40
60
80
100
120
up to 75 kPa
First 5 repeated loading steps
Last 5 repeated loading steps
to virgin compression and unloading

**Appendix G** Conversion between isotach parameters

From the NEN-Bjerrum parameters to the abc-parameters (Den Haan, Essen, & Visschedijk, 2004):

$$a = -\frac{\ln\left[1 - RR\log\left(\frac{p_g}{\sigma_0}\right)\right]}{\ln\left(\frac{p_g}{\sigma_0}\right)}$$

$$b = \frac{\ln\left[1 - \varepsilon_p\right] - \ln\left[1 - \varepsilon_p - CR\log\left(\frac{\sigma'}{p_g}\right)\right]}{\ln\left(\frac{\sigma'}{p_g}\right)},$$

$$c = \frac{\ln\left[1 - \varepsilon_{prim}\right] - \ln\left[1 - \varepsilon_{prim} - C_\alpha\log\left(\frac{t}{t_0}\right)\right]}{\ln\left(\frac{t}{t_0}\right)}$$